PREPARATION AND CHARACTERIZATION OF DICHROIC POLYMER DISPERSED LIQUID CRYSTALS

A

Thesis

Submitted for the Award

of the Degree of

DOCTOR OF PHILOSOPHY

By

PANKAJ KUMAR

SCHOOL OF PHYSICS AND MATERIALS SCIENCE

THAPAR UNIVERSITY, PATIALA-147004, INDIA

July 2007

CONTENTS

CERTIFICATE

This is to certify that the thesis entitled ***"PREPARATION AND CHARACTERIZATION OF DICHROIC POLYMER DISPERSED LIQUID CRYSTALS"*** which is being submitted by ***Mr. Pankaj Kumar*** in fulfillment of the requirement for the award of the degree of ***Doctor of Philosophy*** in the School of Physics and Materials Science, Thapar University Patiala, is a record of candidate's own work carried out by him under my supervision and guidance. The matter presented in this thesis has not been submitted in part or full for the award of any degree in any other University or Institute.

Prof. K. K. Raina Date: 31-07-07

Thapar University Place: Patiala

Patiala-147004, Punjab (India)

Acknowledgement

I would like to take this opportunity to thank many people who have helped and encouraged me through out this study. First of all, it is a matter of extreme honour and privilege for me to offer my grateful acknowledgement to my research supervisor ***Professor K. K. Raina,*** Deputy Director and Dean, faculty affairs, resources and planning generation, Thapar University, Patiala, for providing me an opportunity to work under his guidance and supervision. Behind the work compiled in these pages lie the steady encouragement, fruitful guidance and constant enthusiasm of my guide. I owe the greatest debt of gratitude to him for suggesting the research problem followed by meticulous suggestions, ever-willing help and the freedom extended to me throughout the period of my research. I greatly appreciate his support, guidance and trustful strengthen given to me throughout my years at Thapar University to solve the difficulties not only in research but also in the attitude of living. His compassion and kindness makes me realize how lucky I am to have him as my supervisor.

I am extremely thankful to ***Prof. Abhijit Mukherjee***, Director, Thapar University, Patiala, for providing me the entire necessary infrastructure to carry out the experimental work in the School of Physics and Materials Science and lot of opportunity for the interaction with national and international scientists in the various conferences and seminars held during the tenure of my Ph.D.

I am deeply thankful to ***Dr. Susheel Mittal,*** Dean, Research & Sponsored Projects, Thapar University, Patiala, for his whole hearted support and needful help during the various stage of my work.

I am profoundly obliged to ***Dr. O. P. Pandey,*** Prof. **a**nd Head, School of Physics and Materials Science, Thapar University, Patiala for his whole-hearted support and needful help during the various stages of my work, which paved the path for successful completion of this research work.

Words are inadequate in expressing my sincere thanks to ***Dr. Kulvir Singh,*** Assistant Professor, School of Physics and Materials Science, for his support in every moment of complexity, may be either in the field of research or in any day-to-day problem. His skills, constructive suggestions, motivation and constant inspiration helped me to fulfill this effort.

Special thanks go to ***Dr. G. Sumana***, Scientist 'C', NPL, New Delhi, who worked about seven years in the lab as a research scientist and took much care for me. I will always remember her kindness and affection.

I would like to convey my sincere gratitude to my friends and colleagues ***Dr. Praveen Malik, Dr. Sarabjit Singh, Dr. Kiran Gupta***, ***Dr. Varinder Sapehiyia, Dr. Puneet Sharma, Mr. Rakesh sharma, Mr. Ankush Pathania, Mr. Karamjit Singh, Mr. Vineet Prakash, Mr. Vivek Srivastava, Mr. Vijay Kumar, Mr. Jitendra Kushwaha, Mr. Vishal Choudhary, Ms. Anu Arora, Ms. Zinki Jindal, Ms. Meenakshi Malik, Ms. Shikha, Mrs Raminder Kaur and Ms. Neeraj*** for their whole-hearted co-operation.

I would like to thank to our M. Tech. (Materials Science) students (present and past) in our lab and school for their cheerful company. Also I would like give my best wishes to new M. Tech. and Ph.D. students in the lab and School. I am sure they will keep studying hard and try the best. I hope they will take much care of the lab and will always maintain it neat and clean.

I am grateful to the all other faculty and staff of School of Physics and Materials Science who never turned me down whenever I approached them for any help.

I express my loyal venerable thanks and heartfelt gratitude to all the faculty and research scholar of Thapar University for their affection and co-operation, which has really given me the confidence and positive attitude that broadened my vision.

I am greatly indebted to my respected brother ***Mr. K. K. Singh*** and dearest sister ***Km. Priyanka Singh,*** for their patience, moral support and constant co-operation whenever I was away from them.

The meaning of my life and work is incomplete without paying regards to my respected parents whose blessings and continuous encouragement have shown me the path to achieve my goals. I also acknowledge with thanks for encouragement of my elders and relatives.

…And above all, I pay my regards to the **Almighty** for his love and blessings.

(Pankaj Kumar)

LIST OF FIGURES **Page No.**

CHAPTER 1

CHAPTER 2

CHAPTER 3

CHAPTER 4

LIST OF TABLES

ABBREVIATIONS AND LIST OF SYMBOLS

LC	Liquid crystal
NLC	Nematic liquid crystal
FLC	Ferroelectric liquid crystal
PLC	Polymer liquid crystal
MC-PLC	Main chain polymer dispersed liquid crystal
SC-PLC	Side chain polymer dispersed liquid crystal
PDLC	Polymer dispersed liquid crystal
PDNLC	Polymer dispersed nematic liquid crystal
DPDLC	Dichroic polymer dispersed liquid crystal
PSLC	Polymer stabilized liquid crystal
HPDLC	Holographic polymer dispersed liquid crystal
PS	Phase separation
PIPS	Polymerisation induced phase separation
TIPS	Temperature induced phase separation
SIPS	Solvent induced phase separation
ITO	Indium tin oxide
PDFLC	Polymer dispersed ferroelectric liquid crystal
SSPFLC	Surface-stabilized polymer dispersed ferroelectric liquid crystal
PNSFLC	Polymer network-stabilized ferroelectric liquid crystal
SAPDFLC	Shear aligned polymer dispersed ferroelectric liquid crystal
NOA	Norland optical adhesive
n_o	Ordinary refractive index
n_e	Extra ordinary refractive index
n_p	Polymer refractive index
K	Crystalline
I	Isotropic
N	Nematic

N*	Cholesteric
SmA	Smectic A
SmC	Smectic C
SmC*	Smectic C*
I_0	Incident light intensity
I	Transmitted light intensity
α	Scattering coefficient
β	Absorbance coefficient
ε	Dye extinction coefficient
$\varepsilon_{\perp}$	Dye extinction coefficient measured perpendicular to the nematic director
ε_{II}	Extinction coefficient measured parallel to the nematic director
ε_i	Isotropic extinction coefficient
d	Film thickness
l	Path length
V_{th}	Threshold voltage
ε’	Dielectric permittivity
ε”	Dielectric losses
ε_o	Free-space permittivity
σ_{ac}	Ionic conductance
P_s	Spontaneous polarization

LIST OF PUBLICATIONS

Referred Journals

[1] Morphological and electro-optical responses of dichroic polymer dispersed liquid crystal films, **Pankaj Kumar** and K.K. Raina, ***Current Appl. Phys.* 7** (2007) 636-642.

[2] Morphological control and polarization switching in polymer dispersed liquid crystal materials and devices, K. K. Raina, **Pankaj Kumar** and Praveen Malik, ***Bull. Mat. Sci.* 29** 6 (2006) 596.

[3] Ferroelectric liquid crystal-polymer composites: A novel display material, K. K. Raina, **Pankaj Kumar** and G. Sumana, ***Asian Journal of Chemistry***, **18** 5 (2006) 3384.

[4] Opto-electronic responses of a guest-host polymer dispersed liquid crystal device, Praveen Malik, **Pankaj Kumar** and K.K. Raina, ***Current Appl. Phys***. (communicated) 2007.

[5] Studies of optical and dielectric behaviour of dichroic polymer dispersed liquid crystal-Effect of azo dye, **Pankaj Kumar** and K.K. Raina (communicated).

Referred Conference Proceedings (International/National)

[6] Enhancement of the performance of polymer dispersed liquid crystal with the effect of dye, **Pankaj Kumar** and K. K. Raina, ***National conference on emerging trends in Engineering Materials***, SPMS, TIET Patiala, 1-3 Feb, 2007.

[7] Ferroelectric liquid crystals: Physics, Materials and Applications, K K Raina, **Pankaj Kumar** and Praveen Malik, ***XIVth National seminar on Ferroelectric and Dielectrics***, **IIT Kharagpur**, 19-22 Dec 2006.

[8] Opto-electric switching properties in polymer systems with micro-nano liquid crystal droplet dispersions, K. K. Raina and **Pankaj Kumar**, ***International conference on Liquid Crystal, Uni. of Mumbai,*** 5-8 Dec 2006.

[9] Guest host polymer dispersed liquid crystal display device: Role of dichroic dye, Praveen Malik, **Pankaj Kumar** and K. K. Raina, proceeding, page173, ***Asian symposium on Information Display, IIT Kanpur,*** 8-12 Oct 2006.

[10] Study of the morphologies and polarization switching in polymer dispersed ferroelectric liquid crystal composite films and display devices, **Pankaj Kumar**, K. K. Raina and Praveen Malik, proceeding, page173, ***Asian symposium on Information Display, IIT Kanpur,*** 8-12 Oct 2006.

[11] Influence of droplet orientation and its morphology on the electro-optic performance of polymer dispersed liquid crystal composite films, K. K. Raina, **Pankaj Kumar**, Praveen Malik and G. Sumana, ***Indo-Hungarian meeting on Liquid Crystal***, ***Centre forLliquid Crystal Research, Banglore,*** 2 Dec, 2006.

[12] Morphological and electro-optical responses of polymer dispersed liquid crystal thin films: influences of dichroic dye, **Pankaj Kumar**, Praveen Malik, and K. K. Raina, ***International conference on Optics and Optoelectronics, IRDE Dehradun***, 12-15 Dec, 2005.

[13] Charge induced droplet orientation and optical properties of polymer dispersed liquid crystal thin films, Praveen Malik, **Pankaj Kumar** and K. K. Raina, ***7th International conference on Optoelectronics, Fiber optics, and Photonics***, **CUST, Kochi**, 9-11 Dec. 2004.

[14] Effect of polymer viscosity on morphological, polarizing switching and optical properties of polymer dispersed ferroelectric liquid crystal thin films, Praveen Malik, **Pankaj Kumar,** K. K. Raina and Chandra Prakash, ***Proc. of National seminar on Ferroelectrics and Dielectrics XIII***, Allied Publisher, Nov 23-25 (2004), New Delhi.

[15] Morphological and electro-optical studies of polymer dispersed liquid crystal, K. K. Raina and **Pankaj Kumar**, ***National Seminar on Recent Trends in Polymer Science and Technology***, SLIET Longowal, Dec 10-11 2005.

Best Paper Award

[1] Morphological control and Polarization Switching in Polymer dispersed liquid crystal Materials and Devices, K.K. Raina and **Pankaj Kumar**, ***Indo-Singapore symposium on Advanced Functional Materials, IIT Bombay***, 24-26 Feb 2006.

[2] Guest host polymer dispersed liquid crystal display device: Role of Dichroic Dye, Praveen Malik, **Pankaj Kumar** and K. K. Raina, ***9th Asian Symposium on Information Display, IIT Kanpur***, 8-12 October, 2006.

[3] Effect of polymer viscosity on morphological, polarizing switching and optical properties of polymer dispersed ferroelectric liquid crystal thin films, Praveen Malik, **Pankaj Kumar**, K. K. Raina and Chandra Prakash, ***13th National seminar on Ferroelectric and Dielectrics, Delhi Uni, Delhi***, 23-25 November 2004.

****

Chapter 1

Dichroic Polymer Dispersed Liquid Crystal: An Introduction

Overview

This chapter reviews basic features and classification of liquid crystals (LCs) in general and research works already accomplished by various research groups in the area of polymer dispersed liquid crystal (PDLC) and dichroic polymer dispersed liquid crystal (DPDLC) in particular. The liquid crystalline phases, the order parameter, and the liquid crystal alignments are defined, followed by the concepts of theory and liquid crystal deformations. The preparation methods of polymer dispersed liquid crystal (PDLC) and dichroic polymer dispersed liquid crystal (DPDLC) systems are given in detail. The operation principle of these PDLC and DPDLC system, liquid crystal droplet configuration with and without applied field, is explained. The aim of the present research work has been given at end of the chapter.

1.1 Liquid Crystals

Liquid crystals (LCs) are composed of moderate size organic molecules which tend to be elongated, which exist in one or more intermediate phases, which lie between a solid and an isotropic liquid as shown in fig. 1.1 (a, b). Because of their elongated shape, under appropriate conditions, the molecules exhibit orientational order, such that all the axes line up in a particular direction and form a so-called nematic liquid crystal (NLC) state. The molecules are still able to move around in the fluid, but their orientation remains the same. The average direction of the molecules is called the director. The credit for preparing the first liquid crystal material (cholesteryl benzoate) goes to Friedrich Reinitzer [1-9]. Depending on the type and shape of the molecules and the conditions, not only orientational order appears, but also a positional order is possible. In smectics, the orientation is fixed and the movement is limited

to layers. Many materials exhibit several different smectic phases and many smectic materials also exhibit the nematic phase at higher temperature.

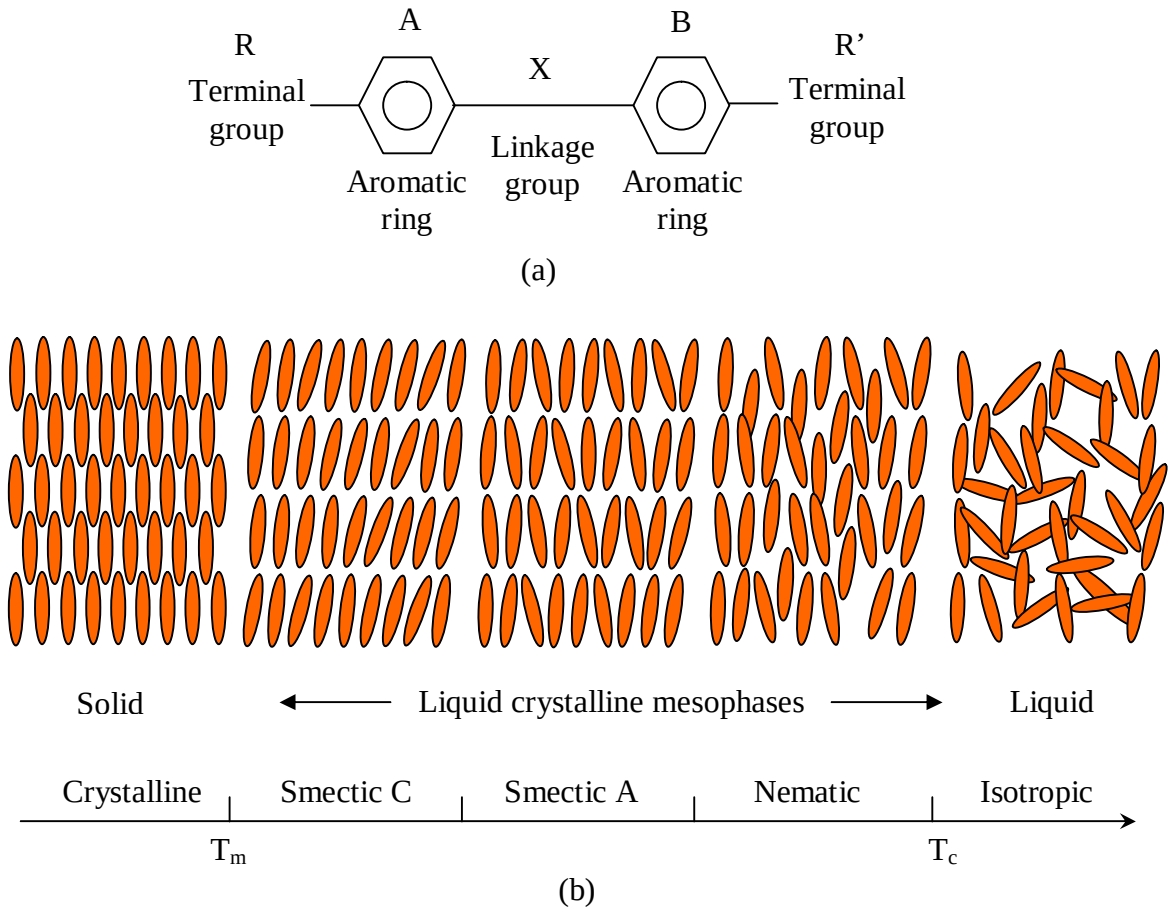

Fig.1.1 (a) Generalised molecular structure template of a typical liquid crystal molecule (b) phase sequence in a liquid crystalline material

1.2 Liquid crystal phases

Based on molecular arrangements such as orientation and positional order of the molecules, liquid crystals can be commonly divided into three types thermotropic, lyotropic and polymeric. Thermotropic systems are classified in to nematics, cholesterics and smectics.

1.2.1 Nematics (N)

An organic molecule with the following chemical structures generally possesses a nematic phase.

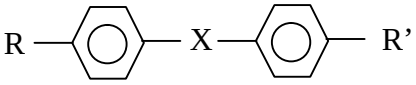

For a molecular, there is a core with two terminals, one at each end, i.e. R and R'. The core consists of two benzene rings with a connector X. One typical example of liquid crystals is p-azoxyanisole (PAA) with the chemical structure:

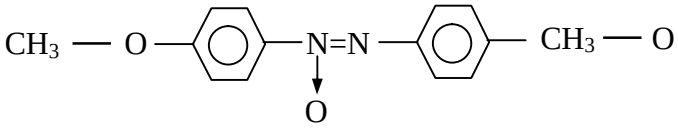

The two benzene rings are nearly coplanar. Such a nematic molecule can be considered as a rigid rod with 20 Å in length and 5 Å in width approximately. Other classical liquid crystalline molecule is methoxy benzilidene butyl aniline (MBBA) with the chemical structure

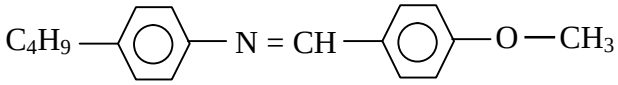

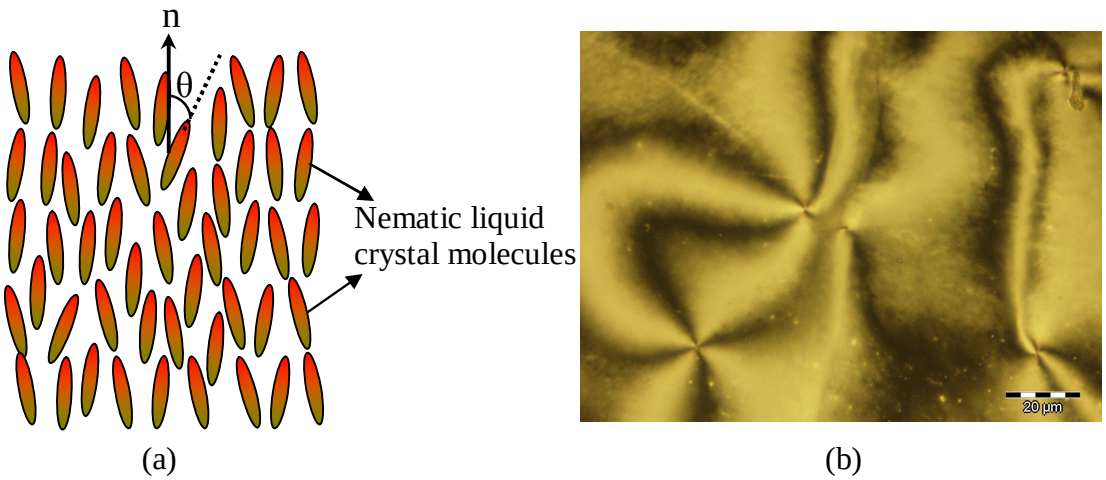

Fig. 1.2 (a) Schematic representation of the two dimensional orientation of the liquid crystal molecules, tending to align along the director (n), (b) optical texture of nematic liquid crystal BL036 between crossed polarizer at a magnification of 100 X.

This material has a wide room temperature nematic phase. Fig.1.2 (a) is the schematic representation for nematics, n is defined as the director axis, which represents the preferred orientation of LC molecules. Nematics possess several main features:

(a) long range orientational order i.e. the molecules tend to align parallel to each other.

(b) fluid-likeness, i.e., there is no long range order in the molecular center of gravity (transitional order).

(c) the states of director n and –n are equivalent. It means that director has no polarity. A nematic molecule is not symmetrical in their structure.

The order parameter for a LC, S_{LC} can be written as

$$S_{LC} = \frac{1}{2}\left\langle 3\cos^2 \theta_{LC} - 1 \right\rangle \qquad (1.1)$$

Where θ_{LC} is the angle between the director and the long axis of an individual LC molecule and the average is taken over the complete ensemble. Typically, S_{LC} is between 0 and 1. S_{LC} for nematic formed by rod-like molecules is between 0.4 (at the highest temperature) and 0.7 (at the lowest temperature). Apparently, the value of S for isotropic liquid is 0, and that for crystal is 1. The micro-texture of typical nematic phase is shown in fig. 1.2 (b), as the Schleiren texture.

1.2.2 Cholesterics

The cholesteric (or chiral nematic) liquid crystal phase is usually composed of nematic mesogenic molecules containing a chiral center; it produces intermolecular forces that favour alignment between molecules at a slight angle to one another. It leads to the formation of a structure which can be visualized as a stack of very thin 2-D nematic like layers with the director in each layer twisted with those above and below as shown in fig. 1.3 (a). In this structure, the directors actually form in a continuous helical pattern about the layer normal. An important characteristic of the cholesteric mesophase is the pitch, defined as the distance it takes for the director to rotate one full turn in the helix. The helical pitch controls the selective reflections of the cholesteric phase and makes them suitable for electro-optic display devices. The pitch can be adjusted to any desired value by adding appropriate amounts of a chiral compound to a nematic structure. However, the necessary condition for the formation of the cholesteric mesophase is that the molecules are chiral (optically active) that is why cholesteric phase is also defined as the chiral nematic phase, represented by N*. When a chiral agent is mixed with a nematic liquid crystal, the pitch of the mixture is given by

$$1/p = 1/(HTP \cdot X_c) \qquad (1.2)$$

This relationship, given by De Gennes and Prost [10], where HTP and X_c are the helical twisting and concentration of the chiral agent, respectively. HTP is mainly a characteristic parameter of the chiral dopant and depends slightly on the nematic host. The optical texture of cholestric phase is shown in fig 1.3(b).

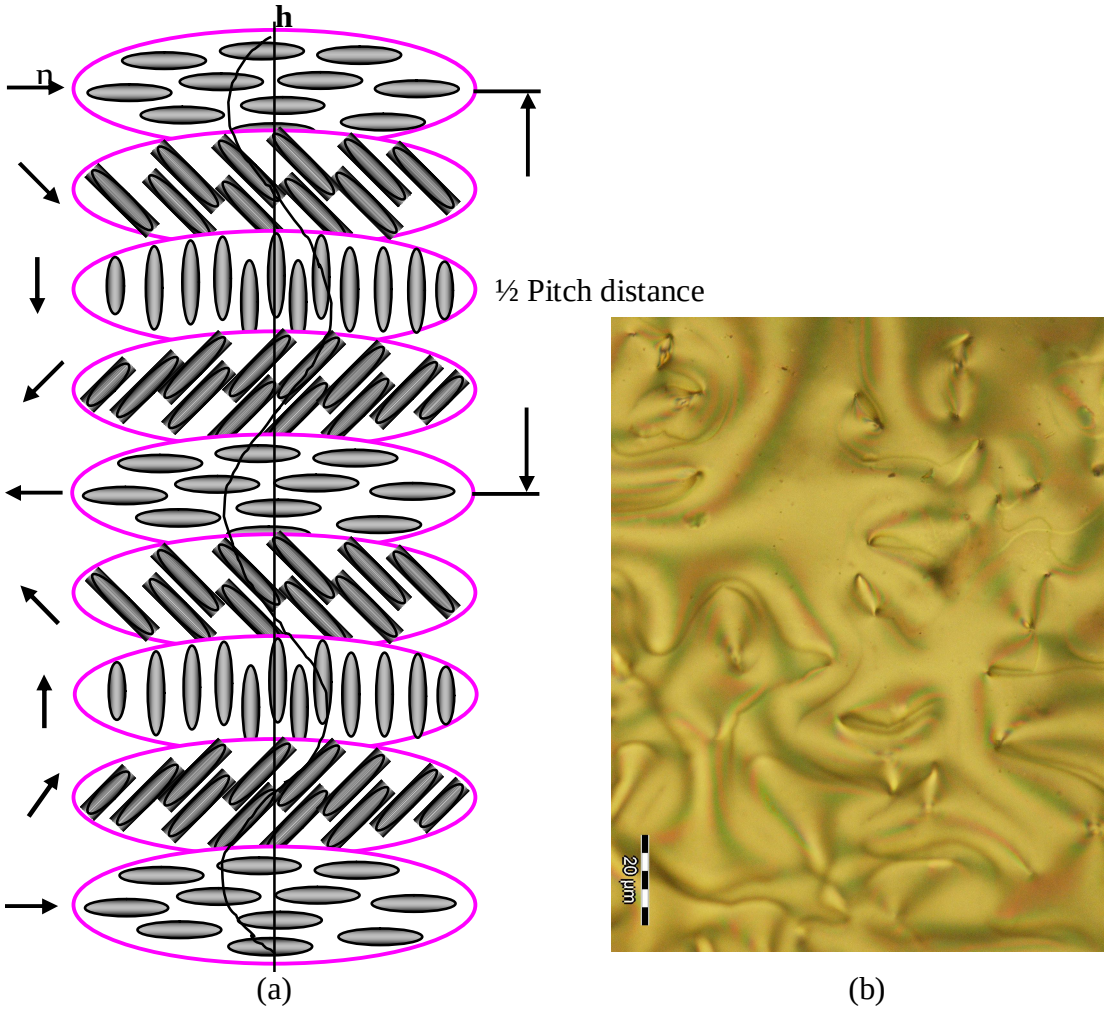

Fig. 1.3 Schematic representation of molecular structure of (a) cholestric liquid crystal (b) optical texture of cholestric phase

1.2.3 Smectic phase

In the smectic phase molecules show a degree of translational order not present in the nematic. In the smectic state, the molecules maintain the general orientational order of nematics, but also tend to align themselves in layers or planes. Motion is possible between the smectic planes, but is hindered within these planes, and separate planes are observed to flow

past each other. The increased order means that the smectic state is more "solid-like" than the nematic. Many compounds are observed to form more than one type of smectic phase. Many different types of different smectics phases have been identified. Halle school (UK) classified them as D, E, F, and G. Further type H had been introduced by de Vries [11] on the basis of X-ray data, but has found to be miscible with smectics B.

1.2.3.1 Smectic A phase

In the smectic-A mesophase, the director is perpendicular to the smectic plane, and these phases are more ordered than nematics and possess positional and orientation order but there is no particular positional order in the layer. These phases usually occur at temperatures below the nematic domain. From the structural point of view, all the smectics have layered structures and are perpendicular to the layer plane with a well-defined interlayer spacing that can be measured by x-ray diffraction. In this system, the molecules can move freely around the long axes within the layer. Optically smectic A is uniaxial with the optical axis direction coinciding with the director (n) as can be seen in fig. 1.4(a). The optical textures of smectic A phase is shown in fig 1.4(b).

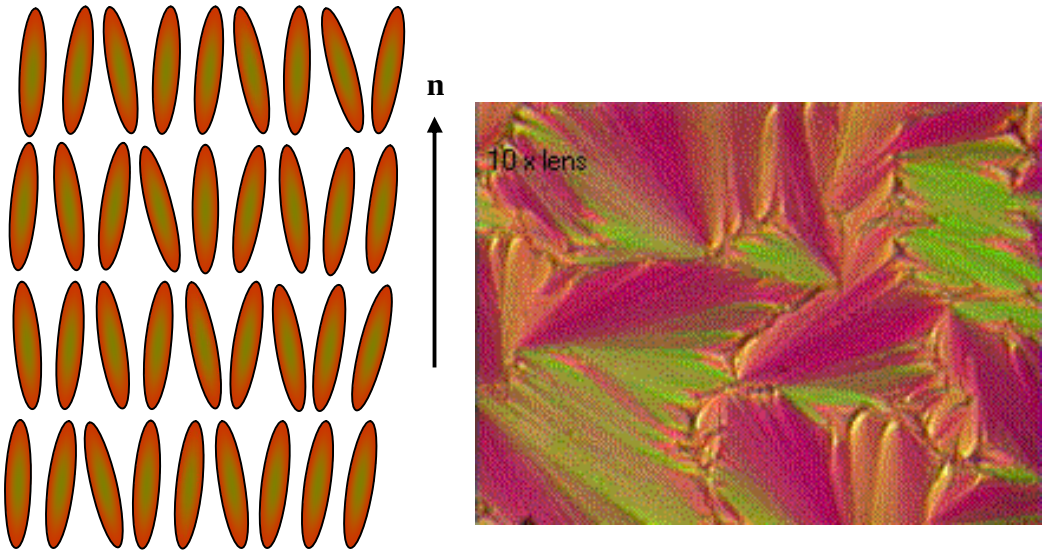

(a) (b)

Fig.1.4 (a) Smectic A phase of liquid crystal. The long axes of the molecules in each layer, on an average, are perpendicular to the layer plane containing the molecules (b) Optical micro texture of smectic A phase

1.2.3.2 Smectic B phase

Similarly, the smectic-B mesophase orients with the director perpendicular to the smectic plane, but the molecules are arranged into a network of hexagons within the layer, just like the SmA phase. In this phase the LC molecules are locally hexagonally packed and are perpendicular to the plane as shown in fig. 1.5.

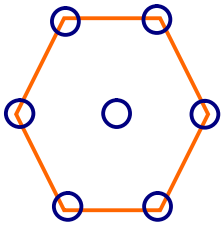

Fig. 1.5 A planar view of molecules within a layer of a hexagonal smectic B phase, the molecules are perpendicular to the smectic plane

1.2.3.3 Smectic C phase

In the smectic-C mesophase, molecules are arranged as in the smectic-A mesophase, but the director is at constant tilt angle measured normally to smectic plane as shown in fig**.** 1.6.

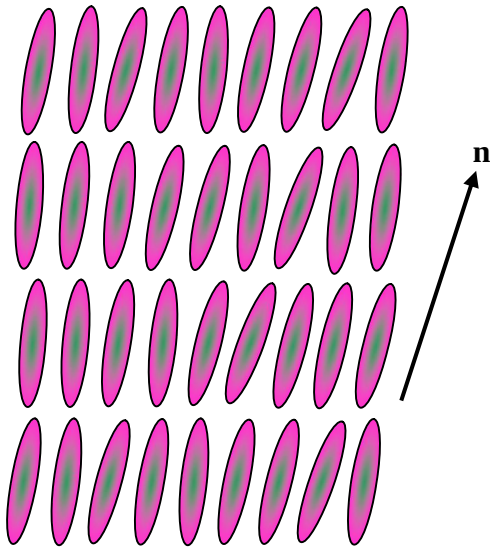

Fig.1.6 Smectic C phase of liquid crystal. The long axes of the molecules in each layer, is tilted at an angle with respect to layer normal

1.2.3.4 Chiral smectic C phase

Smectic phases where long axis of molecule is tilted at an angle with respect to the layer normal, as in SmC phase, can form different helical structures. In these phases the director rotates from layer to layer through a change in tilt direction and describes a helix as shown in fig.1.7 (a). These phases are denoted by SmC*. The optical texture of chiral smectic phase is shown in fig. 1.7 (b).

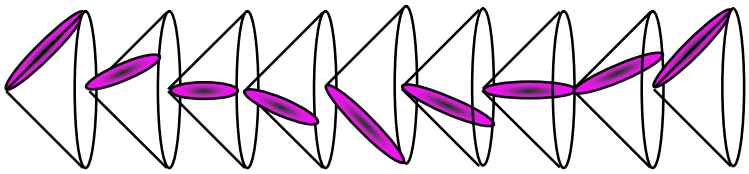

(a)

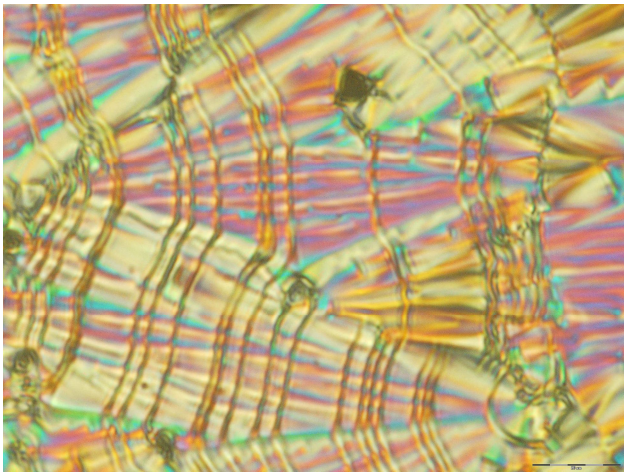

(b)

Fig 1.7 (a) Modulated structure of chiral smectic C (SmC*) phase resulting in the helix formation (b) Micro photograph of the chiral smectic C phase. The parallel lines give the measure of the helical pitch

On the molecular structures, liquid crystal molecules are broadly classified in to three types: (a) the rod-like (b) disc like and (c) lath-like structures.

These are schematically depicted in fig. 1.8 in the nematic phase. Rod-like molecules are the most typical ones, which give rise to the conventional nematics and smectics. Disk-like

molecules form the so called columnar mesophases. Between these two types we can find lath-like molecules which don't process the cylindrical symmetry. These can form optically biaxial nematics and perhaps smectics.

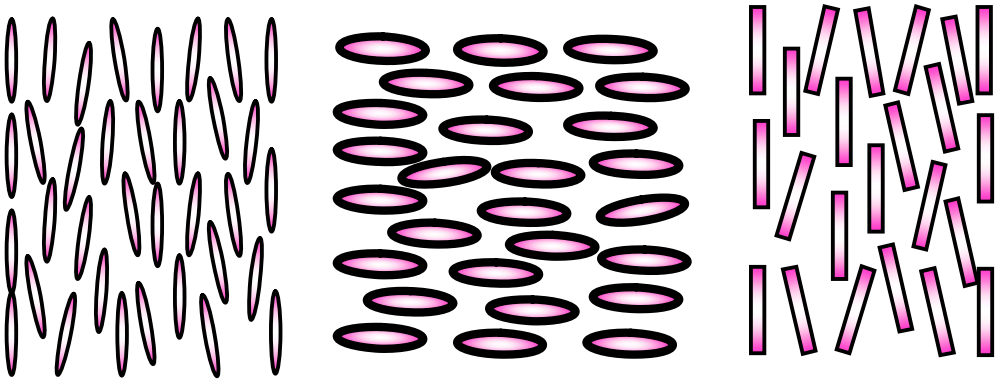

Fig.1.8 Molecular shape of liquid crystal (a) rod-like (b) disc like and (c) lath-like structures

A number of different types of molecules form liquid crystal (LC) phases when heated above their melting point. However, they are all anisotropic, they differ either in their shape or different solubility properties [2].

Over the years, polymers have emerged as important class of systems having important physical properties. These systems with liquid crystal give rise to polymer liquid crystals (PLCs) [12, 13]. These hybrids show the same mesophases characteristic of ordinary liquid crystals, yet retain many of the useful and versatile properties of polymers like.

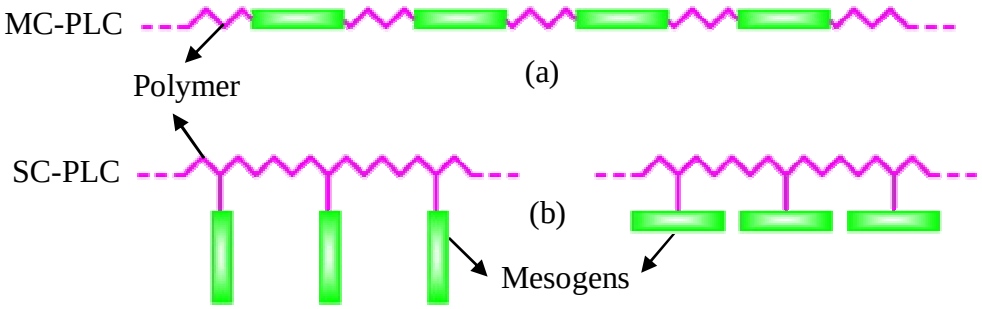

Fig. 1.9 Structural model of (a) main chain and (b) side chain polymer liquid crystal

For normally flexible polymers to display liquid crystal characteristics, rod-like or disk-like elements called mesogens must be incorporated into their chains. The placement of the mesogens plays a significant role in determining the type of PLC that is formed. Main chain

polymer liquid crystals (MC-PLC) are formed when rigid elements are incorporated into the backbone of normally flexible polymers fig. 1.9 (a). These stiff regions along the chain allow the polymer to orient in a manner similar to ordinary liquid crystals, and thus display liquid crystal characteristics. Conversely, side chain polymer liquid crystals (SC-PLC) are formed when the mesogens are connected as side chains to the polymer by a flexible "bridge" (called the spacer) as shown in fig. 1.9 (b).

1.3 Polymer dispersed liquid crystal (PDLC)

De Gennes [14] first contemplated that liquid crystal-polymer gels can form composite materials and shall exhibit interesting electro-optic properties. This idea generated considerable interest in these materials and in mid-1980s, polymer dispersed liquid crystals (PDLCs) attracted significant attention among various scientific groups [15-17]. In 1985, Doane et al. [18, 19] reported first examples of PDLC preparation.

In recent years, thrust of the research activity in liquid crystal shifted to PDLCs, considering their potential use in variety of electro-optical applications like switchable windows, displays and other devices due to their numerous and important properties [20-37]. PDLC materials consist of micron sized nematic droplets dispersed in a polymer matrix and their optical response is based on the electrically controlled light scattering properties of the droplets. An applied electric field aligns the droplets to yield a non-scattering or transparent state. Surface interactions at the droplet wall and a non ideal spherical droplet shape return the droplets to the original orientation in the absence of the field to yield a scattering or opaque state. One mode of operation is that shown in fig. 1.10 (a) where nematic droplets with a positive dielectric anisotropy are randomly oriented in the film in the opaque state. In this state, the film has a translucent white appearance because of the light scattering properties of the droplets. Upon application of a field the droplets align in a direction parallel to the field. If the refractive index $n_{\perp}$ (index perpendicular to the nematic director) approximately matches the refractive index of the polymer matrix, the film will switch to a transparent state, fig. 1.10 (b). Upon removal of the field, the droplets return to their original random orientation and the film returns to its opaque state. Sub-millisecond switching times are possible with these films. Thermally switched films are prepared by matching the refractive index of the polymer with that of the liquid crystal in the isotropic phase, $n_{i.}$ changing the temperature of the film across

the isotropic-nematic phase transition reversibly switches the film from opaque to clear as shown in fig. 1.10 (d).

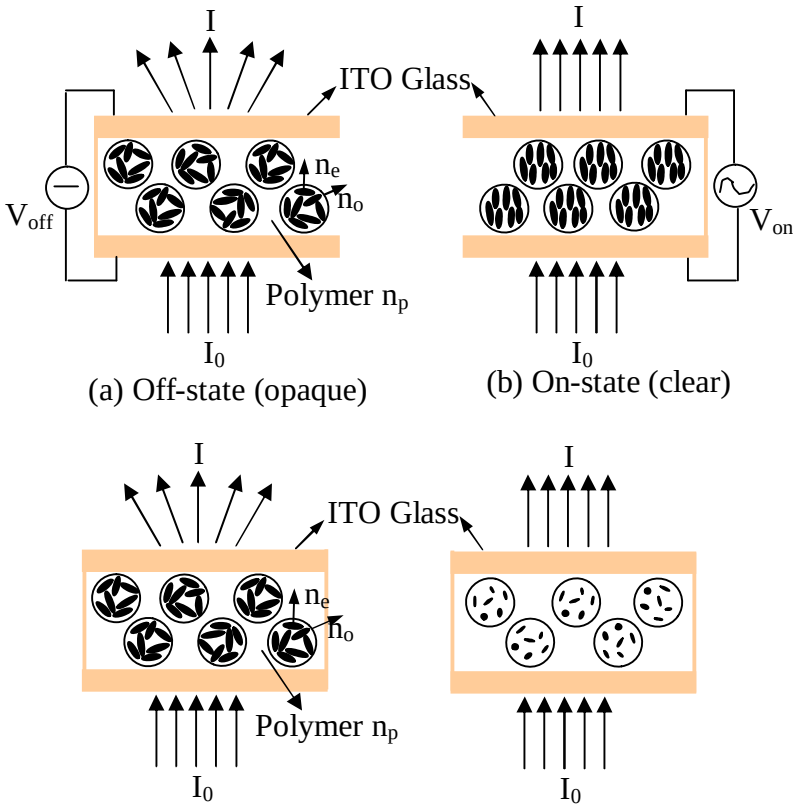

Fig.1.10 Schematic of PDLC light shutter illustrating the opaque state (a) and (c) the electro-optically switched transparent state, (b) with aligned droplets and the thermally switched transparent state, (d) with the droplets in the isotropic phase

It is reported that the electro-optical properties of PDLC displays depend on LC concentration, film thickness, size and shape of LC droplets, anchoring energy on the boundary surface, and physical properties of both components, e.g. elasticity and viscosity parameters, and dielectric anisotropy of the liquid crystal, and the resistivities and refractive index ratios of the liquid crystal and polymer. Fig. 1.11 shows a typical dispersion for nematic liquid crystal (E7) in Norland optical adhesive (NOA65) polymer matrix with low concentration of anthraquinone blue and orange azo dye at an applied voltage 10 volt at room temperature.

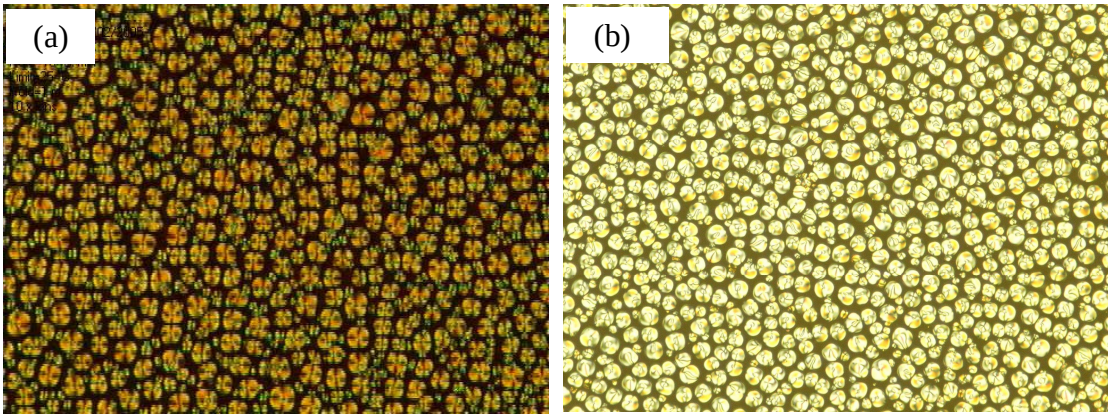

Fig. 1.11 Liquid crystal droplets in a polymer matrix (NOA 65) (a) anthraquinone blue dye and (b) orange azo dye dispersed texture at an applied voltage 10 volt at room temperature

1.4 Methods of PDLC preparation

Polymer dispersed liquid crystals are usually produced in two distinct ways: phase separation and encapsulation. Phase separation (PS) in liquid crystals (LCs) is a subject of intensive studies [38-50].

1.4.1. Phase separation

In order to obtain PDLC by phase separation, a homogenous mixture of polymer (prepolymer) and liquid crystal is first produced. The liquid crystal droplets are then formed by the separation of the two phases. After De Gennes [14] thought, in 1985 Doane et al. reported that phase separation methods could be used to create films with electrically controllable scattering [18, 19]. The phase separation can take place in one of the following three ways.

1.4.1.1 Polymerization induced phase separation (PIPS)

Polymerization induced phase separation (PIPS) occur when a liquid crystal is mixed with a solution that has not undergone polymerization (a pre-polymer). This technique is useful when, pre-polymer materials are miscible with the low molecular weight liquid crystal compounds [22, 23, 25 and 51]. Once a homogenous solution is formed, the polymerization

reaction is initiated either thermally (thermoset polymer) or optically (photo-curable polymer). As the reaction progresses, the liquid crystal molecules come out of solution and begin to form micro droplets. The droplets grow until the polymer binder becomes solid enough that the molecules are trapped and can no longer move easily. The two main factors that influence the size of liquid crystal droplets in PIPS method are the cure temperature and the type and proportions of materials used. The cure rate affects the speed of polymerization as well as the diffusion rate and solubility of the liquid crystal in the polymer. These factors can greatly influence the size of the liquid crystal droplets, which translates into different macroscopic optical properties.

1.4.1.2 Thermally induced phase separation (TIPS)

Thermally induced phase separation (TIPS) can be used when the polymer binder has a melting temperature below its decomposition temperature. In this method, a homogenous mixture of liquid crystal and a melted polymer is formed. The solution is cooled at a specific rate to induce the phase separation. Liquid crystal droplets begin to from as the polymer hardens. The droplet continues to grow until the glass transition temperature of the polymer is crossed. In this method, droplet morphology and droplet size is affected the most by the cooling rate of polymer melt/liquid crystal solution. Fast cooling rates tend to produce small droplets because there is not sufficient time for large particles to form. Therefore, droplet size and cooling rate are relatively inverse to each other. In general, larger concentrations of liquid crystals are required for these films as compared to PIPS.

1.4.1.3 Solvent induced phase separation (SIPS)

Solvent induced phase separation (SIPS) is useful with thermoplastics, which melt above the decomposition temperature of the thermoplastic or the liquid crystal, or where solvent coating techniques are used. The liquid crystal and polymer are dissolved in a common solvent, forming a homogenous solution. The solvent is then removed by evaporation, resulting in phase separation and polymer solidification. The LC droplets come out of solution and start growing until all the solvent removed from the solution. In this case droplet size is dependent on the rate of solvent removal. This combination of the solvent evaporation process followed by thermal annealing adds flexibility and ease to the production of commercial PDLC films.

1.4.2 Encapsulation

Early attempts to produce PDLCs were made with a technique known as micro encapsulation. Micro encapsulation is a technique that has been applied to obtain small capsules of drug release of food products and even of cholesteric liquid crystals in temperature indicating devices. In this method, a liquid crystal is mixed with a water soluble polymer. When the water is evaporated, the liquid crystal is surrounded by a layer of polymers. Thousands of these tiny capsules are produced and distributed through the bulk polymer. Droplets with this method tend to be non-uniform in size and can even be interconnected with each other. Materials manufactured by encapsulation are referred to as 'nematic curvilinear aligned phase' (NCAP) [20, 21].

1.5 Droplet pattern in DPDLC

Ordering in nematic liquid crystals (LCs) has been subject of intensive research for now many years [52]. The main configuration has been the focus of dichroic polymer dispersed liquid crystal (DPDLC). The birefringent spherical droplets of liquid crystal are included in a polymer matrix and contain defects that can be switched between several configurations [53, 54]. The type of defect, generally, depends on the size and shape of the droplets. Droplet shape is important because it can cause LC organizational changes and plays a significant role in governing LC reorientation dynamics [55, 56]. The switching characteristics of PDLCs can be modified mainly through changes in the surface anchoring energy and the inter-molecular interactions [57-59]. The complex variety of behaviors [60] that surface anchoring or boundary conditions impose on the liquid crystals is not only evident in individual PDLC spheres or hexagonal droplets [61], but also in large, cylindrical, polymer cavities [62] and infiltrated opals [63]. In practical devices, droplets having diameters of about 1 μm and a narrow size distribution work best [64, 65]. PDLC film optical properties are often modeled based on the assumption of spheroidal or ellipsoidal droplets of a specific size. We have been tried to better understand the droplet shape classes, size and LC organizations with optical microscopy. In Chapter 3 we will show a series of images that depict some of the different types of droplets that have been observed. The optical microscopic images depict of the expected spheroidal or ellipsoidal droplets for the nematic E7-NOA65-dichroic dye system.

The LC in these droplets is organized in the bipolar configuration. Topographic and optical images of radial and collapsed or toroidal droplets can also be seen [66, 67].

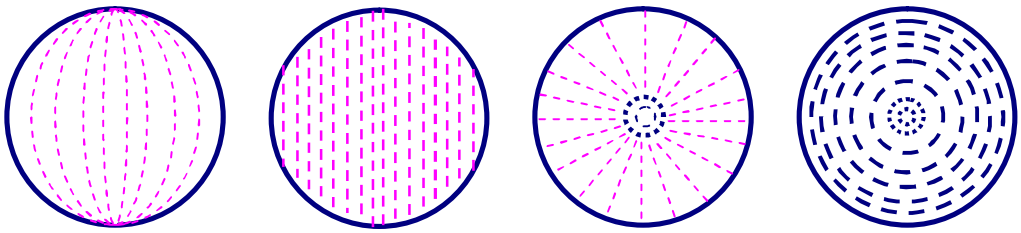

Fig. 1.12 Liquid crystal droplet organization in polymer matrix (a) bipolar (b) axial (c) radial and (d) toroidal droplet

It is also seen that LC droplets distributed in DPDLC films containing azo orange dye forming spheroidal like bipolar droplet configuration in a continuous matrix phase, even when a relatively large amount of dye concentration was introduced. The bipolar configuration is obtained when the elongated molecules of the nematic liquid crystal are anchored tangentially to the droplet wall. This structure is characterized by the presence of two point defects at the poles of the droplet and this model has shown in the fig. 1.12 (a). These point defects in bipolar configuration are classified as 'boojums' [68]. Boojums can exist only at the surface and cannot move into the volume of the droplet. The radial configuration occurs when the liquid crystal molecules are anchored with their long axes perpendicular to the droplet walls. If the anchoring strength is strong or droplet is larger enough, then radial structure is stable. The radial structure possesses a splay-type deformation with a point volume defect at the center topologically classified as 'hedgehog' [69]. The axial configuration of the liquid crystal droplets also occurs when the molecules are oriented perpendicular to the droplet wall [70]. Axial configuration is most stable when surface anchoring is weak and droplet size is sufficiently small or if there is an applied electric field E of suitable strength. This configuration creates a line defect that runs around the equator of the spherical droplet, as shown in fig. 1.12 (b). When an electric field is applied to a radial droplet, the molecules adopt the axial configuration. The radial configuration is returned when the field is removed. Although not yet proven, the appearance of the toroidal droplets likely results from competition between surface energy effects, which tend to yield spheroidal droplets and LC

organizational energy, which favors droplets having no organizational defects (i.e., as occur at the poles of bipolar droplets).

1.6 PDLC with nano-scale morphology

The optical characteristics of the PDLC film are dependent on the details of the polymer structure and thus the nature and rate of polymerization mechanism. Understanding and controlling the polymerization mechanism are especially important for holographic curing of PDLC films (H-PDLC), in which a spatial variation of light intensity results in a patterned LC droplet distribution [71, 72]. Recent HPDLC developments by Bunning group [73, 74] using a free-radical polymerization of highly functional monomers have demonstrated the ability to sequester nanoscale LC domains (<100 nm), thereby eliminating scattering problems associated with larger two-phase structures that result from step-growth polymerizations. For free-radical reactions, a high molecular weight polymer is formed almost instantaneously, while for a step-growth reaction, the molecular weight increases slowly with time. Small-angle X-ray scattering and high-resolution scanning electron microscopy (SAXS/HRSEM) were utilized to examine the nano- (1-100 nm) and meso- (100-1000 nm) scale morphology of PDLC films of varying liquid crystal (LC) concentration. In contrast to the conventional PDLCs derived from photo initiated step-growth polymerizations, these PDLC films were formed using photo irradiation of initially homogeneous syrup comprised of highly functional free-radical monomer and liquid crystal, resulting in rapid molecular weight increase and network formation prior to or in conjunction with phase separation. Two-phase morphology observable with HRSEM was absent below 20% LC, although fine, small modulation features existed on the fracture surface. In contrast, SAXS reveals increasing nanoscale heterogeneity with increasing LC content. Fig. 1.13 is the schematic representation of common liquid crystal and polymer dispersion (LCPD) morphologies.

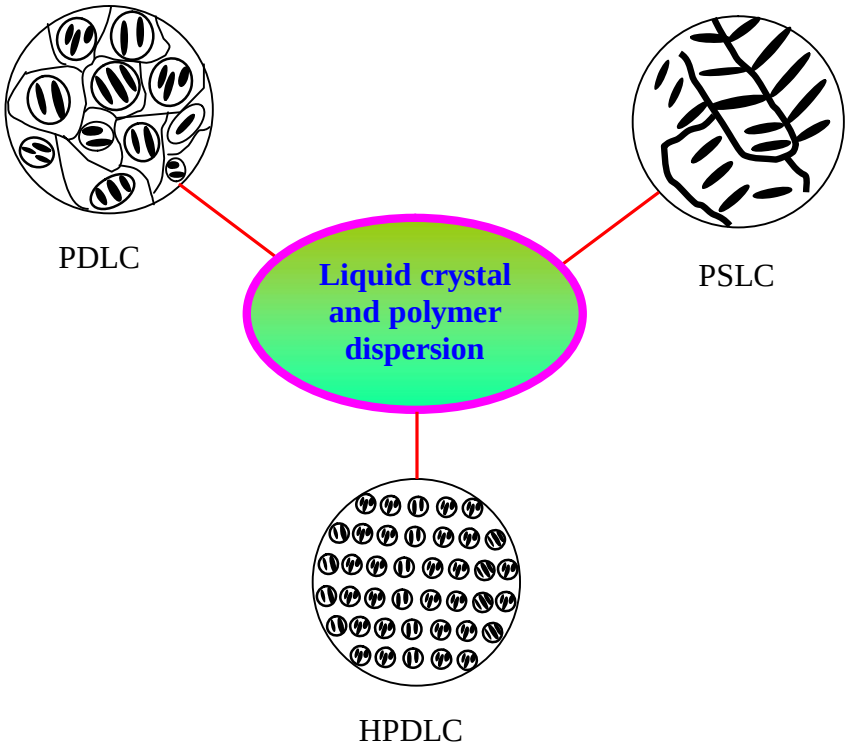

Fig.1.13 Schematic representation of common liquid crystal and polymer dispersion (LCPD) morphologies

1.7 Surface-stabilized polymer dispersed ferroelectric liquid crystal (SSPFLC)

Surface stabilized polymer dispersed ferroelectric liquid crystal (SSPFLC) is prepared by mixing a small amount of polymer (≤ 3 wt %) with the ferroelectric liquid crystal (FLC) materials. The SSFLC device was prepared by injected the mixture between ITO coated rubbed glass substrates. Sakaigawa et al. [75] have investigated the combination of the FLC material and the polymer which provides the stripe domain distribution. The most important feature is the phase separation of dispersed polymer from FLC mixture in the nematic phase and following realignment process at the smectic phase. Thus, the micro scale phase separated polymer aligns along the smectic layer. When the polymer is separated randomly from the nematic phase, it will be aligned along the smectic layer in the smectic phase, by cooling from the nematic phase.

1.8 Polymer network-stabilized ferroelectric liquid crystal (PNSFLC)

Polymer network-stabilized ferroelectric liquid crystals with homogeneous alignment have been produced [50, 51, 76-86] in cells without a surface alignment layer. In this technique, a crosslinkable monomer was mixed into a ferroelectric liquid crystal and polymerized in a magnetic field to form a polymer network that will stabilize the alignment of the ferroelectric liquid crystal. The concentration of the monomer lower than 10 wt% is an important factor in achieving alignment of the ferroelectric liquid crystal. Both the morphology of the final composite layer and the molecular alignment of the host FLC are affected by the curing temperature at which the UV curing of the sample is started.

1.9 Shear aligned polymer dispersed ferroelectric liquid crystal (SAPDFLC)

Molsen and Kitzerow [87] and Leader et al. [88] have shown that thicker than in the case of SSFLC devices can be fabricated using PDFLCs. The essential uniform alignment of the liquid crystal molecules is achieved by shearing the material during the phase separation that occurs between the liquid crystal and the polymer during photo induced cross-linking. In such a shear aligned PDFLC there are no restrictions in principle on the thickness of the device. The size of the droplets and the quality of the alignment of the smectic layers are determined to a large extent by the relative rates of shearing, phase separation and polymerization of the matrix. Coles et al. [89] applied the rate of shearing for the production of the devices of the order of 100 μm/s, far higher then authors previously reported [87, 88]. For this reason they have called the device a fast sheared PDFLC (FS-PDFLC). The starting mix for the fabrication of the FSPDFLC was a one phase solution of one of the low molar mass ferroelectric organosiloxane liquid crystals in a UV-curable optical adhesive (NOA-65, Norland, Inc.). The solution does not spontaneously phase separate at room temperature. The phase separation was induced by control photo polymerization.

1.10 Dichroic polymer dispersed liquid crystal (DPDLC)

In recent years, dichroic polymer dispersed liquid crystals (DPDLCs) have attracted significant interest among various research groups due to its technological applications. The role of dyes in these systems is to allow increase the light absorption thus reducing remarkably the power necessary to induce nonlinear optical effects. Dichroic liquid crystal displays (DLCDs) do not require any polarizer; therefore, they exhibit a high brightness and wide viewing angle [20, 21]. Contrast ratio can improve with suitable dichroic dye concentration.

Very recently, PDLC [71-74, 90-92] and polymer stabilized LC (PSLC) [93, 94] have been widely studied and applied intensively in the field of display devices due to such advantages as their polarizer free and alignment layer free nature, fast response times, simple preparation, etc. however, because of their low contrast ratio and broad switching behaviour, the use of PDLCs for display devices is limited and many studies have been carried out to overcome the problems. Generally, to improve the contrast ratio, use of dichroic dye-doped liquid crystal was proposed [94-96]. As a result, investigation of this phenomenon has been focused on the manufacture of photo-controllable devices which have a high contrast ratio [97-100]. When a dichroic dye with a geometric anisotropy is dissolved in a nematic liquid crystal, the dye molecules tends to arrange itself in such a way that its long molecular axis aligns along the liquid crystal director and a change of colour intensity is obtained by controlling the direction of the liquid crystal molecules. A rod like, long molecular structure is favorable for a strongly dichroic dye. In particular, absorption spectra and dichroic ratios in liquid crystals are the dominant properties with regard to the performances of displays. Since each dye has plural properties that have important effects on performances of displays exchanging dyes means that the plural variables are changed simultaneously.

It is also known that a change in the transmittance of a PDLC can take place by the photochromic reaction of photochromic molecules such as azobenzene derivatives [98-101]. The configuration of azo-benzene derivatives can be transformed reversibly through the process of photoisomerization. Cis-azobenzene is formed using UV light around 366 nm, and transformed into the trans-azobenzene by visible light around 433 nm. When azobenzene derivatives exist in the LC, they affect the LC phase significantly. Cis-azobenzene destablise

the LC phase but, on the contrary, trans-azobenzene is aligned with the LC molecules and enhances the LC phase. This means that the meso phase of an azobenzene-doped LC can be controlled by light irradiation.

It has been demonstrated that a small amount of a dye dissolved in LC (nematic) make it light absorbing can enhance the orientational optical nonlinearity of the material [101]. The explanation proposed by Janossy [102] is connected with the electronically excited metastable states appearing in the molecules of absorbing dye. The interaction of the excited dye molecule with the LC molecules is different from the one of the dye molecule in the ground state. The Janossy model is suitable for the re-orientational bulk effect. A surface driven reorientation effect as a result of the light action on the bulk of a light-sensitive NLC-azo dye mixture was reported by Voloschenko and co-workers. The explanation was the adsorption of dye photo-transformed molecules onto the aligning photopolymer surface [103]. Simoni and co-workers have pointed that the observed huge re-orientational effect in a LC-dye mixture is due to light-induced modifications on the surface-induced nonlinear effect [104]. Their investigations about the diffraction efficiency reveal the basic role of light-induced adsorption and desorption of the dye molecules onto the boundary surfaces [105-107].

1.10.1 Dichroic polymer dispersed liquid crystal (DPDLC) absorbance

Dichroic PDLC displays can possess contrast ratios similar to the best optics obtainable by phase change display [22]. Since PDLC films possess strong scattering properties, it is necessary to correct for film scattering when estimating the dichroic response of the films. It is possible that the absorbance properties of the PDLC films may be complicated by the scattering properties of these films. Film scattering may increase the path length of light passing through the film, and lead to an increased absorbance in the powered state. However the measured absorbance values for the dichroic response of PDLC films do not appear to depend strongly on film scattering [108].

The absorbance β of a dichroic dye contained in a PDLC film is the sum of the absorbance of the dichroic dye dissolved in the polymer binder and nematic droplets and is given by the expression:

$$\beta = \beta_{droplet} + \beta_{binder} \quad (1.3)$$

For the simple alignment described here, the dichroic absorbance of these PDLC films at zero field (β_{OFF}) and high field (β_{ON}) should follow the Beer-Lambert law, given by

$$\beta_{OFF} = -\varepsilon_{OFF} cd \quad (1.4)$$

$$\beta_{ON} = -\varepsilon_{ON} cd \quad (1.5)$$

Where ε_{OFF} and ε_{ON} is the dye extinction coefficient, c is the dye concentration and d is the thickness of the film.

The linear relationship between absorbance and the path length at a fixed concentration of absorbing substance is generalized by Beer's Law [109]

$$\beta = \varepsilon cl \quad (1.6)$$

Where ε is the dye extinction coefficient, c is the dye concentration and l is the path length of light. Because of the anisotropy of the dye molecules dissolved in the liquid crystal droplet, the extinction coefficient is defined for various orientations of the nematic director where $\varepsilon_{\perp}$ is the extinction coefficient measured perpendicular to the nematic director, $\varepsilon_{\parallel}$ is the extinction coefficient measured parallel to the nematic director, and ε_i is the isotropic extinction coefficient. The isotropic extinction coefficient can be defined as a weighted average over the parallel and perpendicular components given by the following relation

$$\varepsilon_i = \frac{2\varepsilon_{\perp} + \varepsilon_{\parallel}}{3} \quad (1.7)$$

The measured dichroic ratio, R, of the dissolved dye in the liquid crystal is defined as

$$R = \frac{\varepsilon_{\perp}}{\varepsilon_{\parallel}} \quad (1.8)$$

In the OFF state, the symmetry axes of the bipolar droplets vary randomly from droplet to droplet and the average extinction coefficient of a collection of droplets is ε_i. The path length in the OFF state can be defined by the relation

$$l = ad \quad (1.9)$$

Where d is the thickness of the PDLC film and a defined as the scattering efficiency. The absorption in the OFF state can then be expressed as

$$\beta_{OFF} = \varepsilon_i Xcad + \varepsilon_i (1-X)cad \quad (1.10)$$

Where X is the fraction of dye in the nematic droplet and 1 - X is the fraction of dye dissolved in the polymer binder after the phase separation process. We assume the extinction coefficient of the dye is the same in a liquid crystal and polymer solvent. Equation (1.6) simplifies to

$$\beta_{OFF} = \varepsilon_i Xcad \tag{1.11}$$

Equation (1.9) allows the scattering efficiency to be determined from the measured β_{OFF}. In the ON state, the droplet directors are aligned perpendicular to the surface of the film, and therefore the dye in the droplet has the perpendicular extinction coefficient and the dye in the binder has the isotropic extinction coefficient. In the ON state, the path length is just the thickness of the film. The absorption in the ON state is thus given by the following expression:

$$\beta_{ON} = \varepsilon_\perp Xcd + \varepsilon_i (1-X)cd \tag{1.12}$$

The fraction of dye in the droplet X can be calculate from eq. (1.12) using the measured on state absorbance and the measured extinction coefficients of the dichroic dye.

1.10.2 Dichroic PDLC devices

Reduction in the operating voltage of PDLC devices is an important goal for compatibility with high-performance drive electronics. Drzaic [108] demonstrated dichroic PDLC materials with 1 V/μm reorientation field. We have studied dichroic PDLC with ~1.1 V/μm reorientation field, (10μm cell thickness) with anthraquinone and azo dye, in our laboratory. The low voltage material is suitable for use in active matrix display applications. The requirements for dyes in active matrix displays are somewhat different, as it is important that the liquid crystal system maintains high impedance over time. If the photoproducts of dyes are ionic in nature the impedance of the system drops and contrast in active matrix applications suffers. Dichroic PDLC systems with sufficiently good charge holding and stability for several years of operation in active matrix devices have been developed [110]. Currently, dichroic PDLC films can be found in many control panel applications for office equipment and appliances. The ability to make large area displays with plastic substrates allows for designs where touch switches are incorporated behind the pixels in the PDLC display. Thus,

the user actually pushes through the display pixel to access the switch, which can be used to control both device and display functions. There is still much space for improvement for dichroic PDLC materials. In particular, more stable dyes are of great interest.

1.10.3 Photostability of dyes in DPDLC films

The stability of dichroic dyes is an important factor in applications of DPDLC devices. Dichroic dyes for liquid crystals tend to be of the azo or anthraquinone types [111]. Decomposition of these dyes has been found to follow [112] a standard rate law for unimolecular photo-processes in a well-stirred medium [113].

$$\text{Log}\,(10^{\beta(t)} - 1) = -RIt + \text{Log}\,(10^{\beta(t)} - 1) \qquad (1.13)$$

Where $\beta(t)$ is the absorbance at time t, β is the initial absorbance, I is the light intensity, and R is a rate constant which includes contributions from the quantum yield, extinction coefficient, and path length. Typically, dichroic dye fading is tested using dyes placed in glass cells, often with degassing of the solution before filling. However, PDLC devices are often used and tested on plastic substrates. Plastic substrates allow for diffusion of oxygen into the system, whereas glass substrates do not. Thus, dye photoreactions in glass cells takes place under anaerobic conditions, while photoreactions in plastic cells usually take place under aerobic conditions. It was found that, in many cases the stability of dichroic dyes can differ significantly under aerobic and anaerobic conditions [108].

1.11 Aim of the present research work

The field of liquid crystal is quite abundant in itself and the documentation and understanding of the physical phenomena found in liquid crystal have attracted the attention of researchers for several decades [1-3] and now they have been involved for the development of composite system including liquid crystal, polymer and dichroic dyes for fabricating many potential devices, e.g. displays, light control devices. The role of dyes in these systems is to allow increase the light absorption thus reducing remarkably the power necessary to induce nonlinear optical effects. As a consequence, we noticed that there were still some unanswered questions and few gaps in understanding the nature of droplet morphology and process of phase separation in these systems under the influence of electric filed, temperature and

different concentrations dichroic dyes. The preparation of a dichroic polymer dispersed liquid crystal (DPDLC) requires a preliminary knowledge of each used material constituting the sample i.e. liquid crystal, dye and polymer matrix. Thus an attempt was made to consider the appropriate combination of liquid crystal, polymer and dichroic dye material which would enhance the optical transmission, contrast ratio, homogeneity in droplet morphology and their electro-optic characteristics. For this purpose, anthraquinone blue and azo orange dichroic dyes with low molar mass nematic and ferroelectric liquid crystal mixtures were dispersed in the polymer matrix (NOA 65) to study their behaviour in detail.

The apparent understanding and scientific curiosity to investigate the properties of DPDLC devices, with minimum threshold and maximum contrast was the main incentive to carry out this experimental work.

References

[1]. P. J. Collings, Liquid Crystals: Nature's Delicate Phase of Matter, Pricenton University Press (1990).

[2]. P. J. Collings and M. Hird, Introduction to Liquid Crystals: Chemistry and Physics, Tayler and Francis Ltd, (1997).

[3]. P. G. De Gennes, The Physics of Liquid Crystal, Oxford University Press (1975).

[4]. S. Chandrasekhar, Liquid Crystal 2nd Edn, Cambridge University Press (1992).

[5]. C. B. McArdle, Side Chain Liquid Crystal Polymers, Champan and Hall: New York (1989).

[6]. A. Ciferri, W. R. Kribaum and R. B. Mayer, Polymer Liquid crystals, Academic Press: New York (1979).

[7]. E. B. Priestley, P. J. Wojtowicz and P. Sheng, Introduction to Liquid Crystal, Plenum Press, New York (1979).

[8]. A. C. Griffin and J. F. Johnson, Liquid Crystals and ordered fluids, **4** (1984)763.

[9]. C. Kittel, Introduction to Solid State Physics, John Wiley and Sons, New York, (1996).

[10] P. G. De Gennes and J. Prost, The Physics of Liquid Crystals, 2nd edition, oxford, Clarendon Press 1973, 282.

[11] A. De Vries and D. L. Fishel, Molecular Crystal Liquid Crystal, **16** (1972) 311.

[12]. Cifferi, W. R. Krigbaum and R. B. Meyer, Polymer Liquid Crystals, Academic Press: Network (1982).

[13] C. B. Mcardle, Side Chain Liquid Crystal Polymer, Champan and Hall: Newyork (1989).

[14] P. G. de Gennes, Scaling Concepts in Polymer Science, Cornell University Press, Ithaca, Chapter 5 p.131 (1979).

[15] J. L. Fergason, Encapsulated liquid crystal and method. US Patent **4**, 435 (1984) 047.

[16] J. L. Fergason, Polymer encapsulated liquid crystals for display and light control applications. Tech Digest SID Int Symp, **16** (1985) 68.

[17] P. S. Drzaic, Liquid crystal dispersion. Series on liquid crystals, Singapore: World Scientific, (1995).

[18] J. W. Doane, N. A. Vaz, B. G. Wu and S. Zumer, Appl. Phys. Lett. **48** (1986) 269.

[19] J. W. Doane, G. Chidichim and N. A. Vaz, US Patent **4**, 688, (1987) 900.

[20] B. Bahadur, Liquid Crystals Applications and Uses, World Scientific: Singapore, Vol. **3**, Ch. 11 (1992).

[21] S. T. Wu and D. K. Yang, Reflective Liquid Crystal Displays, Wiley: New York, Ch. 6 (2001).

[22] H. S. Cole and R. A. Kashnow, Appl. Phys. Lett. **30** (1977) 619.

[23] D. L. White and G. N. Taylor, J. Appl. Phys. **45** (1974) 4718.

[24] T. Uchida, H. Seki, C. Shishido and M. Wada, Proc. SID, **22** (1981) 41.

[25] R. Stannarius, G .P. Crawford, L. C. Chien and J. W.Doane, J. Appl. Phys. **70** (1991) 135.

[26] R. A. M. Hikmet, Mol. Cryst. Liq. Cryst. **213** (1991) 117.

[27] D. K. Yang, L. C. Chien and J. W. Doane, Appl. Phys. Lett. **60** (1992) 3102.

[28] H. S. Kitzerow, Liq. Cryst. **16** (1994) 1.

[29] J. W. Doane, A. Golemme, J. L. West, J. B. Jr. Whitehead and B.G. Wu., Mol. Cryst. Liq. Cryst. **165** (1988) 511.

[30] J. R. Kelly and P. Palffy-Muhoray, Mol. Cryst. Liq. Cryst. **243** (1994) 11.

[31] S. Zumer, A. Golemme and J. W. Doane, J. Opt. Soc. Am. **6** (1989) 403.

[32] G. W. Smith and N. A..Vaz, Mol. Cryst. Liq. Cryst. Sci. Technol. A **237** (1993) 243.

[33] B. G. Wu, J. H. Erdmann and J. W. Doane, Liq. Cryst, **5** (1989) 1453.

[34] A. Y. G. Fuh, M. S. Tsai, C. R. Lee and Y. H. Fan, Phys. Rev. E **62** (2000) 3702.

[35] M. Macchione, D. Cupelli, G. De Filpo, F. P. Nicoletta and G. Chidichimo, Liq. Cryst. **27** (2000) 1337.

[36] C. H. Choi, B.K. Kim and T. Kajiyama, Mol. Cryst. Liq. Cryst. **247** (1994) 303.

[37] H. Kikuchi, F. Usui and T. Kajiyama, Polym. J. **28** (1996) 35.

[38] R. Yamaguchi, N. Sudo and S. Sato, Mol. Cryst. Liq. Cryst. **262** (1995)119.

[39] J. B. Jr. Whitehead and G. P Crawford, Mol. Cryst. Liq. Cryst. **262** (1995) 25.

[40] B. K. Kim, Y. S. Ok and C. H. Choi, J. Polym. Sci. B: Polym. Phys. **33** (1995) 707.

[41] J. L. West, Mol. Cryst. Liq. Cryst. **157**(1988) 427.

[42] J. W. Doane and B. Bahadur, editor. Liquid crystal application and used, Vol.**1**. Singapore: World Scientific; 1990, chapter 14.

[43] J. L. West, Polymer dispersed liquid crystal displays. In: Weiss RA, Ober CK, editors. Liquid crystal polymers. ACS symposium series, **435** (1990) 475.

[44] L. Bouteiller and P. L. Barny, Liq. Cryst. **21** (1996) 157.

[45] G. P. Crawford and S. Zumer, edited liquid crystals in complex geometries, Taylor & Francis, London, (1996).

[46] I. Dierking, L. L. Kosbar, A. Afzali-Ardakani, A. C. Lowe and G. A. Held, Appl. Phys. Lett. **71** (1997) 2454.

[47] R. A. M. Hikmet and H. Kemperman, Nature (London), **392** (1998) 476.

[48] K. Amundson, A.Van Blaaderen and P. Wiltzius, Phys. Rev. E **55** (1997) 1646.

[49] T. J. Bunning, L. V. Natarajan, V. P. Tondiglia and R. L. Sutherland, Annu. Rev. Mater. Sci. **30** (2000) 83.

[50] Y. Kim, J. Francl, B. Taheri and J. L. West, Appl. Phys. Lett. **72** (1998) 2253.

[51] A. M. Lapena, S. C. Glotzer, S. A. Langer and A. J. Liu, Phys. Rev. E **60** (1999) 29.

[52] G. P. Crawford and S. Zumer, eds. (Taylor & Francis, London, 1996).

[53] J. H. Erdmann, S. Zumer and J. W. Doane, Phys. Rev. Lett. **64** 1907 (1990).

[54] V. Yu Reshetnyak, T. J. Sluckin and S. J. Cox, J. Phys. D: Appl. Phys. **30** (1997) 3253.

[55] P. S. Drzaic, Liq. Cryst. **3** (1988) 1543.

[56] B. G. Wu, J. H. Erdmann and J. W.Doane, Liq. Cryst. **5** (1989) 1453.

[57] W. Y. Li and S. H. Chen, Jap. J. Appl Phys. **138**, 1482 (1999).

[58] M. Abbate, P. Mormile, E. Martuscelli, P. Musto, L. Petti, G. Ragosta and P. Villano, J. Mat. Sci. **35** (2000) 999.

[59] S. C. Sharma, L. Zhang, A. J. Tapiawala and P. C. Jain, Phys. Rev. Lett. **87** (2001) 105501 (4).

[60] O. Lavrentovich, Liq. Crys. **24** (1998) 117.

[61] A. Fernandez-Nieves, D. R. Link, D. Rudhardt and D. A.Weitz, Phys. Rev. Lett. **92** (2004) 105503 (4).

[62] T. Yamaguchi, Y. Kawata and Y. Mori, Appl. Phys. Lett. **72** (1998) 1170.

[63] P. Mach, P. Wiltzius, M. Megens, D. A. Weitz, K. H. Lin, T. C. Lubensky and A. G. Yodhi, Phys. Rev. E **65** (2002) 031720(3).

[64] G. P. Montgomery, J. L West, Tamura-Lis and W. Light, J. Appl. Phys. **69** (1991) 1605.

[65] P. S. Drzaic, Mol. Cryst. Liq. Cryst. Sci. Technol. Sect.A, **261** (1995) 383.

[66] E. Mei and D. A. Higgins and Langmuir, **14** (1998) 1945.

[67] G. H. Springer and D. A.Higgins, J. Am. Chem. Soc. **122** (2000) 6801.

[68] J. W. Doane, MRS Bulletion, **16** (1991) 22.

[69] G. E. Volovik and O. D. Laurentovich, Zh. Eksp. Teor. Fiz **85** (1983) 1997 [Sov. Phys. JETP, **58** (1983) 1159].

[70] J. H. Erdmann, S. Zumer and J. W. Doane, Phys. Rev. Lett. **64** (1990) 1907.

[71] K. Tanaka, K. Kato, S. Tsuru and S. Sakai, J. Soc. Inform. Display, **2** (1994) 37.

[72] R. L. Sutherland, V.P. Tondiglia, L.V. Natarajan, T. J. Bunning and W.W. Adams, Chem. Mater. **5** (1993) 1533.

[73] R. T. Pogue, R. L. Sutherland, M. G. Schmitt, L. V. Natarajan, S. A. Siwecki, V. P. Tondiglia and T. J Bunning, Appl. Spectrosc. **54** (2000) 1.

[74] R. A. Vaia, D. W. Tomlin, M. D. Schulte and T. J Bunning, Polymer, **42** (2001) 1055.

[75] A. Sakaigawa, T. Sako and M. Koden., Mol. Cryst. Liq. Cryst. **328** (1999) 201.

[76] V. Vorflusev and S. Kumar, Science, **283** (1999) 1903.

[77] J. B. Nephew, T. C. Nihei and S. A. Carter, Phys. Rev. Lett. **80** (1998) 3276.

[78] J. C. Loudet, P. Barois and P. Poulin, Nature (London), **407** (2000) 611.

[79] G. A. Held, L. L. Kosbar, I. Dierking, A. C. Lowe, G. Grinstein, V. Lee and R. D. Miller, Phys. Rev. Lett. **79** (1997) 3443.

[80] D. Voloschenko and O. D. Lavrentovich, J. Appl. Phys. **86** (1999) 4843.

[81] S. W. Kang, S. Sprunt and L. C. Chien, Appl. Phys. Lett. **76** (2000) 3516.

[82] N. A. Vaz, G. W. Smith and Jr. G. P. Montgomery, Mol. Cryst. Liq. Cryst. **146** (1987) 17.

[83] J. L. Fergason, SID Digest, **16** (1985) 68.

[84] H. G. Craighead, J. Cheng and S. Hackwood, Appl. Phys. Lett. **40** (1982) 22.

[85] H. Liu, H.Duig and J. R.Kelly, Mol.Cryst.Liq. Cryst. **26** (1995) 99.

[86] J. W. Hax, T. J. Kaxg and G. Park, J. Korean Phys. Soc. **36** (2000) 156.

[87] H. Molsen and H. S. Kitzerow, J Appl Phys. **75** (1994) 710.

[88] C. M. Leader, W. Zheng, J. Tipping and H. J. Coles, Liq. Cryst. **19** (1995) 415.

[89] M. J. Coles, C. Carboni and H. J. Coles, Liq Cryst. **26** (1999) 679.

[90] A. Miyamoto, H. Kikuchi, S. Kobayashi, Y. Morimura and T. Kajiyama, Macromolecules, **24** (1991) 3915.

[91] E. Grosicka and M. Mucha, Mol. Cryst. Liq. Cryst., **353** (2000) 417.

[92] L. Petti, P. Mormile and W. J. Blau. Mol. Cryst. Liq. Cryst. (2001) **359** 53.

[93] H. G. Craighead, J. Cheng, and S. Hackwood, Appl. Phys. Lett. **40** (1982) 22.

[94] N. Kawatsuki and H. Ono, J. appl. poly. Sci. **55** (1995) 911.

[95] E. Shimada and T. Uchida, Jpn. J. appl. Phys. **31** (1992) 352.

[96] J. W. Doane, A. Golemme, J. L.West, J. R. Whitehead and B. G. Wu, Mol. Cryst. liq. Cryst. **65** (1998) 511.

[97] S. Pane, M. Caporusso and H. Hakemi, Liq. Cryst. **23** (1997) 861.

[98] L. C. Chien, C. Lin, D. S. Fredley and J. W. McCargar, Macromolecules, **25** (1992) 133.

[99] C. V. Rajaram, S. D. Hudson and L. C. Chien, Chem. Mater. **7** (1995) 2300.

[100] C. V. Rajaram, S. D. Hudson and L. C. Chien, Chem. Mater. **8** (1996) 2451.

[101] I. Janossy, A. D. Lloyd and B. S. Wherrett, Mol. Cryst. Liq. Cryst. **179** (1990) 1.

[102] I. Janossy, Phys. Rev. E **49** (1994) 2957.

[103] F. Simoni, G. Cipparrone and C. Umeton, Appl. Phy. Lett. **57** (1990)1949.

[104] F. Simoni, G. Cipparrone, D. Duca and I. C. Khoo, Opt. Lett. **16** (1991) 360.

[105] P. S. Drzaic, R. Wiley and J. McCoy, Proc. SPIE, **1080** (1989) 41.

[106] S. Zumer, Phys. Rev. A **37** (1988) 4006.

[107] Jr. G. P. Montgomery, J. L. West and W. J. Tamura-Lis, Appl. Phys. **69** (1991) 89.

[108] P. S. Drzaic, Pure & Appl. Chem. **68** 7 (1996) 1435.

[109] A. Knowles and C Burgess, Practical Absorption Spectrometry (University Press, London, 1984).

[110] P. S. Drzaic, A. M. Gonzales, P. Jones and W. Montoya, SID**,** Digest, **571** (1992)**.**

[111] A. V. Ivashchenko, Dichroic dyes for liquid crystal displays., Boca Raton: CRC Press (1994).

[112] S. Aftergut and H. S. Cole, Mol. Cryst. Liq. Cryst. **188** (1990) 147.

[113] R. L. Jackson and D. G. Lishan, J. Phys. Chem. **88** (1984) 5986.

Chapter 2

Characterization of PDLC Sample and Techniques

Overview

This chapter presents the experimental techniques for preparation and characterization of study the various PDLC, DPDLC, DPDFLC samples and their physical parameters. The characteristics of the dyes and the liquid crystals that were used in the experiments, along with their molecular structures, selection of materials and description of instruments, are also provided. Optical textures studies have been performed with optical polarizing microscope under different condition of sample preparation and temperatures.

2.1 Introduction

In the past more than three decades, material scientists have been exploring novel materials for applications in various electro-optical control and display devices such as optical shutters, switchable privacy windows, and reflective color displays. Dichroic polymer dispersed liquid crystal(DPDLC) and polymer dispersed liquid crystal (PDLC) is a class of materials, normally prepared via polymerization-induced phase separation (PIPS) of an initially homogeneous solution of liquid crystal (LC), dichroic dye and prepolymer. Therefore the selection of materials plays an important role on the performance of PDLC devices. The selections of materials in the present study has been made on the basis of their physical properties e.g. refractive index, homogeneous mixing of polymer and liquid crystal, solubility of dyes in liquid crystals, their purity, resistivity, chemical and photo stability and the most important is the dye concentration in DPDLC devices. DPDLC films were made by photo polymerization-induced phase separation using UV-curable NOA polymer and nematic liquid crystal. Several factors, i.e. UV intensity, ratio of the concentrations of liquid crystal and polymer, concentration of dyes, chemical structure of monomers and the size of the spacer, were adjusted to obtain the film.

2.2 Materials

In the present work, the liquid crystal mixtures used in our experiments were commercially available nematic liquid crystal mixture (E7) [1], ferroelectric liquid crystal mixture ZLI-3654 (FLC-I) [2] and a synthesized ferroelectric liquid crystalline material (FLC-II) laterally substituted by the methyl group as shown in fig. 2.2. An optical adhesive UV curable polymer NOA-65 (Norland, NJ) [3] was used as matrix element in the preparation of DPDLC films. The dichroic dyes used in the experiments were anthraquinone and azo. The blue anthraquinone dichroic dye was obtained from Rollick, Switzerland where as disperse orange 3 azobenzene dichroic dye was obtained from Sigma Aldrich. The molecular structure of the nematic liquid crystal mixture E7, ferroelectric liquid crystals and dichroic dyes are shown in figs. 2.1-2.4. Transition temperatures in Celsius are also provided in the figures, where K, N, and I stand for crystalline phase, nematic phase and isotropic liquid phase, respectively. Some of the physical parameters for the liquid crystals and liquid crystal mixtures used in the experiments are listed in Tables 2.1 and 2.2. The physical properties NOA 65 polymer are shown in Table 2.3 whereas the physical properties of the dichroic dyes can be found in Table 2.4 and 2.5.

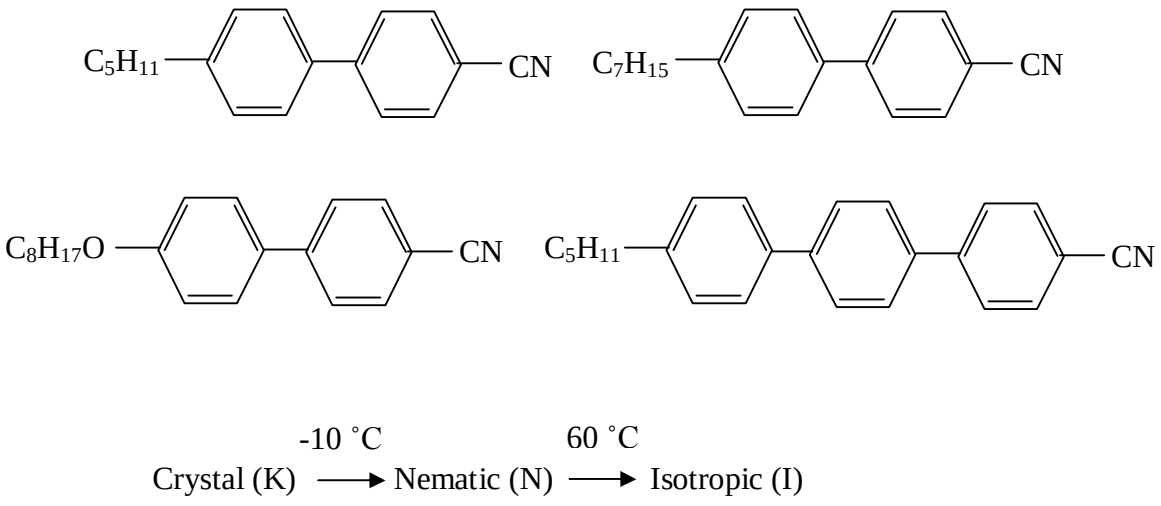

Fig 2.1 Molecular structure of the components and phase sequence of liquid crystal mixture E7 [4]

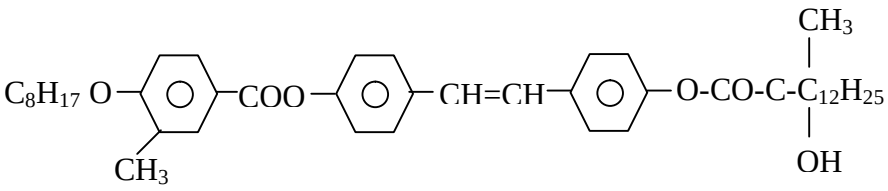

Fig 2.2 Molecular structure and phase sequence of the chiral ferroelectric smectic C* liquid crystal (FLC-II)

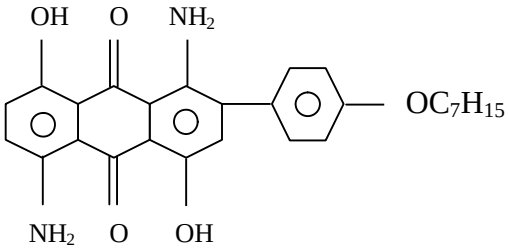

Fig.2.3 Molecular Structure of anthraquinone dye molecule

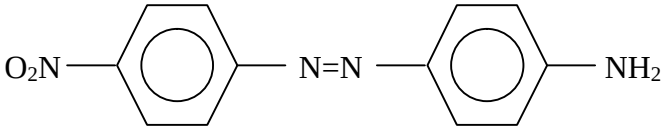

Fig.2.4 Molecular structure of disperse orange3 azo dye molecule

Table 2.1 Physical properties of nematic liquid crystal E7 used in the experiment

Materials	***Phase sequence***	***Refractive index***
Nematic liquid crystals E7	Crystal $\xrightarrow{-10\ ^{o}C}$ Nematic $\xrightarrow{60\ ^{o}C}$ Isotropic	$n_e = 1.7464$ $n_o = 1.5211$

Table 2.2 Physical properties of liquid crystal materials FLC-I and FLC-II used in the experiment

Materials	***Properties***	***Values***
Ferroelectric liquid crystal mixture FLC-I	Phase sequence	K-30 ^{0}C SmC*-62 ^{0}C SmA76 ^{0}C Ch 86 ^{0}C I
	Tilt angle at 20 ^{o}C	25 ^{o}
	Spontaneous Polarization (nC/cm^2)	-29
	Switching Time (μsec)	44
	Pitch (μm)	3
Ferroelectric smectic C* liquid crystal FLC-II	Phase sequence	Crystal $\xrightarrow{67\ ^o\text{C}}$ SmC* $\xrightarrow{121\ ^o\text{C}}$ N* $\xrightarrow{129\ ^o\text{C}}$ Isotropic
	Spontaneous Polarization (nC/cm^2) at d=5 μm sample, at 50 ˚C.	~ 200
	Switching Time (μsec), at 50 ˚C	~ 270
	Pitch (μm)	~ 1

Table 2.3 Physical properties of UV curable NOA 65 polymer used in the experiment

Physical Properties	***NOA- 65 Polymer***
Polymer Viscosity at 25^o C (CPS)	1000
Refractive index at cured polymer	1.52
Tensile (Psi)	1500
Modulus (Psi)	2000

Table 2.4 Physical properties of azobenzene dichroic dye used in the experiment

Properties	***Value***
Solubility	100%
Colour	Brown powder
λ_{max}	~ 440 nm
Melting point (˚C)	200
Molecular weight	242.24
Dye content	~ 90 %

Table 2.5 Physical properties of anthraquinone dichroic dye used in experiment

Properties	***Value***
Solubility	100%
Colour	Blue
λ_{max}	630 nm

2.3 Sample cells assembly

Dichroic polymer dispersed liquid crystal (DPDLC) and polymer dispersed liquid crystal (PDLC) sample cells were prepared using conducting indium tin oxide (ITO) coated glass substrates. These substrates were procured from Bharat Electronics Limited (BEL), Bangalore. Some commercial cells obtained from M/S Linkam Instruments, UK were also used in the experiment. These ITO coated glass substrates were highly transparent with resistivity of the order of few 140-180 ohm-m. The substrates were initially washed with soap solution, rinsed with acetone (purity 99.9%), distilled water and then dried in a vacuum chamber. These substrates were then put in dust free (laminar flow) chamber (fig. 2.5) to ensure proper cleaning conditions. For DPDLC devices there is no need of any surface treatment and polarizers to get the higher contrast and better optical properties [5-7]. The characterization with respect to transmission, contrast ratio, switching responses and

absorbance factor etc was carried out in homogenous (planar) cells. Out of the two basic forms of alignment for liquid crystalline compounds or mixtures i.e. the homeotropic and homogenous [8-12], we used homogenous alignment method. In this method constituents molecules of LC phase are oriented parallel to the supporting substrates. The conducting sides of these ITO coated glass substrates were joined together and separation between the substrates was maintained with the help of mylar spacer of different thickness such as 5 and 10 μm. These two glass plates were sealed with optical adhesive (UV curable polymer), and then cured the cell in presence of UV light. The electrodes were connected at the ITO coated substrate surface of the cell using indium (metal) ingot to obtaining better contact.

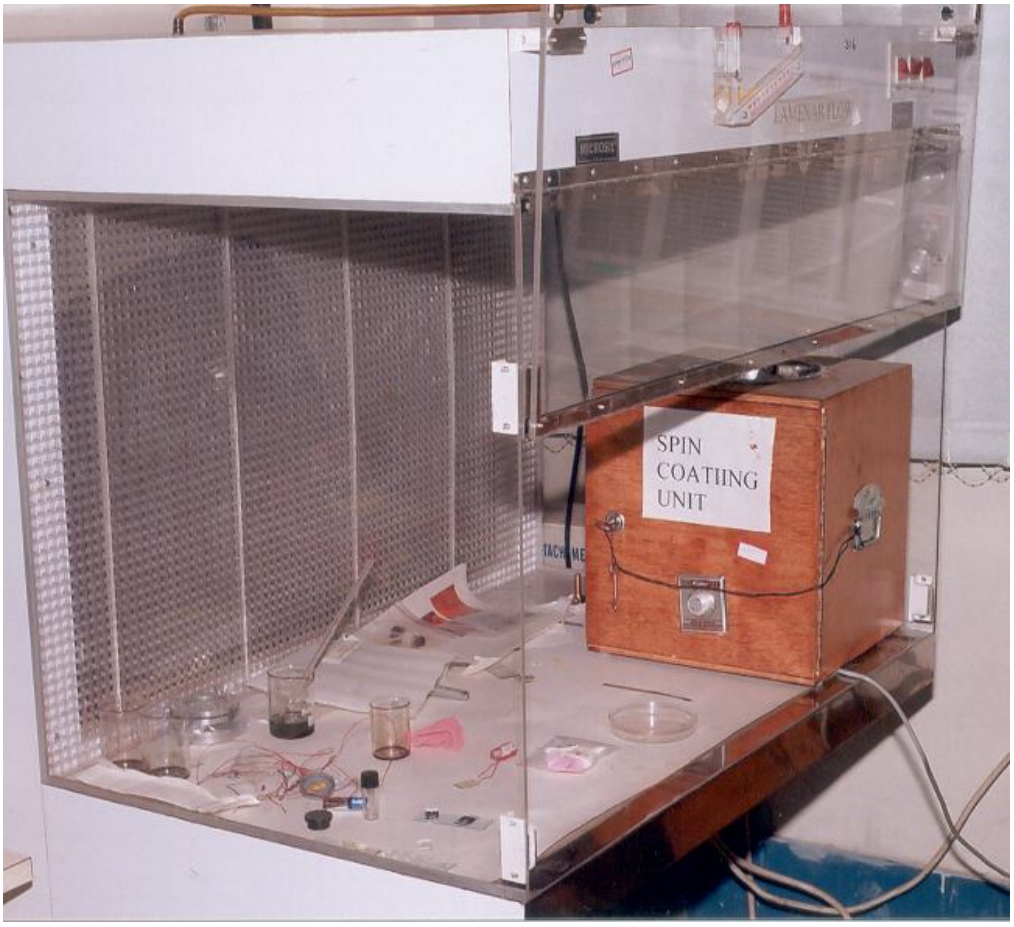

Fig. 2.5 Dust free (laminar flow) chamber for liquid crystal cell preparation

2.4 Preparation of dichroic polymer dispersed liquid crystal samples

In the preparing process of a PDLC sample, the index matching between the polymeric matrix and the LC is very important. In order to design an electrically-activated switch it is necessary to choose the refractive index of the polymer matrix n_p matching with the ordinary refractive index of the LC n_o so that the effective refractive index of the LC droplets n_{eff} is larger than n_o in the OFF state (the film is opaque) while $n_{eff} = n_o \approx n_p$ in the ON state (the film is transparent). Generally, the typical value of the effective refractive index n_{eff} is $n_o \leq n_{eff} \leq n_p$ for the PDLC samples.

In our work we used PIPS method with UV initiation for the preparation of the dichroic-dye-based PDLC films. In this technique, polymer and liquid crystal were mixed in equal or in different wt./wt. ratio in a vial. For the preparation of DPDLC samples, the dye molecules were dissolved in low concentration. First dye was doped with the liquid crystal and then dispersed in the polymer matrix in the wt./wt. ratio. In order to ensure proper mixing, this homogenous mixture was heated to isotropic temperature of the liquid crystal and simultaneously shaken in a vacuum chamber. The mixture was then filled in between indium tin oxide (ITO) coated glass substrates by capillary action. The sample cells were sealed by optical adhesive and then cured under UV light (intensity ~ 2 mW/cm^2) for about an hour at room temperature. An assembly of sample cells in unfilled and filled state is shown in fig.2.6 (a, b, c). The complete methodology of samples preparation is shown in fig. 2.7 in the form of flow chart.

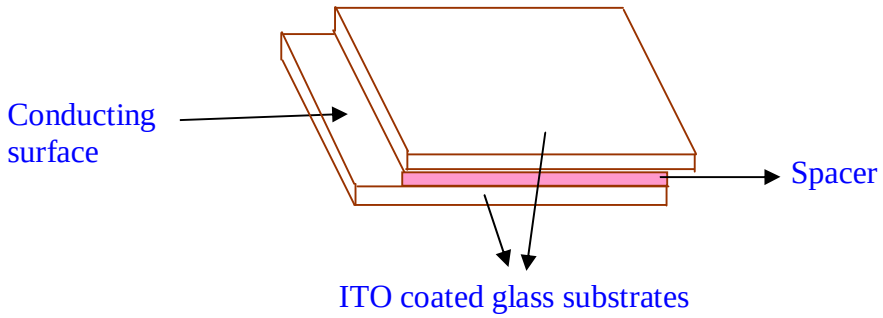

(a)

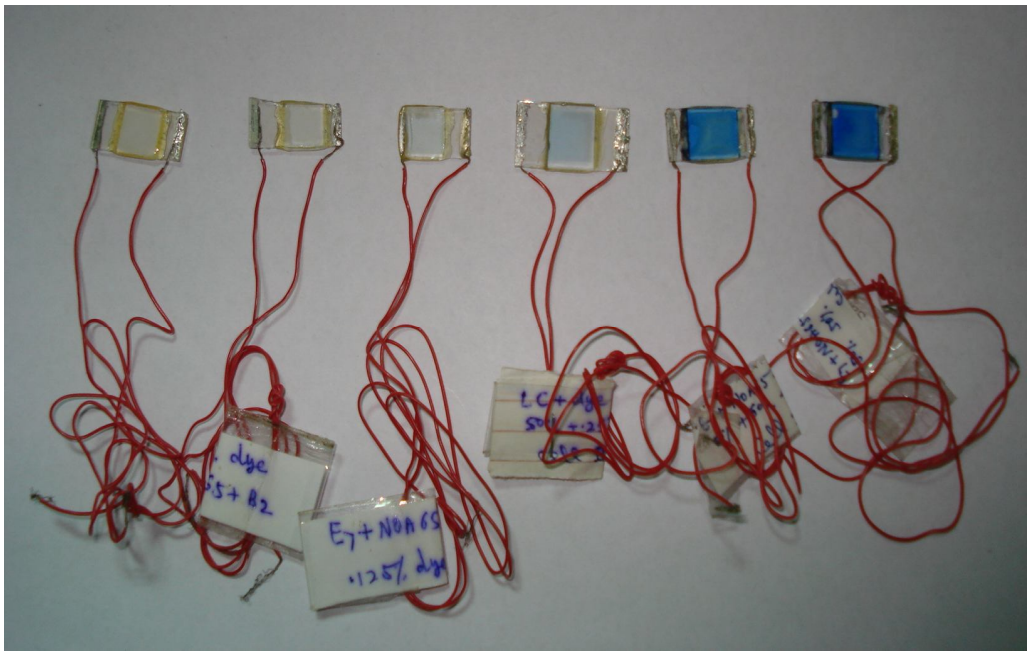

(b)

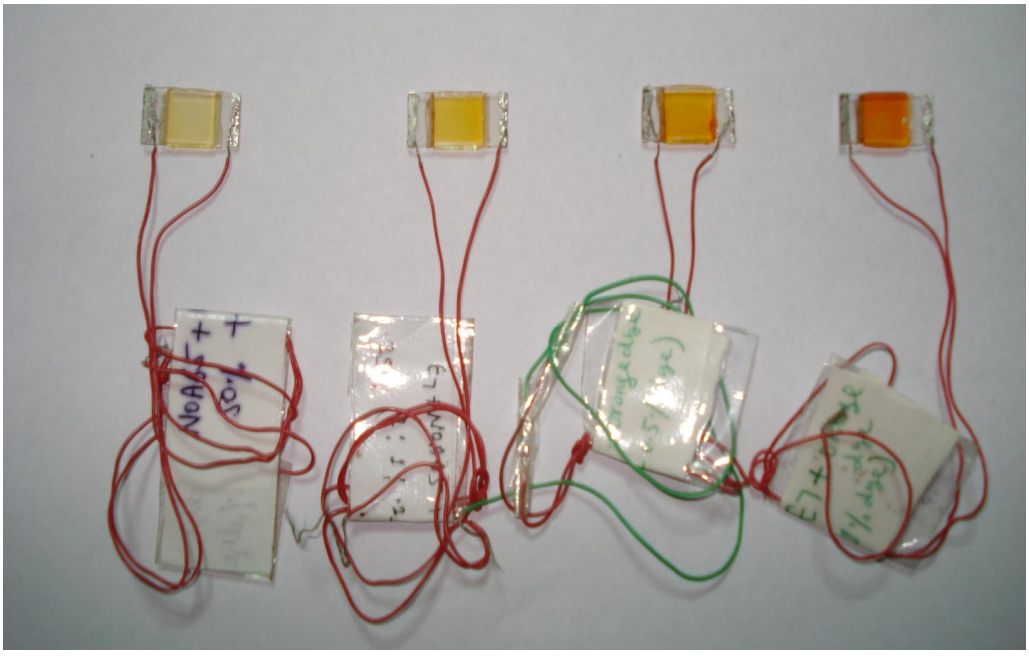

(c)

Fig.2.6 (a) Assembled unfilled sample cell (b) filled DPDNLC sample cells with varying content of anthraquinone blue dye and (c) filled DPDNLC sample cells with varying content of azo orange dye.

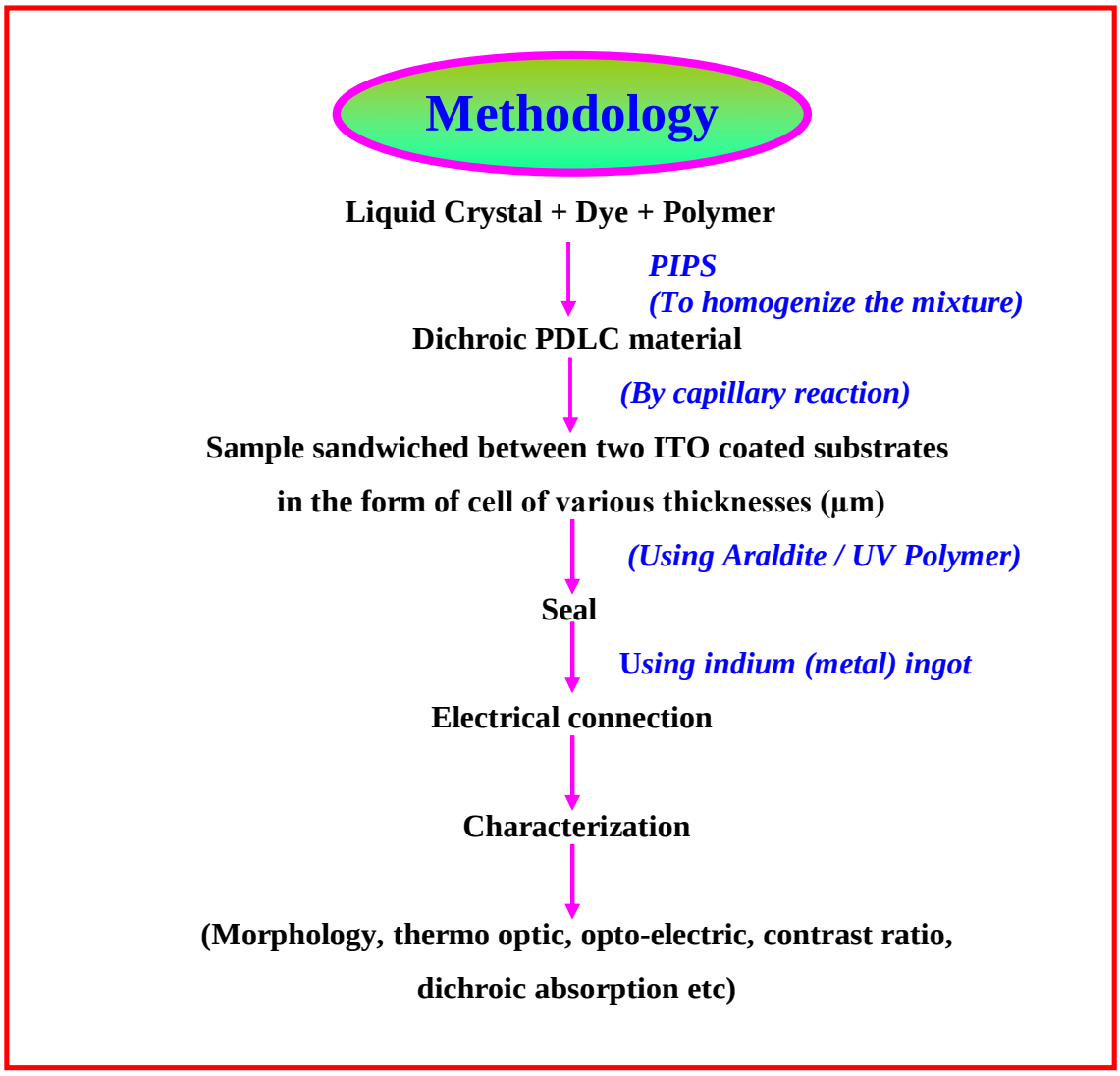

Fig. 2.7 Flow chart for the preparation and characterization of dichroic PDLC cell

2.4.1 Dichroic polymer dispersed nematic liquid crystal (DPDNLC) samples

Dichroic PDNLC films were prepared by polymer induced phase separation (PIPS) method. The materials used were nematic liquid crystal E7, UV curable optical adhesive NOA-65, blue anthraquinone (Rolic, Switzerland) and orange azo (Sigma Aldrich) dichroic dye. The nematic liquid crystal shows a wide temperature range of nematic phase in which the dye molecules were dissolved in low concentrations (0.0625%, 0.125%, 0.25%, 0.50% and 1.0% wt./wt).

To achieve complete phase separation and best droplet morphology, we preferred 50:50 wt./wt. ratio of nematic liquid crystal and polymer, in the preparation of samples. This homogenous mixture of DPDLC material was heated to isotropic temperature in an oven after shaking to ensure proper mixing. A thin sample cell of thickness 10 μm, consisting of two ITO coated glass substrates was used to filling this homogenous mixture by capillary reaction on heating the mixture at its isotropic phase. The sample cell was sealed and exposed to UV light (intensity ~ 2 mW/cm^2) for about an hour at room temperature. The cell assembly was placed in a programmable temperature controller coupled to hot stage (Linkam Model TP 94 and THMS 600) and then cooled down to room temperature @ 0.1^oC per min. Uniform dispersion of dichroic LC droplets in the polymer matrix were viewed under crossed polarizers at a total magnification of 100X and 500X through polarizing microscope (Olympus Model BX-51P) fitted with charge coupling device (CCD) digital camera interfaced to a computer. The electro-optic responses were studied when an electric field was applied to the sample using a function generator (Philips FG -8002). The output responses were recorded and detected on digital storage oscilloscope (Tektronix Model TDS 2024) using a photo-multiplier tube (Model RCA 931-A) for analyses.

2.4.2 Dichroic polymer dispersed ferroelectric liquid crystal (DPDFLC) samples

Dichroic PDFLC film using ferroelectric liquid crystal mixtures FLC-I, FLC-II and NOA-65 with different concentration of anthraquinone dichroic dye was also studied. In the preparation of DPDFLC samples of different dye concentration and for achieving comprehensive phase separation and best droplet morphology, the FLC-II was heated at its melting temperature and mixed with the NOA-65 in an 80:20 wt/wt ratio whereas the mixture FLC-I was mixed with NOA-65 at room temperature in a 50:50 wt/wt ratio of liquid crystal and polymer. To ensure completing mixing of dye in ferroelectric liquid crystal, first dye was doped with the liquid crystal and then dispersed in the polymer matrix. The cell gaps were maintained with Mylar spacer between the substrates in all the samples. PDFLCs samples were sealed and exposed to UV light at the same intensity $2mW/cm^2$ for an hour at room temperature. Electric connections with ITO coated glass substrates were made in all the

samples using an indium solder. After sealing and curing, the samples were placed in a LINKAM temperature programmer cum hot-stage.

The optical micro-texture and LC droplet morphology were viewed at a magnification of 100X and 500X through Olympus polarizing microscope fitted with charge coupling device (CCD) camera. The LC droplet morphology, its size and orientation was detected and acquired on a P IV computer using Linksys and RTVMS software. The electric field was applied using a function generator and the output responses were detected on a digital storage oscilloscope using wave-star software. The detailed investigation on LC droplet morphology, behaviour of droplet in the polymer matrix and other parameters such as spontaneous polarization, response time, absorbance factor etc as a function of temperature, electric filed, dye concentrations etc are given in the chapter 4.

2.5 Experimental

In order to study the liquid crystal droplet morphology and phase transition temperatures, Olympus polarizing microscope (Model- BX51P) and Linkam temperature programmer cum hot stage (Model TP94 and THMS 600) were used. The electric field was applied to the sample through Scientech function generator (Model ST 4060), Philips function generator (Model FG8002). The microscopic optical textures were captured through the charge coupling device (CCD) digital camera (Olympus DP 12 JAPAN) fitted on polarizing microscope and interfaced to a computer. A block diagram of our experimental set-up for the investigation of optical textures, electro-optic properties and other parameters of liquid crystal is shown in fig. 2.8. The temperature of the DPDLC sample cell was controlled using temperature controller interfaced with computer through RS232 port and the output response as a function of field was recorded on a Tektronix Oscilloscope (Model TDS2024). Uniform dispersion of dichroic LC droplets in the polymer matrix and all the optical textures were viewed under crossed polarizers at a total magnification of 100X and 500X in the transmission mode. The complete experimental set-up to study electro-optical properties is also shown in fig. 2.9.

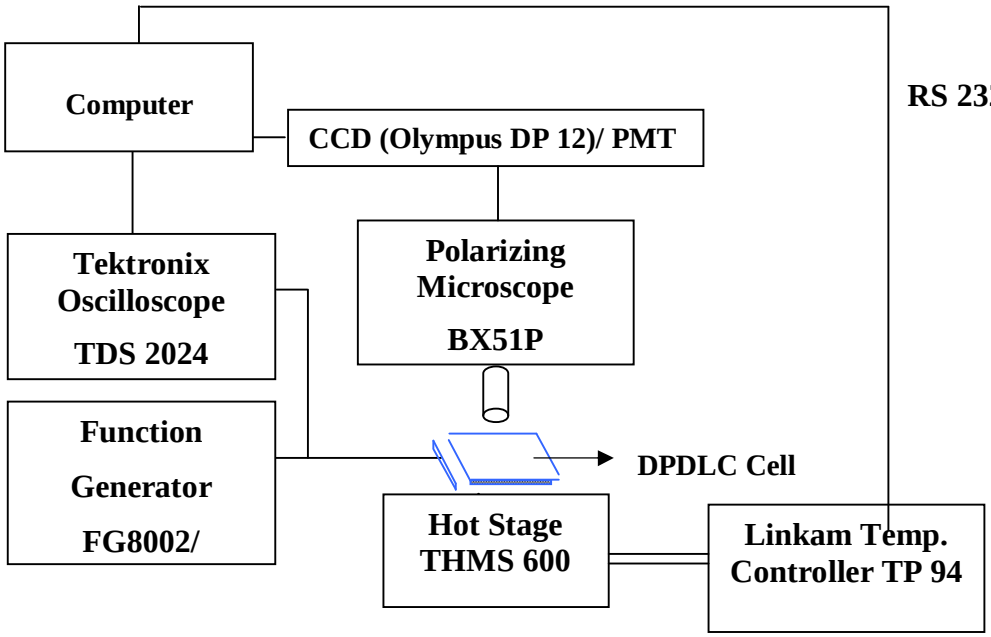

Fig. 2.8 Block diagram of the experimental set-up to study electro-optical properties

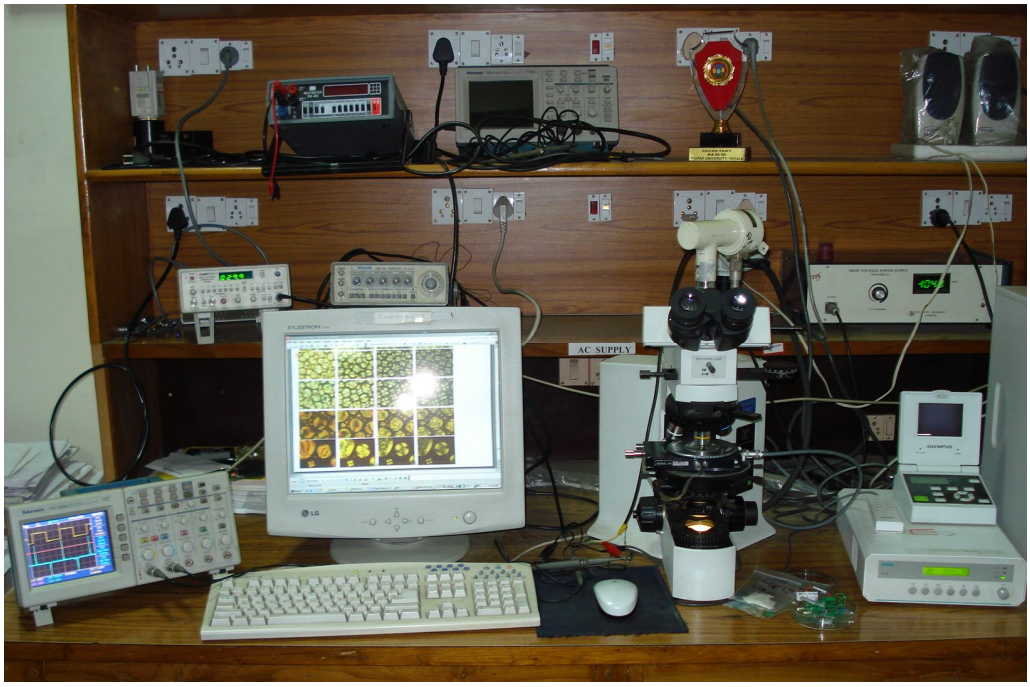

Fig. 2.9 Experimental set-up to study the opto-electric properties of DPDLC samples

2.5.1 Optical polarizing microscopy

The optical studies observed in nematic liquid crystals, ferroelectric liquid crystal and guest host systems were investigated using an Olympus optical polarizing microscope (Model BX51P) at a magnification of 100X and 500 X under crossed polarizers using long working distance objective lens. The optical micro-textures of LC materials were also investigated as a function of temperature, voltage and other physical parameters.

2.5.2 Temperature programmer along with hot stage

In thermal microscopy studies, we used Linkam temperature programmer TP94 and hot stage THMS 600. The TP94 is specifically designed for precise temperature control of the Linkam heating/freezing stages with accuracy ± 0.1 ^{0}C. The stage sensor is digitally linearized to give accurate temperature readout, the controls and their functions have been carefully chosen for simple and easy operation. The temperature range is –196 ^{o}C to 600 ^{o}C. Heating or cooling rates can be changed almost instantly using the three rate keys. The heat ranges are from 0.1 to 0.9^{o}C/min at 0.1 degree intervals from 1.0 to 9.0 ^{o}C/min at 1.0 degree intervals and from 10 to 90^{o}C degree intervals. A varying dc signal is used to control the stage and results in an even application of power, which avoids the bursts seen with conventional burst fire ac techniques. An optional remote control gives single key control of three programmable heating/cooling rates and the HEAT, COOL and HOLD functions. The three programmable heating/cooling rates are held in memory when power is switched OFF. The temperature and limit values can also be stored and recalled using the remote control facility.

2.5.3 Differential scanning calorimetry (DSC)

Differential scanning calorimetry (DSC) is a thermal analysis technique that measurers heat flow to and from a specimen as a function of time and temperature. DSC is one of the most widely used analytical instrument because of the ease with which it can provide large amount of thermodynamic data. Properly used, information on the phase transitions of a sample, such as transition temperature, enthalpy, heat capacity, specific heat, can all be calculated from a single data run. Enthalpy, a term often used in physical chemistry, is a measure of the chemistry, is a measure of the energy of the system that includes the energy due to the volume that the system occupies. This experiment was an attempt to use DSC to examine the phase

transitions and thermodynamic properties of the liquid crystal E7 possess a wide nematic phase, anthraquinone and azo dichroic dye and dichroic polymer dispersed liquid crystal containing different concentration of dyes. The phase transition temperature of the materials, noted through thermal polarizing microscopy was fully supported by differential scanning calorimetry. The DSC (Lineseis DSC L 63) used in the experiment was controlled by a compatible computer running the LINESEIS DSC instrumental software. The software collected data and provided graphical analysis tools to determine transition temperatures with measurement accuracy of ± 0 to 2 K. The DSC (Lineseis DSC L 63) used in the experiment is shown in the fig. 2.10.

2.5.4 UV-VIS Spectrophotometer for absorbance and transmission studies

The UV-VIS absorbance of light by dye and dichroic polymer dispersed liquid crystal sample cells were also investigated by using ultra violet visible (UV-VIS) Spectrophotometer (Model - SPECORD 200PC) in the wave length range of 200–800 nm with an accuracy of ± 0.5nm interfaced with computer. The out put responses of the PDLC sample cells were measured with the help of photo multiplier tube (PMT) (Model RCA931-A) fitted on the polarizing microscope and interfaced with computer as shown in fig. 2.9. Light falls on the PMT and a current results (through the photo electric effect) and it was measured with the help of electrometer (Keithley Model-6514) of three and half to six and half digits. The range of current measurement was 20PA to 20mA with ± 5% error.

2.5.5 Droplet size measurements

The LC droplet sizes have been by considering the large no of droplets manually. OLYSIA Bioreport software was used to measure the partial development of these droplets and then averaged out. The precession in measurement was about ± 1 μm. The droplet size of small droplets exhibiting between the two major droplets was also taken. Fig. 2.11 depicts the measurement of LC droplet size by drawing the horizontal scale bar on the major and minor axes of the droplet.

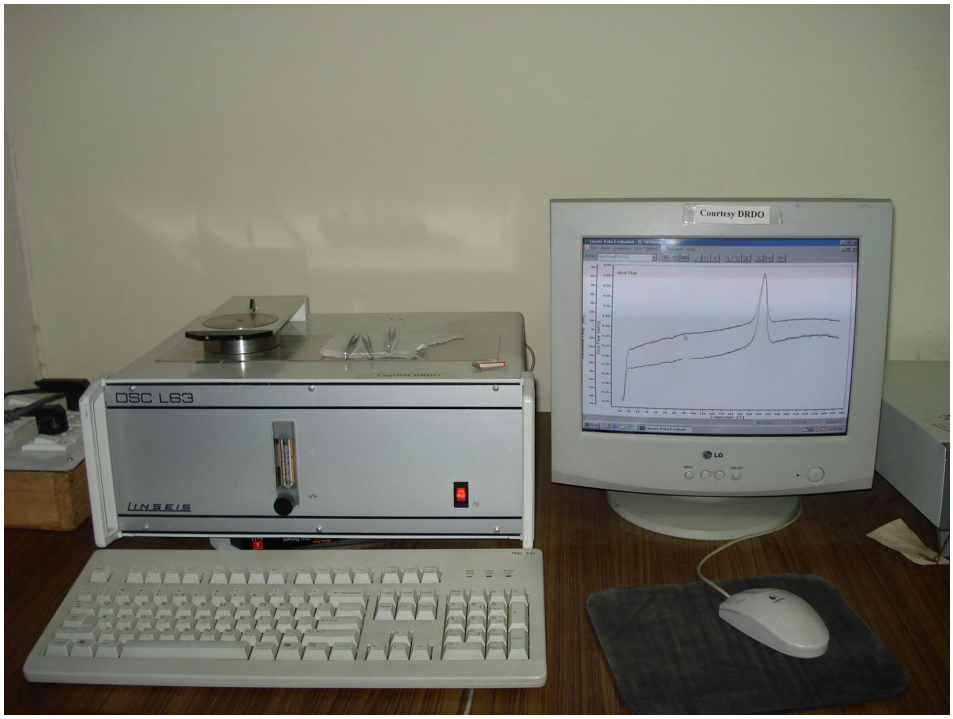

Fig. 2.10 Differential scanning calorimeter

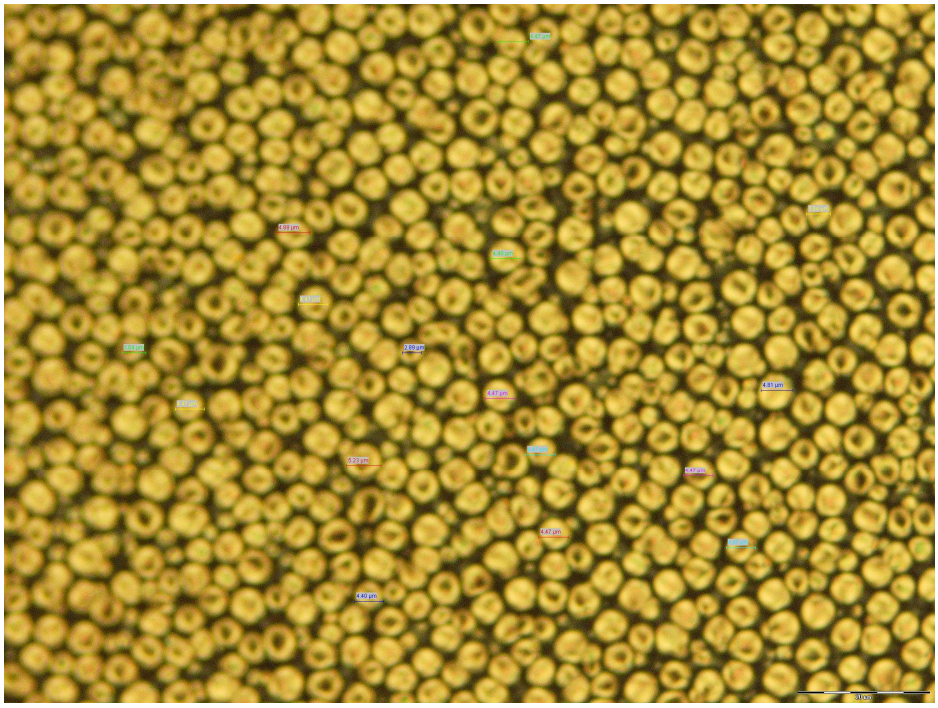

Fig. 2.11 LC droplet size measurement in 0.0625% dichroic PDLC film at room temperature

References

[1] E. Merck, UK

[2] BDH, UK

[3] Data sheet, Norland, NJ, USA.

[4] Thomas Tanggaard Alkeskjold, Jesper Lægsgaard, Anders Bjarklev, David Sparre, Hermann, Anawati, Jes Broeng, Jun Li, Shin-Tson Wu, OPTICS EXPRESS, **12** 24 (2004) 5857.

[5] P. S. Drazic, Liquid Crystal Dispersion, World Scientific, Singapore, (1995).

[6] P. Malik, J. K. Ahuja and K. K. Raina, Curr. Appl. Phys. **3** (2003) 325.

[7] G. Sumana and K. K. Raina, Curr. Appl. Phys. **5** (2005) 277.

[8] P. J. Colling, Liquid Crystal: Nature's Delicate Phase of Matter, Pricenton: University Press (1990).

[9] P. J. Colling and Michael Hird, Introduction to Liquid Crystal: Chemistry and Physics, Taylor and Francis Ltd (1997).

[10] S. Chandrasekhar, Liquid Crystal 2nd Edn. Cambridge: Cambridge University Press (1992).

[11] P. G. De Gennes, The Physics of Liquid Crystal: Oxford University Press (1975).

[12] I. C. Khoo, Physics of Liquid Crystalline Materials (Amsterdam: Golden and Breach) (1991).

Chapter3

Dichroic Polymer Dispersed Nematic Liquid Crystal Systems

Overview

In this chapter, we present experimental results on the dispersion of nematic liquid crystal in polymer matrix with and without dye concentration. The morphological and electro-optical responses of dichroic polymer-dispersed liquid crystal films (DPDLCs) doped with anthraquinone and azo dichroic dyes have been studied in detail. For the preparation of DPDLCs, the polymerization-induced phase separation is considered using UV radiation curing process. The anomalous behavior is attributed to the orientation of molecules in the presence of dye molecules in dispersed liquid crystal droplets. The optical transmission of doped PDLC cells in crossed polarizers exhibits an anomalous dependence on the droplet morphology. In addition the concentration of dyes was changed to improve film performance and determine the best electro-optic response in terms of parameters, such as optical transmission, threshold voltage, contrast ratio, switching time and absorbance factor as a function of applied voltage, temperature and dye concentration. Our result indicates that low dye concentration DPDLCs shows better optical properties and higher contrast ratio. The effects of azo dye and droplet size on the dielectric properties were also examined over a wide frequency range 50 Hz-1MHz. Relaxation modes has been observed with relaxation frequencies in the range of 500 kHz to 89 kHz.

3.1 Introduction

Polymer dispersed liquid crystals (PDLCs), a novel class of optical composites made from polymer and liquid crystal (LC) materials in an appropriate ratio have been the focus of many researchers because of their potential applications. Micron-sized nematic liquid crystal (NLC) droplets are uniformly dispersed in a transparent polymer matrix and thus possess a highly scattering OFF-state. In presence of an electric field, PDLC systems can be switched from

scattered opaque to transparent state. Based on this technique, PDLCs have attracted attention as novel class of optical materials suitable for light valves and other displays [1-4]. PDLCs are also convenient systems to study the confinement and surface effects. The required high surface to volume ratio is here achieved by the formation of a large number of micrometer or sub micrometer spherical liquid crystal droplets embedded in polymer matrix. The structure of a droplet depends on the properties (particularly elastic) of the liquid crystal and the polymer, temperature and the external applied field. It is characterized by the spatial dependence of the director field and orientational order parameter. The director configuration of the nematics droplets depends essentially on the type of molecular anchoring at the interface. When liquid crystal molecules are confined to small droplets, curvature induces significant deformations in the director alignment. In this case when the molecules are strongly anchored parallel to the surface and the elastic constant for the splay, twist, and bend deformation do not differ considerably, the bipolar structure [5] results with two point of defect on the axis of cylindrical symmetry. On the other hand, if the bend elastic constant is smaller than the splay elastic constant, the toroidal structure [6] takes place.

Recently PDLC [7-21] and polymer stabilized LC (PSLC) [22, 23] have been widely studied and applied intensively in the field of display devices due to such advantages as their polarizer free and alignment layer free nature, fast response times, simple preparation, etc. however, because of their low contrast ratio and broad switching behaviour, the use of PDLCs for display devices is limited and many studies have been carried out to overcome the problems. Generally, to improve the contrast ratio, the use of dichroic dye-doped liquid crystal was proposed [24-26]. Some dichroic dyes show the attractive property of photo-isomerization using light. As a result, investigation of this phenomenon has been focused on the manufacture of photo-controllable devices which have a high contrast ratio [27–30]. It is known that a change in the transmittance of a PDLC can take place by the photo-chromic reaction of photo-chromic molecules such as azobenzene derivatives [24-26]. The configuration of azo-benzene derivatives can be transformed reversibly through the process of photo-isomerization. cis-azobenzene is formed using UV light around 366 nm, and transformed into the trans-azobenzene by visible light around 433 nm. When azobenzene derivatives exist in the LC, they affect the LC phase significantly. Cis-azobenzene destabilizes the LC phase but, on the contrary, trans-azobenzene is aligned with the LC

molecules and enhances the LC phase. This means that the mesophase of an azobenzene-doped LC can be controlled by light irradiation.

The addition of dye to a liquid crystal affects some parameters of the liquid crystal such as refractive index, dielectric constant, the orientational order, the phase transition temperature and molecular association [31-35] because of the strong microscopic mutual interactions among the dye and liquid crystal molecules. When a dichroic dye with a geometric anisotropy is dissolved in a in a nematic liquid crystal, the dye molecules tends to arrange itself in such a way that its long molecular axis aligns along the liquid crystal director and a change of colour intensity is obtained by controlling the direction of the liquid crystal molecules (fig.3.1a). A rod like, long molecular structure is favorable for a strongly dichroic dye. In particular, absorption spectra and dichroic ratios in liquid crystals are the dominant properties with regard to the performances of displays. Since each dye has plural properties that have important effects on performances of displays exchanging dyes means that the plural variables are changed simultaneously.

Recently it was demonstrated that a small amount of a dye dissolved in NLC can enhance the reorientation by almost two orders of magnitude and, in some cases, can even change its sign [36]. The explanation proposed by Janossy [37] is connected with the electronically excited metastable states appearing in the molecules of absorbing dye. The interaction of the excited dye molecule with the LC molecules is different from the one of the dye molecule in the ground state. The Janossy model is suitable for the reorientational bulk effect. A surface driven reorientation effect as a result of the light action on the bulk of a light-sensitive NLC-azo dye mixture was reported by Voloschenko and co-workers. The explanation was the adsorption of dye photo-transformed molecules onto the aligning photopolymer surface [38]. Simoni and co-workers have pointed that the observed huge reorientational effect in a LC-dye mixture is due to light-induced modifications on the surface-induced nonlinear effect [39]. Their investigations about the diffraction efficiency revealed the basic role of light-induced adsorption and desorption of the dye molecules onto the boundary surfaces [40, 41]. PDLC films with dichroic dye (DD) dissolved in the liquid crystal possess a controllable absorbance and scattering as well. This combination can be used to produce high contrast displays [42]. We also know that the scattering effect of the film in the OFF state depends on the LC droplet size [43, 44]. Thus for a constant dye concentration, the UV intensity should be optimized to

obtain a suitable droplet size such that the transmittance at the OFF state can be minimized to improve the contrast ratio.

This is observed that the use of controlled amount of dichroic dye should be useful for improving device performance and advancing the development of functional PDLCs. Moreover by controlling the concentration of dye, it should be possible to improve the optical efficiency and reduce the operating voltage of DPDLC. One of the major criteria for evaluating the performance of these films in terms of electro-optical responses is to achieve the high contrast ratio. The orientation of the elongated dye molecule is governed by the nematic director configuration inside the droplet. Therefore, the dye absorbance is modulated by the alignment of the nematic director with an external field. In the OFF-state, we assume random orientation from droplet to droplet of the symmetry axes of the bipolar droplets resulting in random orientation of the dye molecules [fig. 3.1(c)]. The extinction coefficient is therefore averaged over all droplets and is equal to the isotropic extinction coefficient of the dye. In the ON state, the droplet director and the dichroic dye molecules in the droplet are aligned normal to the surface of the film [fig. 3.1(d)] and the dye extinction coefficient is equal to the perpendicular extinction coefficient. Dichroic dye that remains dissolved in the polymer binder will be unaffected by the external field and remain randomly oriented. Therefore, only the dye dissolved in the nematic droplet will exhibit dichroic properties and enhance the contrast of the film.

Dielectric spectroscopy yields valuable information about the complex electrical nature of the liquid crystal (LC) droplets in the PDLC materials arises because of the strong dipole moments of the LC along with interfacial charge layers between the droplets and the polymer matrix or between the electrodes and the PDLC samples as a result of the interactions with the applied electric field [45]. This method is very often used to study the molecular dynamics in various liquid crystalline phases because of its wide frequency range and its ability to follow the reorientational movements of dipolar groups or whole molecules. Since dispersion of a liquid crystal in polymer leads to a large surface-to-volume ratio, the electro-optical properties of the PDLC films are essentially determined by the interactions between the liquid crystal and polymer. On the other hand, the PDLC composites are heterogeneous and the interfacial effects are also of great significance. The dielectric relaxation spectroscopy method can be used to detect these electric complications over a wide temperature and frequency range, and

is also very sensitive to the dc conductivities due to conducting impurities and the interfacial charge layer effect. The existing theories on dielectric behavior in heterogeneous systems can be adapted to the PDLC system as a result of its phase separated nature [46, 47]. Here we also present the results of the dielectric relaxation studies performed for DPDLC films consisting of the nematic dispersed in the polymer with different concentration of azo dye at room temperature.

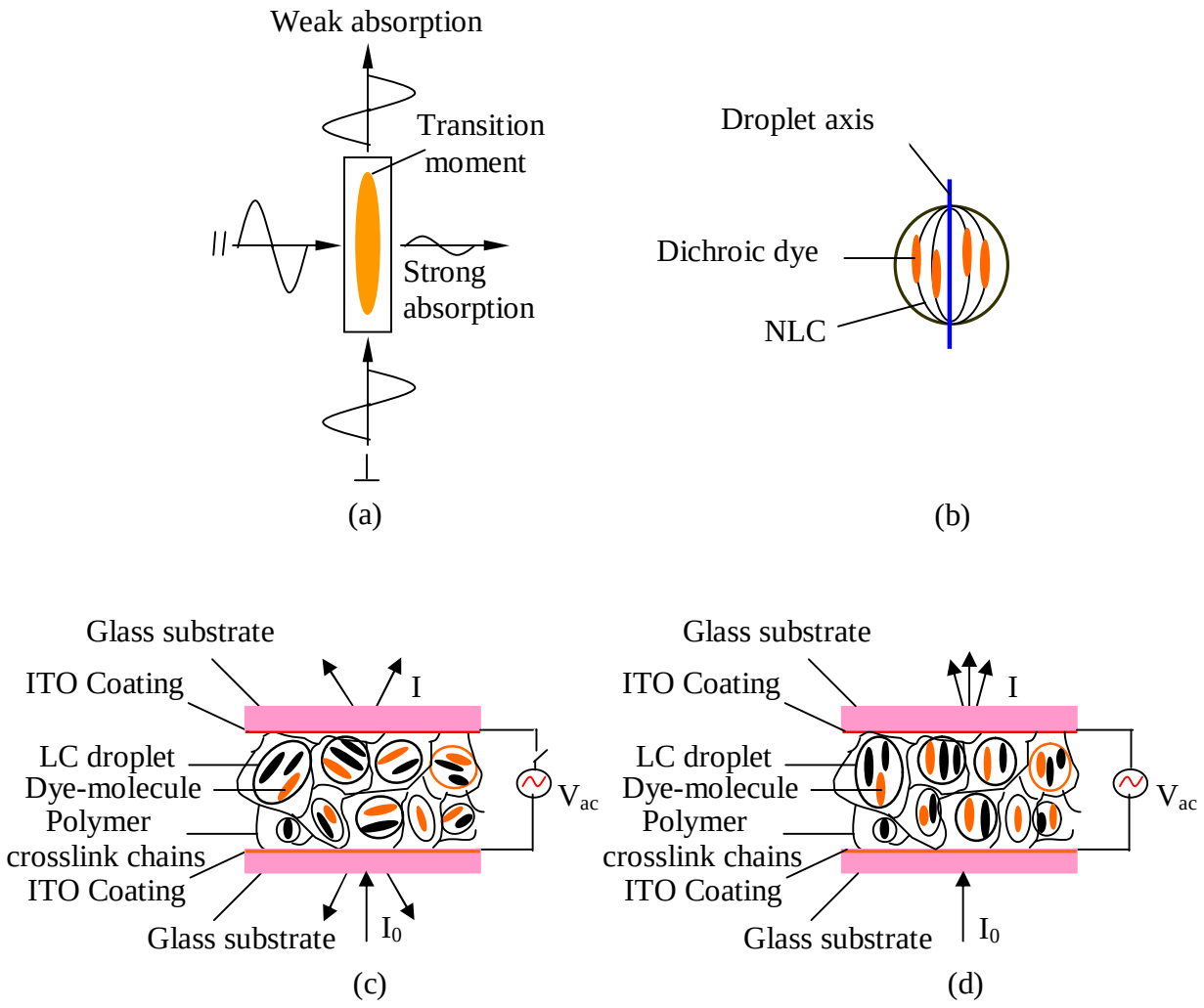

Fig. 3.1 (a) UV- VIS absorbance of dichroic dye molecule (b) alignment of dye molecules in a dichroic NLC droplet (c) random orientation from droplet to droplet of the symmetry axes of the bipolar droplets (OFF state) and (d) alignment of the liquid crystal and dye molecules with the application of field (ON state) in DPDLC film

3.2 Principle of DPDLC device

We consider the OFF state normal mode dichroic PDLC film as shown in fig 3.1(c). Here we assume that before UV curing the dye molecules are randomly aligned in the DPDC and hence the extinction coefficient of the dye is equal to the isotropic extinction coefficient. After polymerization with UV curing, the liquid crystal droplets are formed, and the results in random orientations of the dye molecules. Therefore, when the film is thin or the scattering effect is not too much, the extinction coefficient is averaged over all droplets and approximates the isotropic extinction coefficient of the dye. The transmittance of the normal incident light can be measured. In practice, the dye concentration is low and the DPDLC film is thin, hence we can assume that there is no correlation between absorption and scattering. According to Beer's law (48), the extinction coefficient γ can be defined as

$$\gamma = \alpha + \beta \tag{3.1}$$

Then the Off-state transmittance can be expressed as

$$T = \frac{I}{I_0} = \exp\left[-(\alpha + \beta)d\right] \tag{3.2}$$

Where I_0 of the incident light intensity, I is the transmitted light intensity, α is the scattering coefficient, β is the absorption coefficient and d is the thickness of the film. The scattering coefficient α is a function of the liquid crystal droplet size and curing temperature. Because polymer and liquid crystal molecules absorb nearly no visible light, the absorption of a DPDLC film results from dye. Thus following Beer's law, the absorption coefficient β can be defined as

$$\beta = \varepsilon c l \tag{3.3}$$

Where ε is the dye extinction coefficient, c is the dye concentration, and l is the ratio of the distance traveled by light to the film thickness d. Even for normal incidence l is always larger than one because of scattering. When the film is thin or the scattering effect is small, l is near unity. Then, similar to Beer's law, the OFF-state transmittance of the DPDLC film can be expressed as

$$T = \frac{I}{I_0} = \exp(-\gamma d) \tag{3.4}$$

In the ON-state, as in fig. 3.1(d), the symmetry axes of the dichroic NLC droplets move in only one direction, the dichroic dye molecules are absorbed only slightly, and because $n_p \approx n_0$, the largest portion of the incident light I_0 is transmitted through the dye-doped PDLC film. The path length of light is just the thickness of the film because there is no scattering. All of the films have the same film thickness d and made of the same PDLC materials, except the dye concentration, and then the optical properties are determined by the dye concentration on which β depends. From Beer's law using equation (3.2), we can show a symbolic expression of the relationship between the ON state maximum transmittance of light and dye concentration, as shown in fig.3.2.

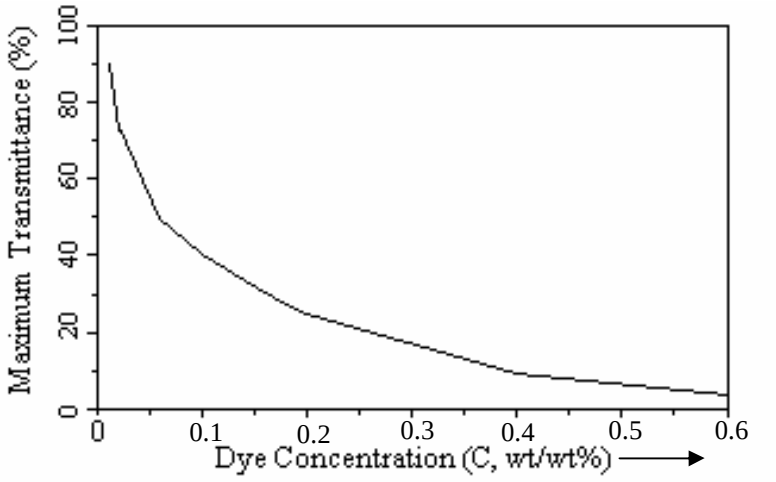

Fig 3.2 Symbolic expression of the relationship of the ON state maximum transmittance of visible light, T_{ON}, to the dye concentration C

3.3 Results and discussion

3.3.1 Transition temperature

The phase transition temperature of liquid crystal E7 possess a wide nematic phase was noted through thermal polarizing microscopy and differential scanning calorimetry (Lineseis DSC L 63) and given by

$$\text{Crystal} \xrightarrow{-10\ ^\circ\text{C}} \text{Nematic} \xrightarrow{60\ ^\circ\text{C}} \text{Isotropic}$$

After dye addition in different concentrations, we noticed a considerable change in transition temperature (at T_{N-I}) was observed. Table 3.1 shows this variation as a function of anthraquinone dye concentration.

Table 3.1 Variation in T_{N-I} as a function of anthraquinone blue dichroic dye concentration

Material	T_{N-I} (˚C)
E7	60.0
NOA 65/E7 (1:1)	59.6
NOA65/E7/B2 (0.0625%wt)	59.4
NOA 65/E7/D (0.125%wt)	59.0
NOA 65/E7/D (0.25%wt)	57.3
NOA 65/E7/D (0.5%wt)	55.0
NOA 65/E7/D (1.0%wt)	41.0

(* D is the dye concentration)

The phase transition temperature of DPDLC films containing azo (disperse orange 3) dichroic dye was also noted through thermal polarizing microscopy and confirmed by differential scanning calorimetry (DSC) (Lineseis DSC L 63) as shown in fig.3.3 for (a) dichroic dye (b) nematic E7, (c) PDLC (c) 0.125% DPDLC and (d) 0.25% DPDLC. We analysed the behaviour of the LC molecules thermally to study the relationship between the temperature dependence of characteristics and the phase transition of LC in DPDLC films. We peeled dichroic PDLC films from glass plates and measured these films with at a temperature scanning rate of 5˚C/min. The peaks of the phase transition in the DSC curves of the films (fig.3.3) agreed well with each other within the measurement precision of the optical polarizing microscopy experiment, indicating that the phase transition of the LC droplets was decreased in the dichroic PDLC with the addition of dyes. Table 3.2 shows this variation as a function of azo dye concentration.

It is noticed that at higher dye concentration, the T_{N-I} shows large variation as compared to the low dye concentration. We believe that this difference in the transition temperature may be due to larger concentration of some ionic impurities arising from dye and monomer molecules

when dissolved in LCs [49]. The light absorption of the dye molecules at higher concentration may also contribute to lowering the T_{N-I}.

Table 3.2 Variation in T_{N-I} as a function of azo orange dye concentration

Material	T_{N-I} (˚C)
E7	60.0
NOA 65/E7 (1:1)	59.6
NOA 65/E7/D (0.0625%wt)	59.0
NOA 65/E7/D (0.125%wt)	56.0
NOA 65/E7/D (0.25%wt)	53.4
NOA 65/E7/D (0.5%wt)	51.0
NOA 65/E7/D (1.0%wt)	49.0

(* D is the dye concentration)

The other possible reason to lowering the T_{N-I} may be that the azo molecule which shows a rod-like shape when in the trans form, but is bent and banana-like in the cis form acts like an impurity and therefore destabilizes the liquid crystalline phase. As shown in fig. 3.4 (b) there is a sharp absorbance peak at around 340 nm indicating that the trans-cis photoisomerization has taken place.

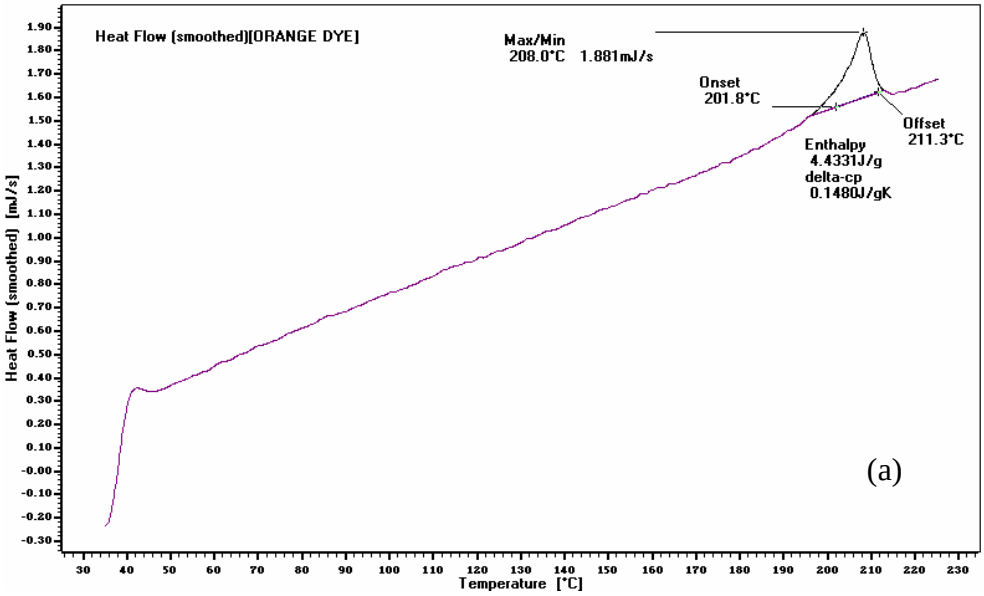

Conti.

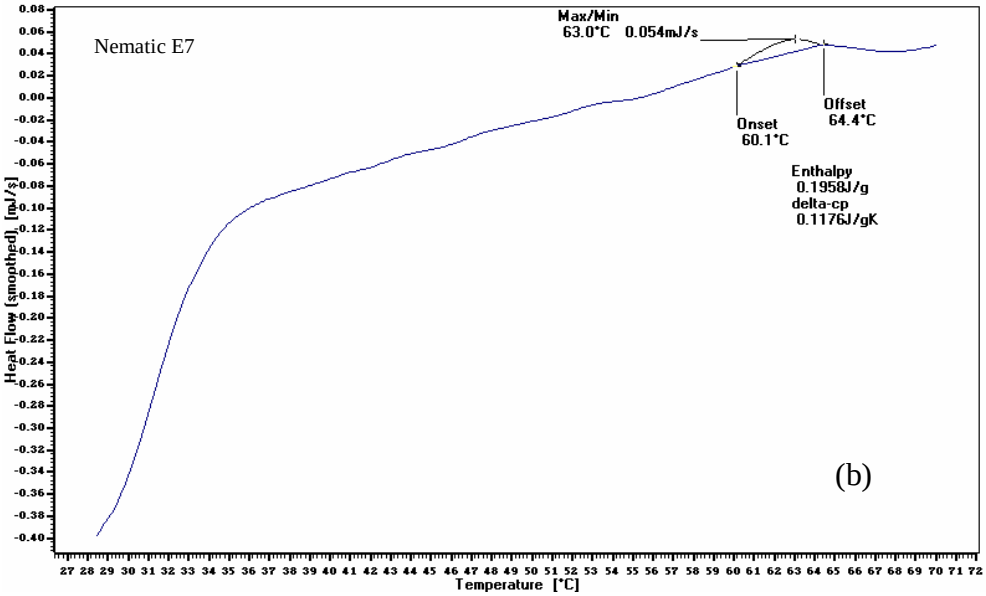
Nematic E7
Max/Min
63.0°C 0.054mJ/s
Onset
60.1°C
Offset
64.4°C
Enthalpy
0.1958J/g
delta-cp
0.1176J/gK
Heat Flow (smoothed) [mJ/s]
Temperature [°C]
(b)

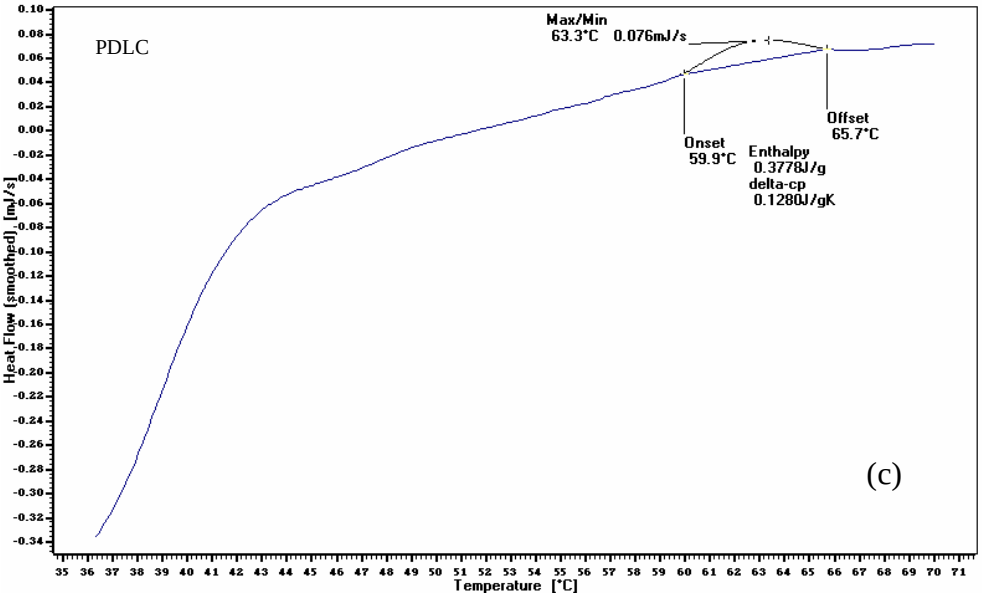
PDLC
Max/Min
63.3°C 0.076mJ/s
Onset
59.9°C
Offset
65.7°C
Enthalpy
0.3778J/g
delta-cp
0.1280J/gK
Heat Flow (smoothed) [mJ/s]
Temperature [°C]
(c)

Conti.

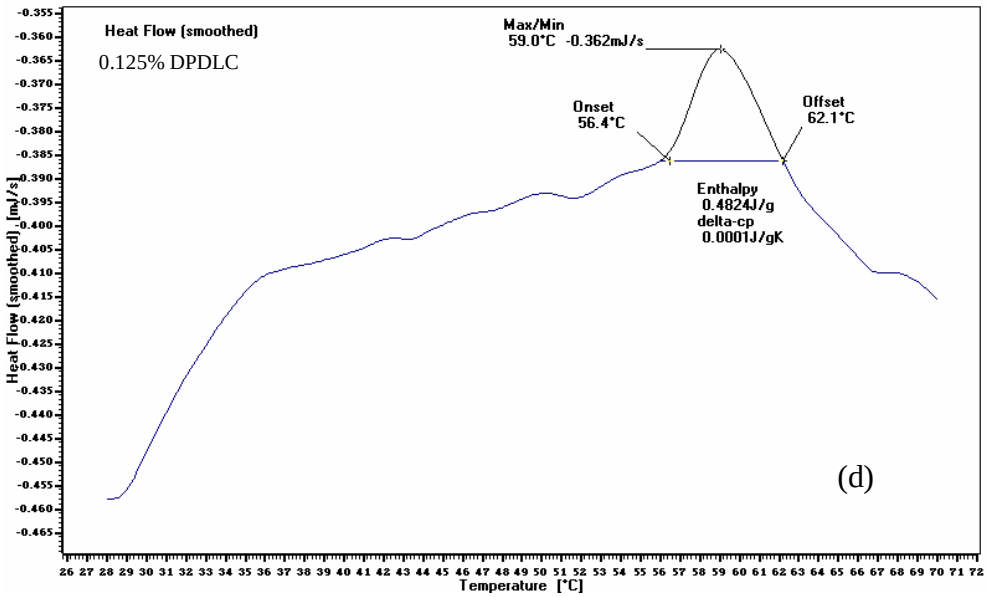

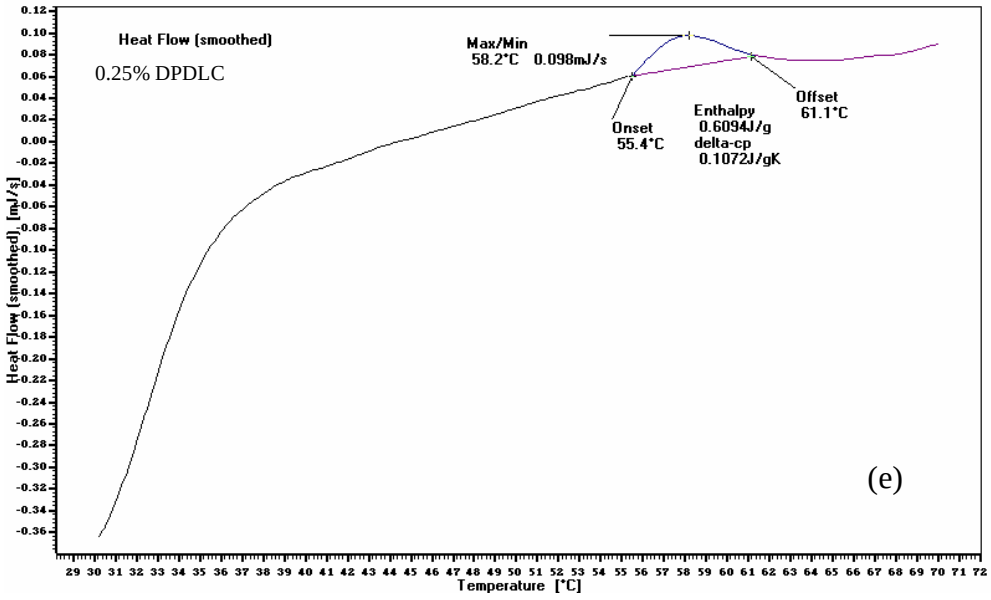

Fig.3.3 Dfferential scanning thermograms of (a) azo (orange) dye (b) liquid crystal E7 (c) PDLC and DPDLC containing (d) 0.125%, (e) 0.25% azo dye

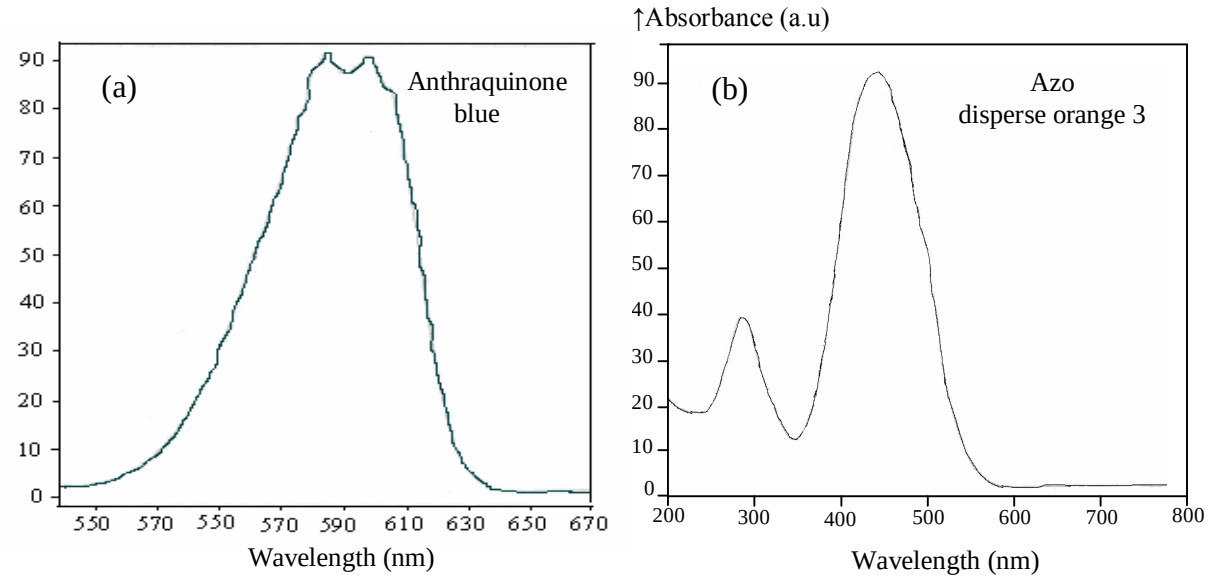

Fig.3.4 Absorption spectrum of (a) anthraquinone blue dye and (b) azo (disperse orange3) dye molecule

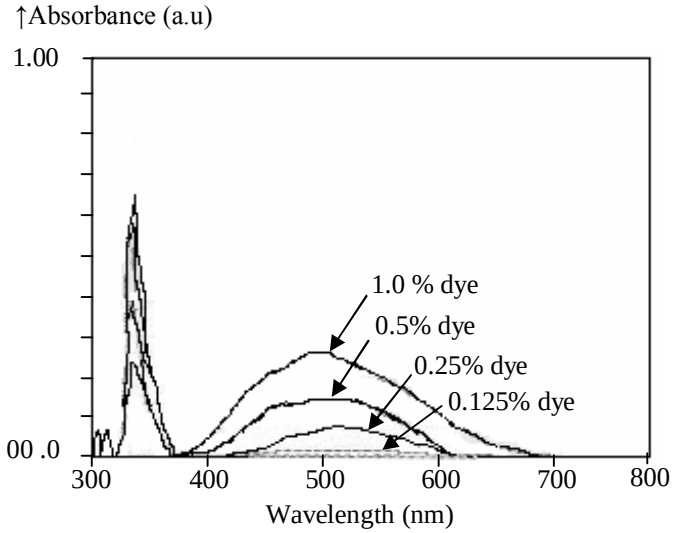

Fig. 3.5 UV-VIS absorbance of dichroic liquid crystal mixture with azo dye

3.3.2 Droplet morphology

A. Droplet morphology with anthraquinone dye

Fig.3.6 shows the droplet morphology of DPDNLC with different concentration of anthraquinone dye at room temperature. It is seen that LC droplet size is relatively smaller (~10-15 μm) and rather more uniformly distributed forming spheroidal bipolar droplet configuration [fig. 3.6 (a, b)] at lower dye concentration (≤ 0.25%) than higher dye

concentration [fig. 3.6 (c, d)]. It may be due to the less free volume available for the dispersed low dye concentration droplets in the polymer matrix. At 0.5% dye concentration, the droplet morphology is shown in fig 3.7. The molecular orientations depict the combination of several other configurations [bipolar, axial, radial and toroidal (or collapsed)] which appear simultaneously.

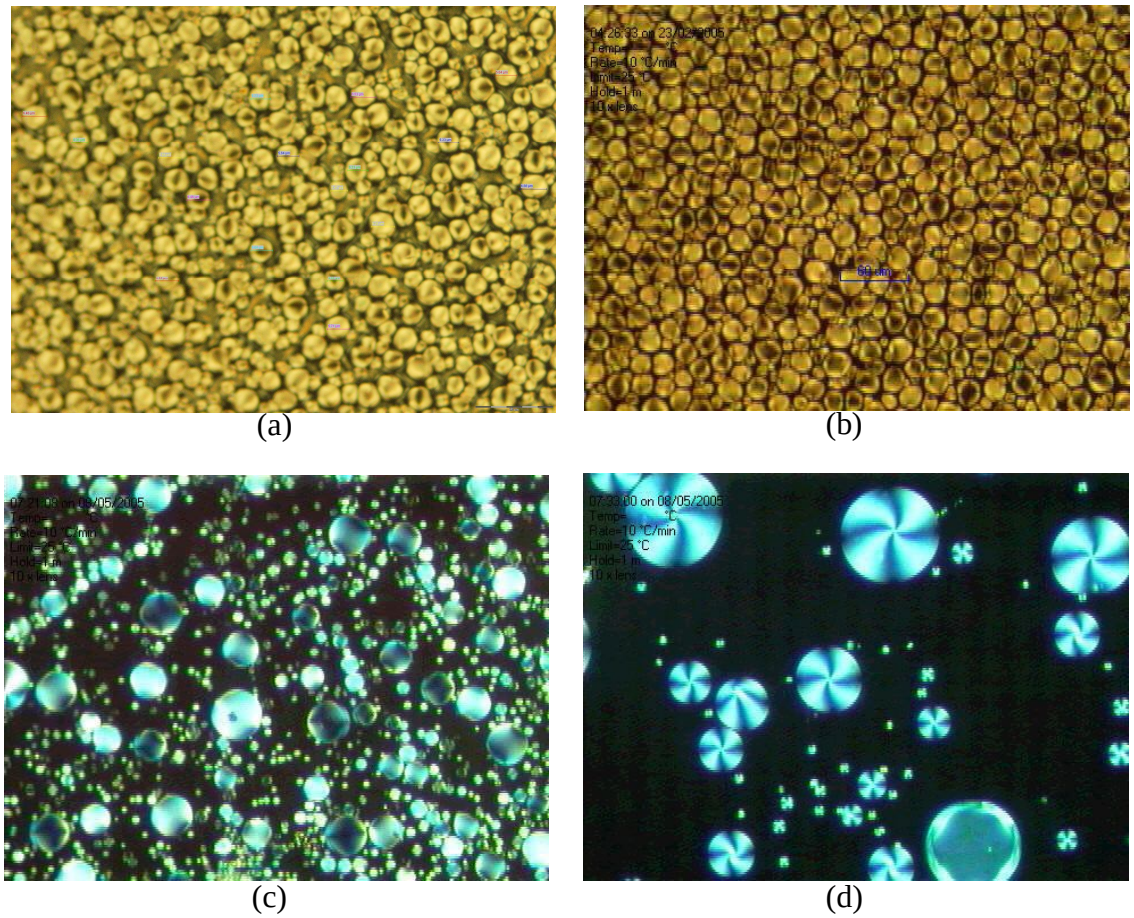

Fig. 3.6 Droplet morphologies of dichroic polymer dispersed nematic liquid crystals with varying anthraquinone dye contents of (a) 0.125% (b) 0.25% (c) 0.5% and (d) 1.0%, at a magnification of 100X

We believe that toroidal LC droplet form spontaneously by collapse of polymer shell covering the LC droplet thus forming a toroidal cavity in the film. The dye molecules absorbed at the polymer/LC interface may weaken the polymer shell, causing it to collapse under certain condition. A reduction in interfacial energy can cause an increase in the fraction of toroidal

LC droplets. Several groups reported the formation of toroidal LC droplets in PDLC and DPDLC composite films [50-52].

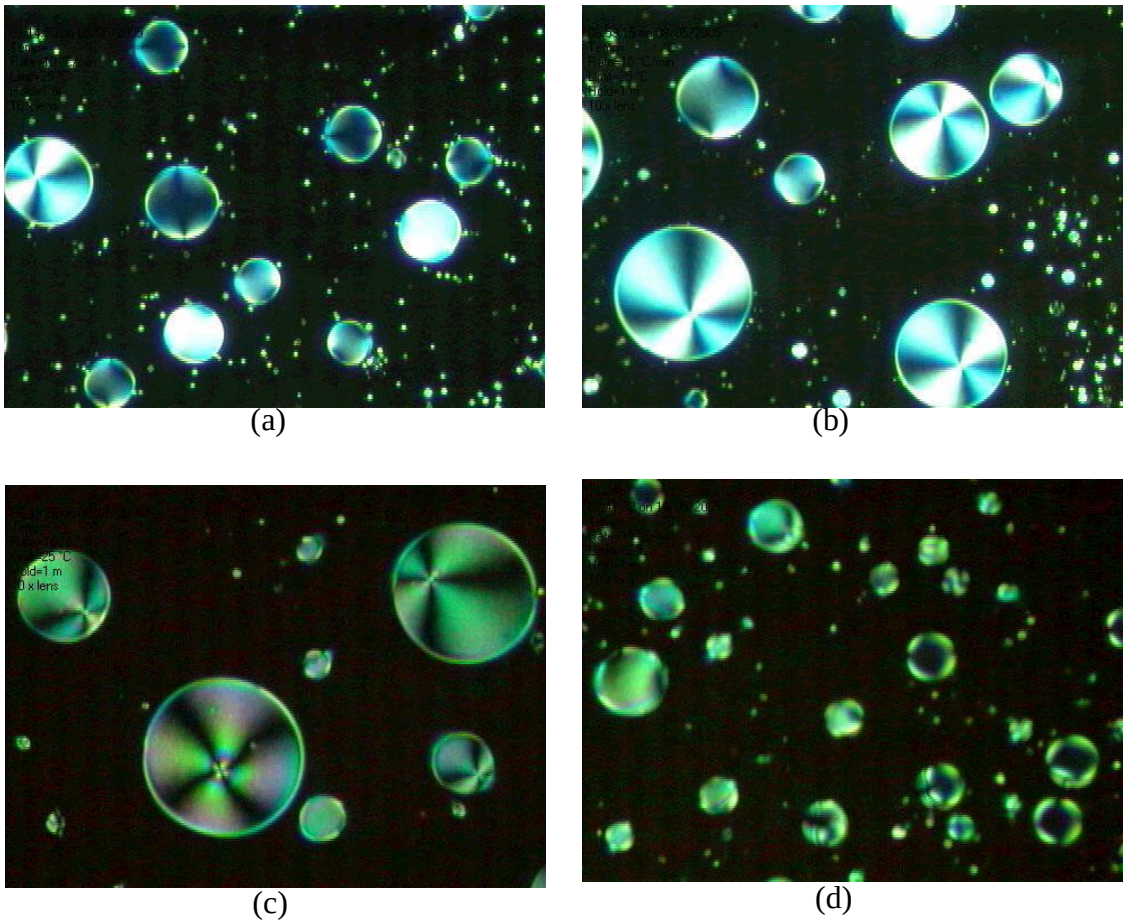

(a) (b)

(c) (d)

Fig. 3.7 Several LC droplets image of (0.5%) dichroic PDLC sample (a) spheroidal or ellipsoidal droplets, droplets is organized in the bipolar configuration (b,c) radial configuration of droplets (d) topographic images of collapsed (toroidal) droplets, at a magnification of 100X

Fig. 3.8 shows the influence of external field on the droplet morphology at room temperature. It can be seen that dichroic LC droplets have a bipolar configuration and their bipolar axes are randomly distributed inside polymer matrix. A model for the LC director field in a spheroidal PDLC droplet is shown in fig. 3.1(b). In this configuration the director field is anchored parallel at the interface. The director field possesses cylindrical symmetry, with the symmetry axis defined by two point defects which lie at the opposite ends of the droplet. Most polymers

tend to induce a parallel alignment of the nematics so that bipolar droplets most often found in PDLC films.

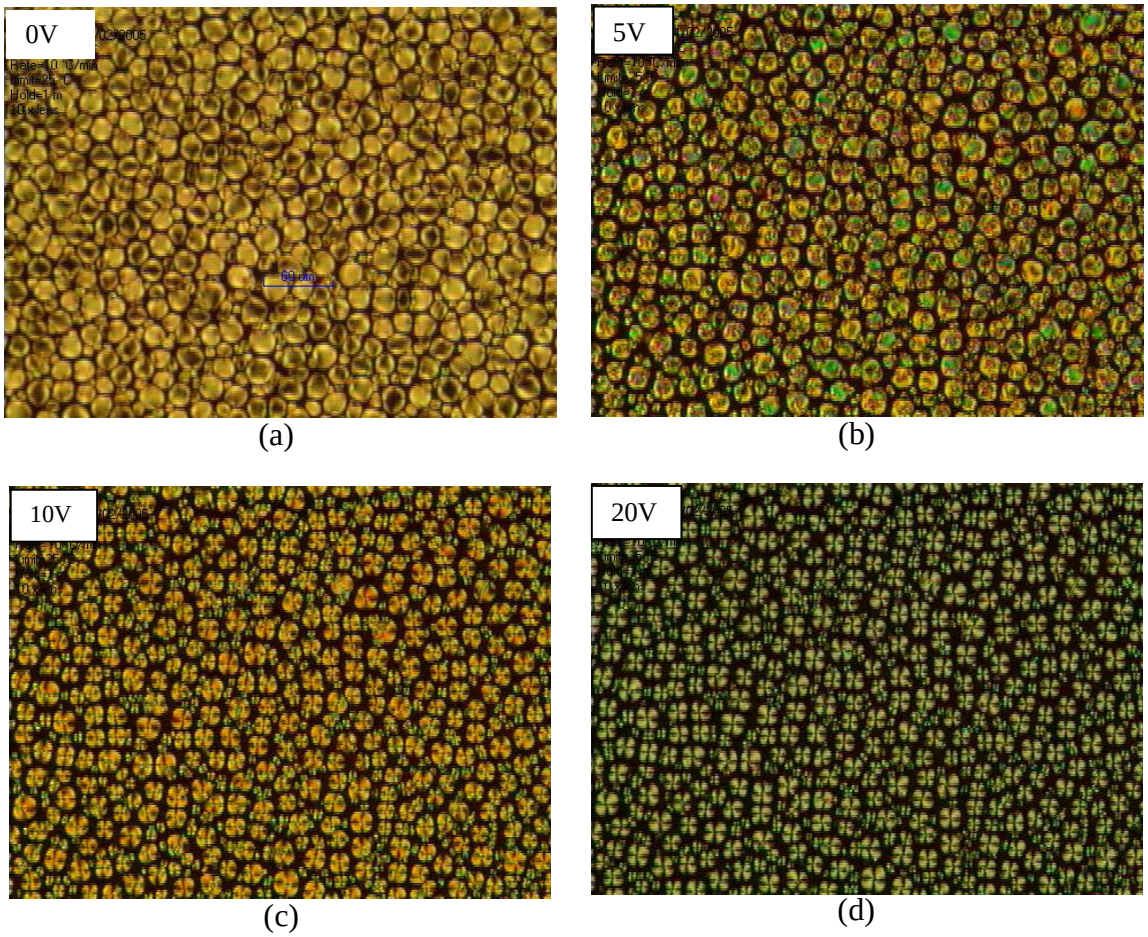

Fig. 3.8 Droplet orientation of dichroic (0.25% dye) polymer dispersed liquid crystal under electric field (a) 0 $V_{P\text{-}P}$, (b) 5 $V_{P\text{-}P}$, (c) 10 $V_{P\text{-}P}$ and (d) 20 $V_{P\text{-}P}$

The optical axis orientation, corresponding to the average nematic director alignment, varies randomly from droplet to droplet with no applied voltage. Upon application of an applied voltage across the film, we observed a bulk distortion of the LC droplet at low applied voltage. The rotation of bipolar axes is associated with the individual droplets, [figs. 3.8 (b, c)] in such a way that the bipolar axes tend to align along the direction of the applied field. However, at higher voltage (~$20V_{p\text{-}p}$) the LC droplets exhibits a well defined maltese type crosses [fig. 3.8 (d)].

B. Droplet morphology with azo dye

Fig. 3.9 shows the droplet morphology of DPDNLC with different concentration of azo dye at room temperature. It is seen that LC droplets distributed in DPDLC films forming spheroidal like bipolar droplet configuration [fig. 3.9 (a-f)] in a continuous matrix phase. Microscope observations revealed the presence of spherical LC droplets, even when a relatively large amount of azo dye concentration was introduced. It is also observed that the droplet size is relatively smaller and rather more uniform [fig. 3.9 (b-d)] at lower dye concentration (≤ 0.25%) than higher dye concentration. The average maximum diameter of liquid crystal droplets were 4.20, 4.50, 6.83, 9.90, and 19.60 μm for 0.0625, 0.125, 0.25, 0.5 and 1.0% DPDLC respectively. These results also supported our work done with anthraquinone dye [53] which may be due to the less free volume available for the dispersed low dye concentration droplets in the polymer matrix.

Further it is clear from the UV-VIS absorbance as shown in fig. 3.5, the azo dye in the films absorbs UV light and absorbance increases with the increase of dye concentration, which reduced the UV curing intensity results in an increase of the droplet size [54]. The lower UV cure rate results in a slower freezing of the PDLC once phase separation is induced, allowing more time for the liquid crystal to form larger droplets. It is reasonable to assert that the degree of polymerization, when the drops first form, is an important determiner of drop growth and eventual film morphology. Drop growth requires diffusion of liquid crystal material towards and diffusion of monomer and polymer away from the drop, and movement of the drop boundary in to the polymer rich region. Further with increasing the dye concentration the DPDLC mixture moves closer to the phase boundary resulting in less developed polymer matrix when phase separation occurs and more time liquid crystal to form large droplets.

Fig. 3.10 shows the influence of external field on the droplet morphology at room temperature. It can be seen that dichroic LC droplets have a bipolar configuration and their bipolar axes are randomly distributed inside polymer matrix relatively at low applied field 5 volt peak to peak for all the DPDLC films. However, at higher voltage (~$20V_{p\text{-}p}$) the LC droplets exhibits a well defined maltese type crosses for low concentration (≤ 0.25%) of azo dye [fig. 3.9 (b)] whereas the liquid crystal droplets containing 0.5 and 1.0 % azo dye, have

shown the nematic texture in these DPDLC films, which may be due to the incomplete phase separation with these concentrations of dye and due the much lower transition temperature from nematic to isotropic phase and large size of outcome droplets.

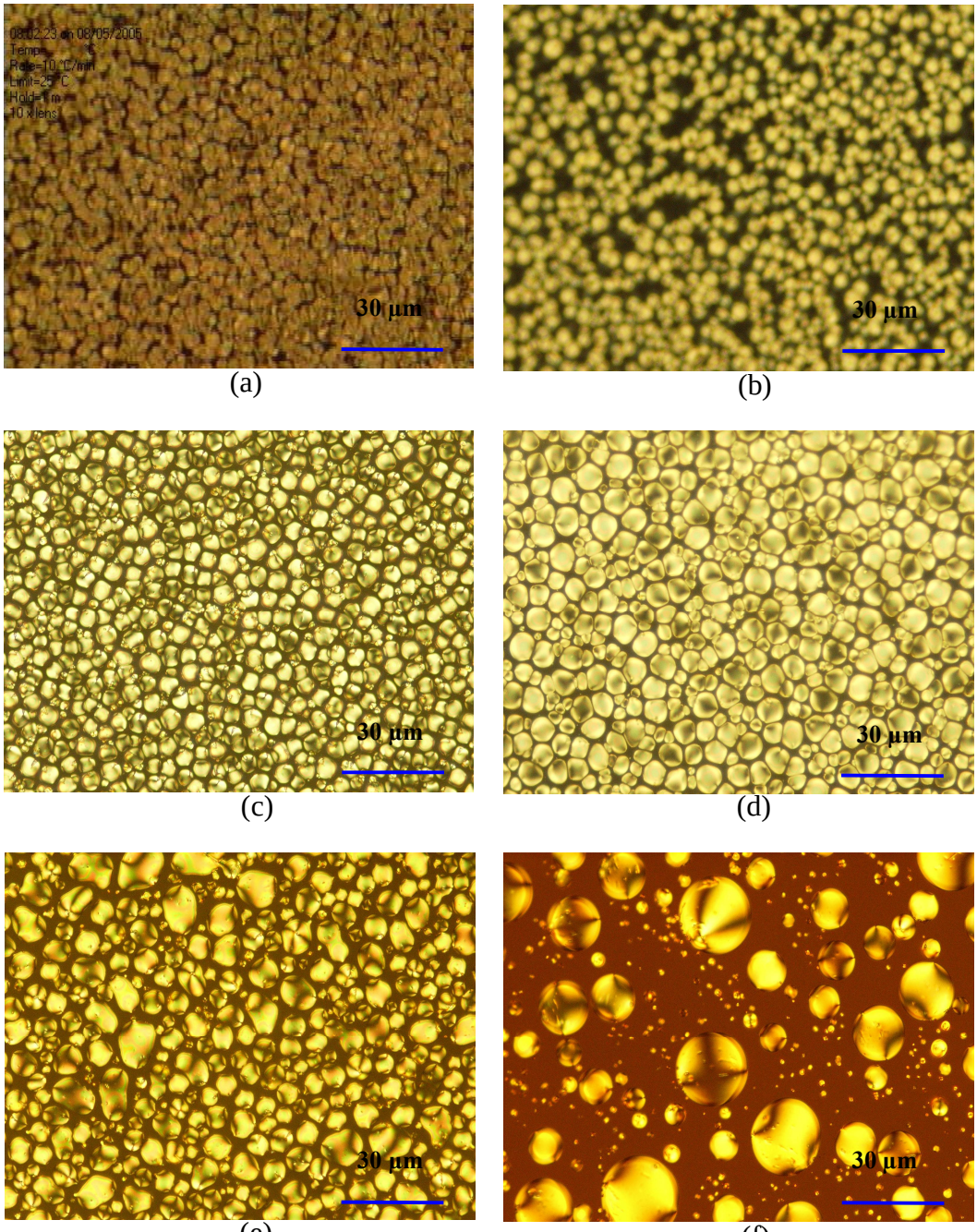

(a) (b) (c) (d) (e) (f)

Fig.3.9 Droplet morphology of DPDNLC at room temperature with varying azo (orange) dye contents (a) 0.0625% (b) 0.125% (c) 0.25% (d) 0.5% and (e) 1.0%, at a magnification of 100X

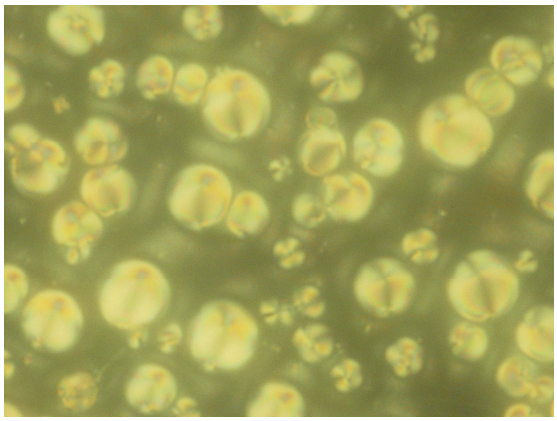

(a)

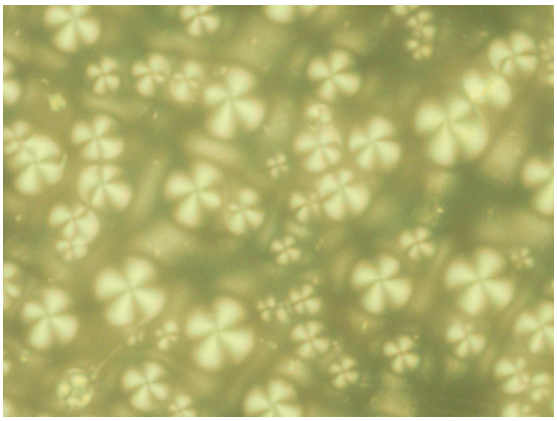

(a*)

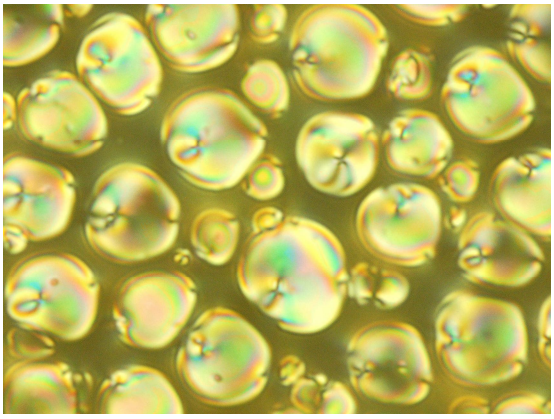

(b)

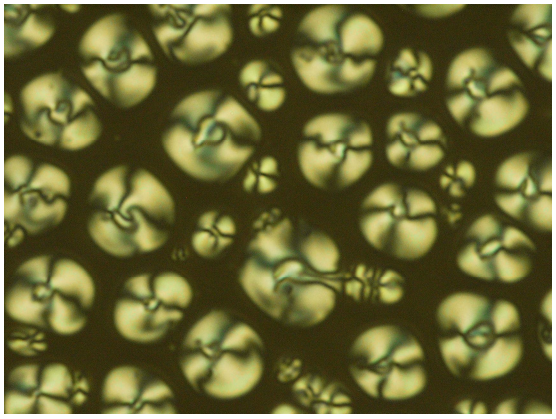

(b*)

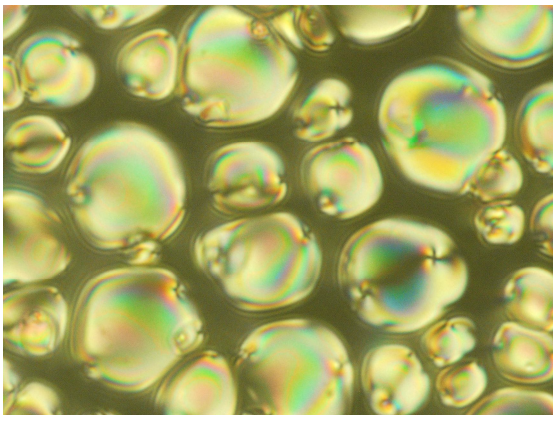

(c)

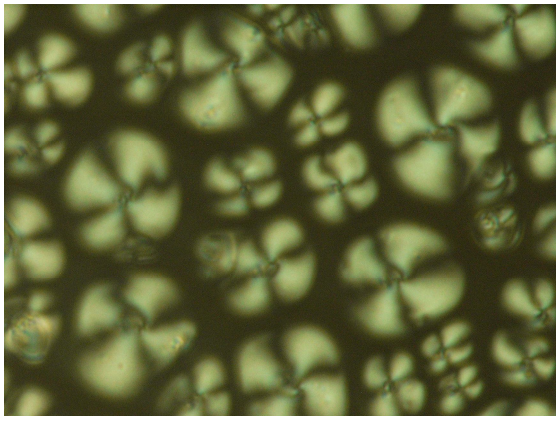

(c*)

Conti.

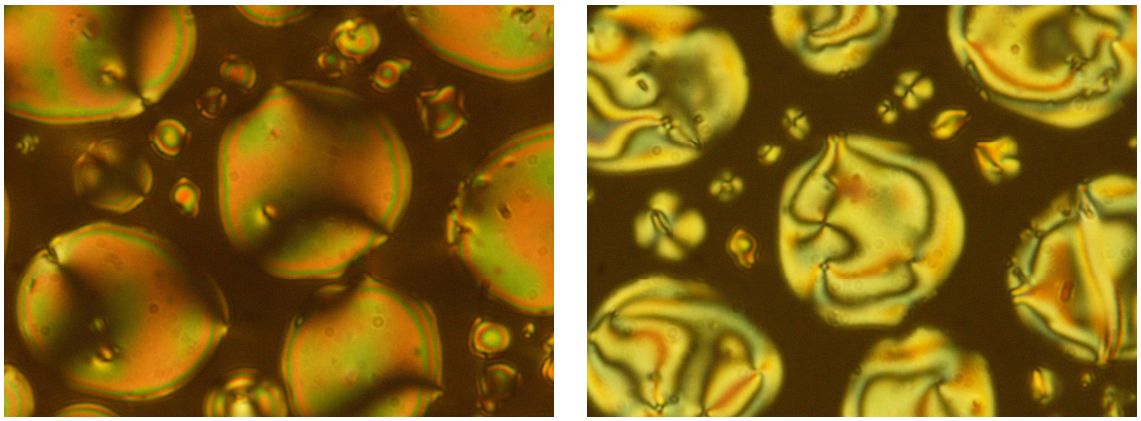

(d) (d*)

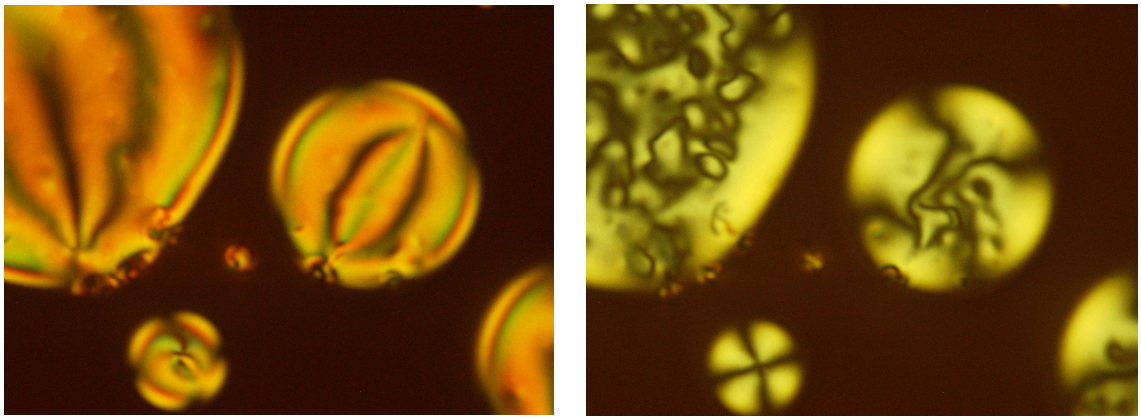

(e) (e*)

Fig.3.10 Droplet orientation of DPDLC films (0.0625% to 1.0 % azo dye) under electric field (a-e) 5 V_{P-P}, and (a*-e*) 20 $V_{P-P,}$ at a magnification of 500X at 20 ˚C

3.3.3 Electro-optics

A. Effect of anthraquinone dye

A.1 Transmission study

The light transmission as a function of applied voltage of PDLC and DPDLC films with corresponding different concentration of anthraquinone dye is shown in fig. 3.11. We see that as temperature increases, transmission decreases. One conceivable reason for this unusual behaviour may be the decrease in dichroic ratio with temperature due to stronger absorption by dye molecules leading to a lower transmission and also the variation of refractive index of the materials as a function of temperature.

Fig. 3.11 shows that the driving voltages from minimum (T_{min}) to maximum transmission (T_{max}) for these dichroic PDLC films are different. This finding implies that the value of threshold voltage V_{th} is approximately 8 V/µm for pure PDLC (without dye), where as the threshold voltages are approximately 4 V/µm, 2 V/µm and 1 V/µm for 0.125%, 0.25% and 0.5% dye respectively doped PDLC . It hints that as dye concentration increases, the threshold voltage decreases. It is expected that a small amount of anthraquinone dye dissolved in nematics liquid crystal makes it light absorbing and then can greatly enhance the orientational optical nonlinearity of the material which indicates that the photo-excited anthraquinone dye molecules induced a positive torque, similar to what has been predicted by Janossy et al [55].

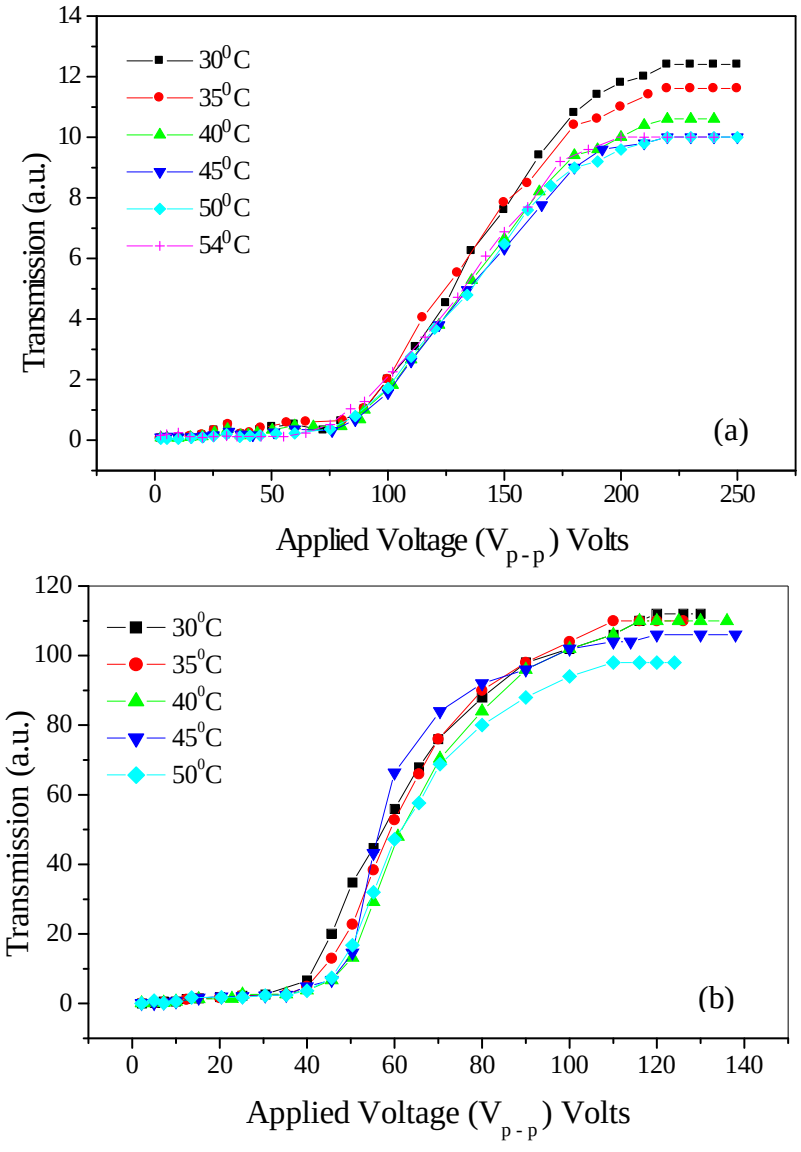

Conti.

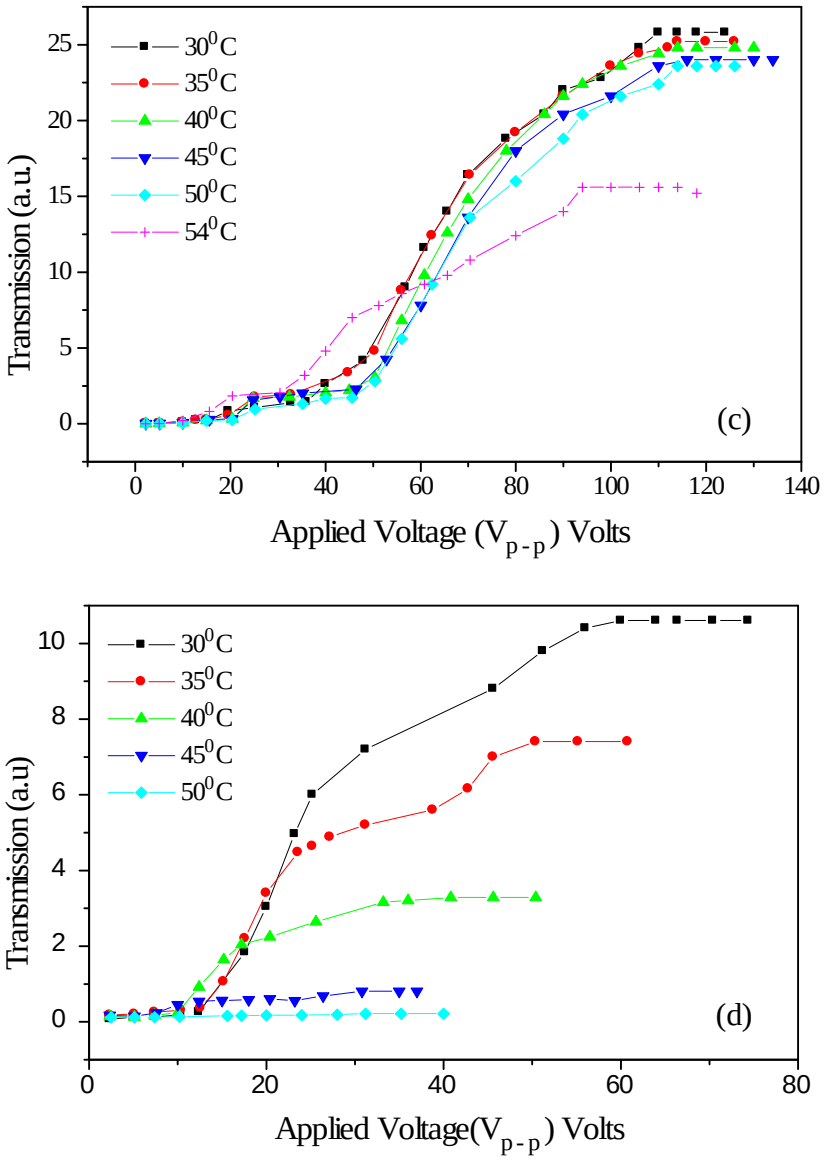

Fig. 3.11 Temperature dependence transmission characteristics of dichroic PDLC films with different anthraquinone dye contents: (a) without dye (b) 0.125 wt% (c) 0.25 wt% and (d) 0.5 wt% as a function of the applied voltage (50 Hz)

The absorption coefficient is obtained by measuring the transmittances of PDLC films containing different anthraquinone dye concentration. From the measured transmittances of the films, the dye extinction coefficient can be obtained using eq. (3.4). By least square fitting of the experimental data, we found that the straight line is least squares fit to the experimental data as shown in fig.3.12. The relationship between the maximum transmission of the films

and the dye concentrations is shown in fig. 3.13. The theoretical results fully support our experimental data.

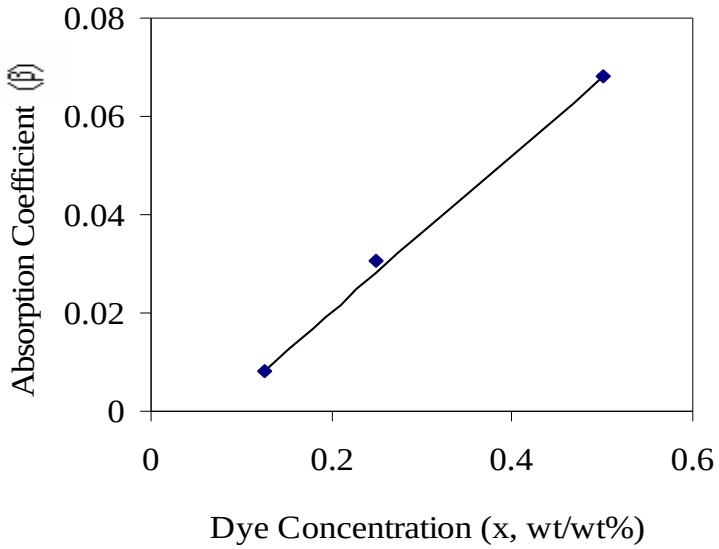

Fig. 3.12 OFF-state light absorption coefficient (β) Vs anthraquinone dye concentration, the straight line is least squares fit to the experimental data (squares)

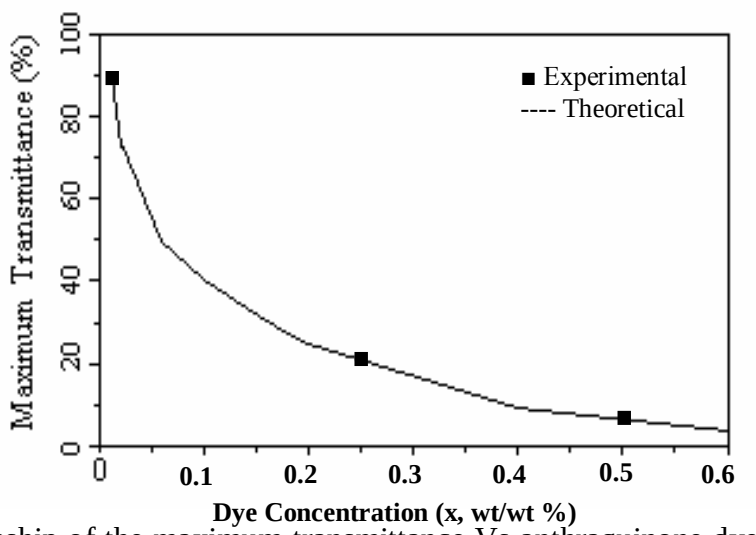

Fig. 3.13 Relationship of the maximum transmittance Vs anthraquinone dye concentration in the ON state at 30^0C, the theoretical line is fit to the experimental data

A.2 Contrast ratio

It can be seen from fig. 3.14 that as temperature increases contrast ratio decreases but in case of lower dye concentration dichroic PDLC film it is higher. A decrease in contrast ratio is also due to reduction in order parameter with increasing the temperature. At higher temperature DPDLC sample shows more absorption and produce lower transmission in comparison to low

temperature [fig.3.15]. The contrast ratios of dichroic PDLC were also measured as a function of the applied voltage. As shown in fig.3.16, the contrast ratio increases with increasing applied voltage, reaches a maximum and then maintains the constant value. The PDLC film with 0.125 wt% anthraquinone dye has higher contrast ratio with respect to other concentrations under same applied electric field.

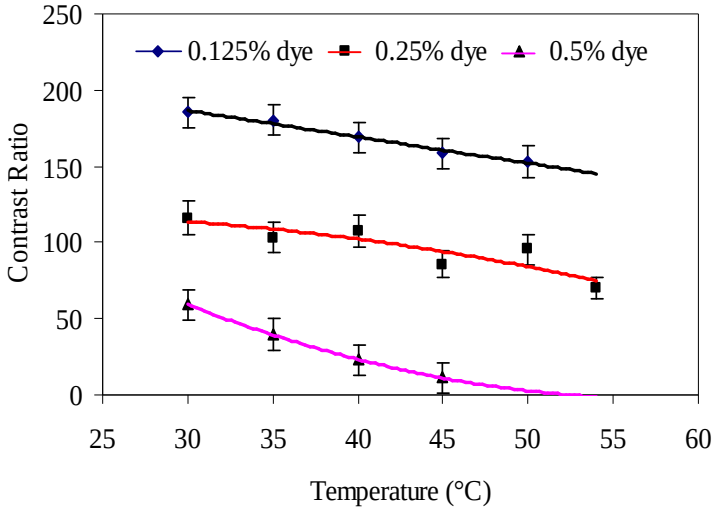

Fig.3.14 Temperature dependence contrast ratio of dichroic PDLC films

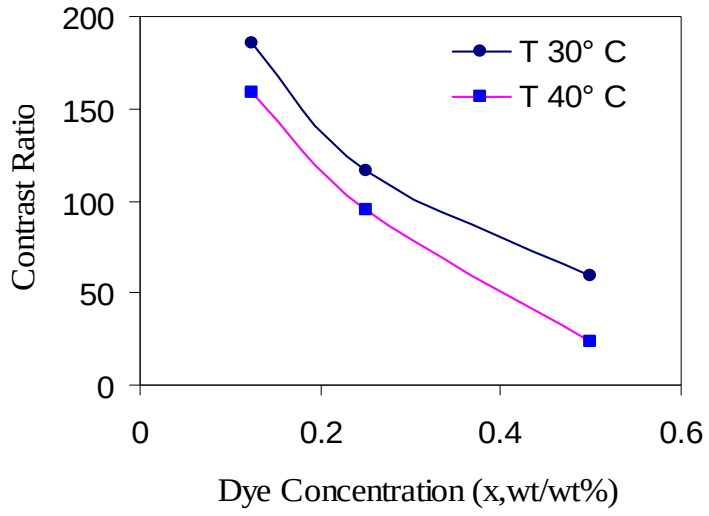

Fig.3.15 Anthraquinone dye dependence contrast ratio of dichroic PDLC films

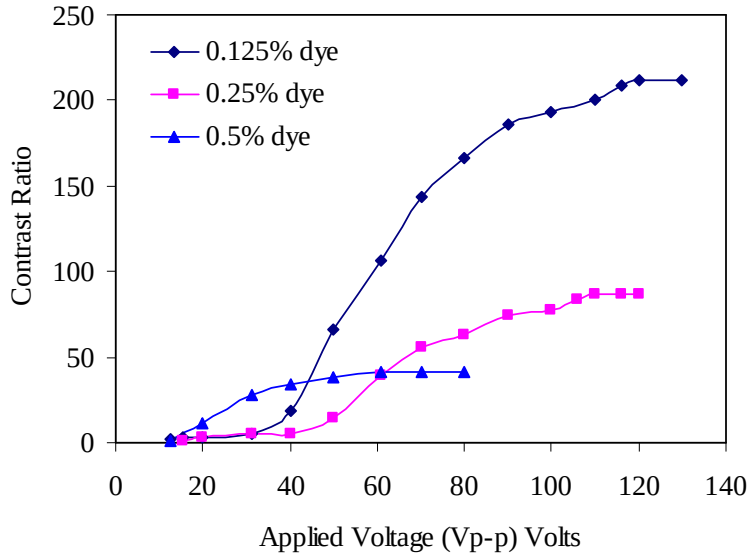

Fig.3.16 Contrast ratio of dichroic PDLC films as a function of applied voltage

B. Effect of azo dye

B.1 Transmission study

The temperature dependence of the light transmission as a function of applied voltage of DPDLC films with corresponding different concentration of azo dye is shown in fig.3.17. We found that as temperature increases, transmission decreases. One conceivable reason for this unusual behaviour may be the decrease in dichroic ratio with temperature due to stronger absorption by dye molecules leading to a lower transmission and also the variation of refractive index of the materials as a function of temperature. The transmission increases with applied electric field up to a fixed voltage, beyond which it is independent on the applied electric field for all the DPDLC films, indicating that the director orientation is almost completed at that electric field and transmission reaches its maximum. Very low transmission was observed initially at low applied voltage [inset 3.17(a)]. Fig. 3.17(f) illustrates the influence of transmission as a function of electric field for various dye concentration in DPDLCs. In comparing the transmission of DPDLC samples we found that the maximum transmission shifted to lower values with the increase of dye concentration because the ordinary refractive index of the liquid crystal matches more closely with that of the polymer (1.5028, observed experimentally in the lab) at low dye concentration at a temperature of 20 ˚C, as shown in fig. 3.18.

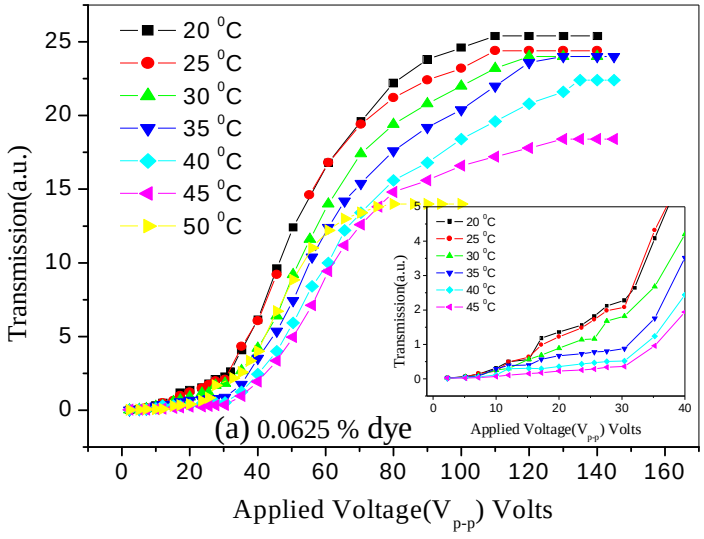
20 °C
25 °C
30 °C
35 °C
40 °C
45 °C
50 °C
Transmission(a.u.)
Applied Voltage(V p-p) Volts
(a) 0.0625 % dye

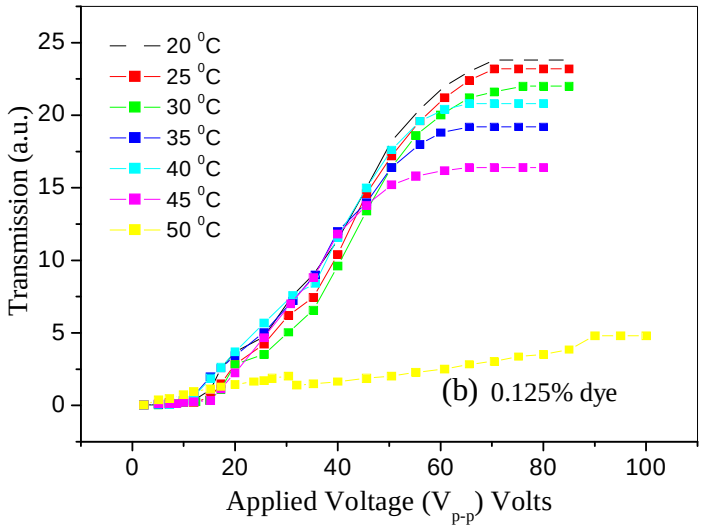
20 °C
25 °C
30 °C
35 °C
40 °C
45 °C
50 °C
Transmission (a.u.)
Applied Voltage (V p-p) Volts
(b) 0.125% dye

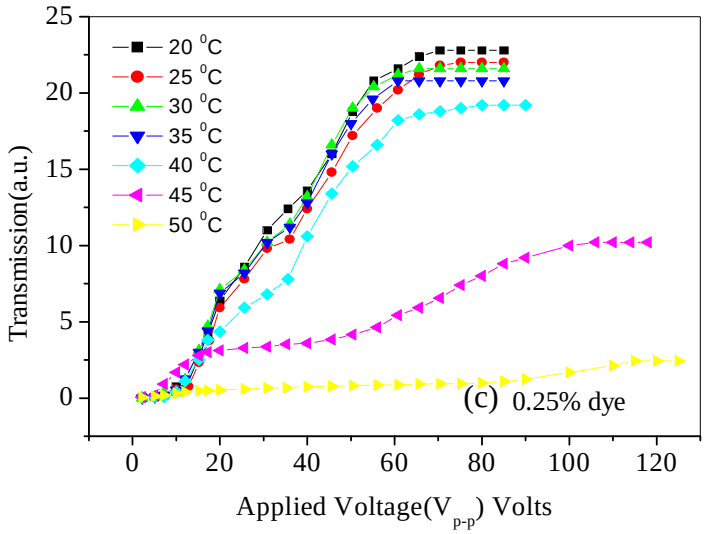
20 °C
25 °C
30 °C
35 °C
40 °C
45 °C
50 °C
Transmission(a.u.)
Applied Voltage(V p-p) Volts
(c) 0.25% dye

Conti.

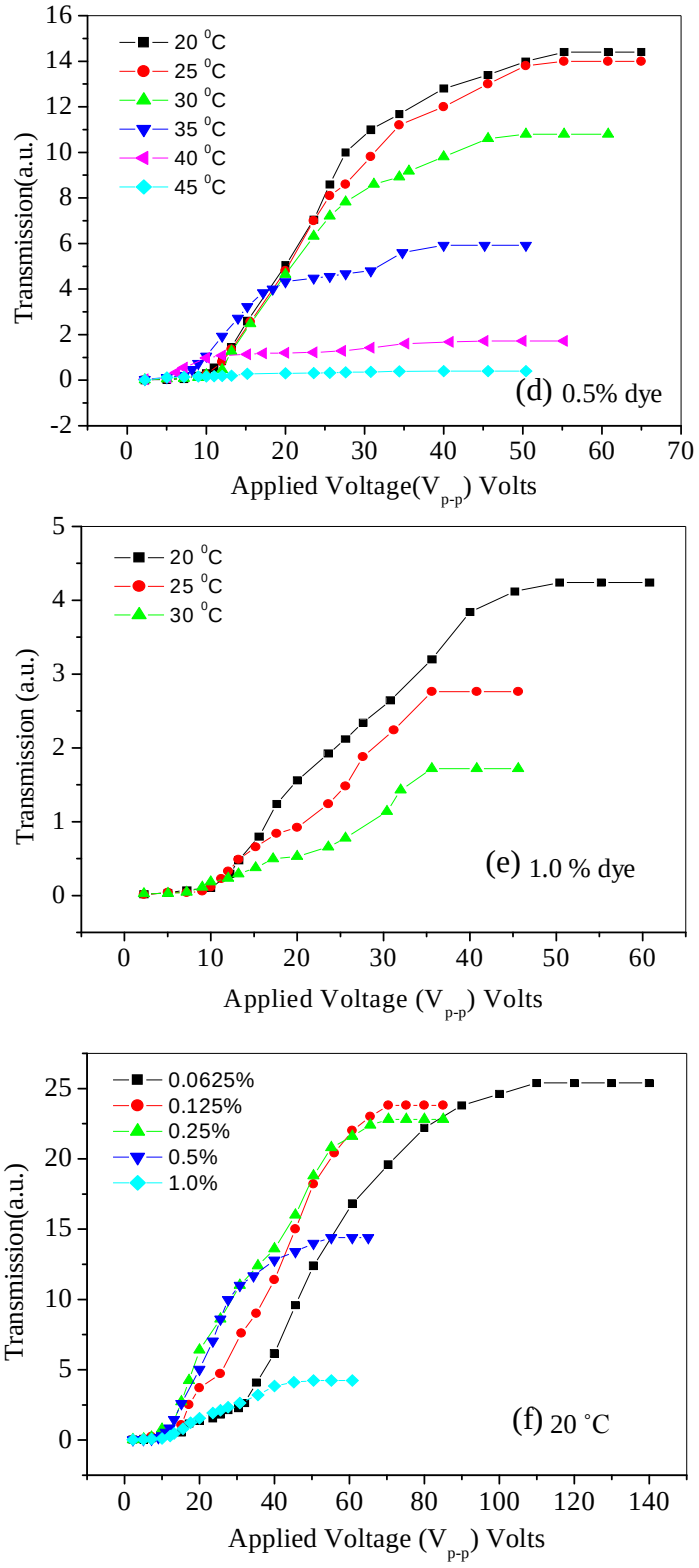

Fig. 3.17 Temperature dependence transmission characteristics of dichroic PDLCs with varing dye contents: (a) 0.0625 % (b) 0.125 wt% (c) 0.25 wt% (d) 0.5 wt% (e) 1.0 wt% and

(f) dye dependence transmission at 20 ˚C, as a function of the applied voltage at a fixed frequency 50 Hz

These results may also be related to the fact that higher absorbance of the visible light at higher dye concentration relatively as shown in fig. 3.5, results in lower transmission. It is noticed here that the DPDLC film containing 0.0625% dye concentration shows no absorption peak in visible region, it hints that the dye molecules with this small quantity reduces the scattering with the alignment of the liquid crystal molecules along the director and enhances transmission in the on state. The electro-optic characteristic of higher dye concentration PDLC films not responding to an electric field at higher temperature as shown in fig. 3.17 (d, e), can be explained by the LC in films being in the isotropic phase.

Fig. 3.17 shows that the driving voltages from minimum (T_{min}) to maximum transmission (T_{max}) for these dichroic PDLC films are different. This finding implies that the value of threshold voltage V_{th} is approximately 8 V/μm for pure PDLC (without dye) [53], where as the threshold voltages are approximately 4.0 V/μm, 2.0 V/μm, 1.7 V/μm, and 1.1 V/μm, for 0.0625%, 0.125%, 0.25% and 0.5% dye respectively for doped PDLC . It indicates that as dye concentration increases, the threshold voltage decreases. It is expected that a small amount of azo dye dissolved in nematics liquid crystal makes it light absorbing and then can greatly enhance the orientational optical nonlinearity of the material which indicates that the photo-excited azo dye molecules induced a positive torque, similar to what has been predicted previously by Raina et al [53] in the case of anthraquinone dichroic dye. We also presume that the threshold voltage in the dichroic PDLC is also affected by the droplet size. Because the surface effect is greater for smaller dichroic PDLC droplets therefore anchoring force from the surfaces is greater for the low dye concentration.

B.2 Contrast ratio and absorption coefficients

To investigate the effect of dye concentration on the contrast we measure the contrast ratio (T_{ON}/T_{OFF}). The accuracy in measurement is ± 5%. As shown in table 3.3, dye concentration increases from 0.0625% to 0.125%, the T_{ON} decreases slightly but T_{OFF} decreases much more which gives the maximum contrast relatively to all concentrations of dye ranging from 0.0625 to 1.0%. From the results we can infer that the maximum contrast is 2.55 times to the minimum contrast served in the experiment. The absorption coefficient is obtained by

measuring the transmittances of PDLC films containing different dye concentration. From the measured transmittances of the films, the dye extinction coefficient can be obtained using eq. (3.4). By least square fitting of the experimental data, we found that the straight line is least squares fit to the experimental data as shown in fig. 3.19. The theoretical results are in agreement with our experimental data. It is evident that refractive index decreases with increasing dye concentration. Table 3.3 shows the variation in contrast ratio as a function of dye concentration.

Table 3.3 Variation in Contrast ratio as a function of dye concentration

Dye concentration (wt %)	**T_{ON} (%)**	**T_{OF} (%)**	**Contrast ratio**
0.0625	90.00	1.10	81.81
0.125	86.33	0.825	104.64
0.25	81.793	0.816	100.23
0.5	51.024	0.694	73.52
1.0	15.024	0.368	40.82

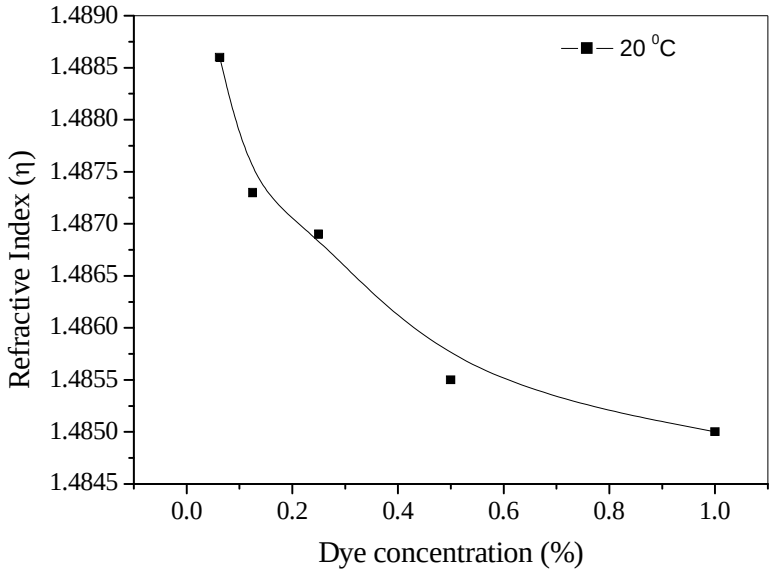

Fig. 3.18 Dependence of refractive index of dichroic PDLC as a function of dye concentration at temperature 20 ˚C

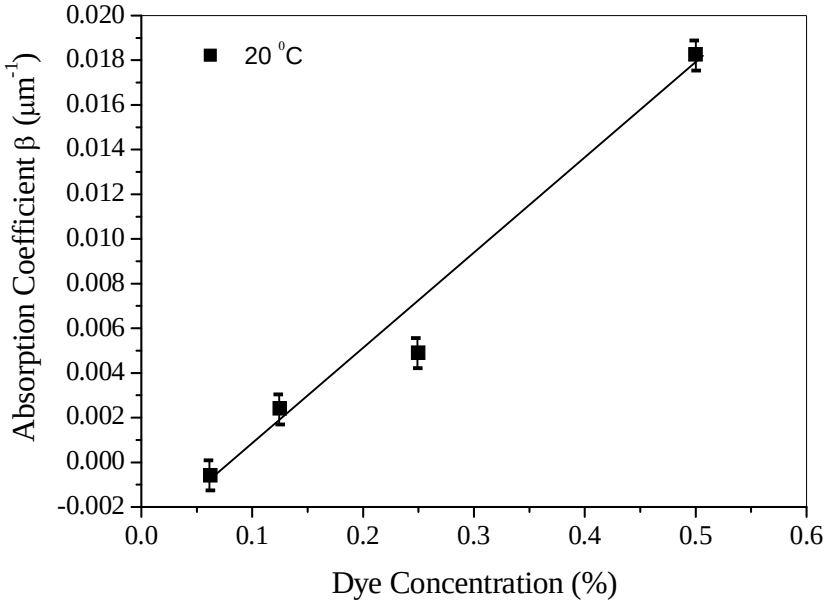

Fig. 3.19 Absorption coefficient (β) as a function of dye concentration, the straight line is least squares fit to the experimental data (squares)

3.3.4 Dielectric behaviour of DPDLCs

The dielectric measurements were carried out using a programmable automatic RCL meter (FLUKE PM 6306) in the frequency range 50Hz to 1MHz. The cells were calibrated using air and benzene as standard references. The frequency and bias dependence of the real and imaginary parts of the complex dielectric permittivity have been studied in detail at room temperature. The dielectric properties of DPDLC were made in the well aligend of applied voltages that produced alignment (and therefore, optical switching) of the LC phase. Dipolar relaxation and ion-conduction-related processes were observed for samples. The dielectric behavior gave information on the reorientational motions of dipoles and the conduction behavior of extrinsic ions in the samples. The relation between the complex dielectric constant (ε*), dielectric permittivity (ε') and dielectric loss is given by the following

$$\varepsilon^* = \varepsilon' - i\varepsilon'' \qquad (3.5)$$

At the low frequencies (especially below 1KHz) significantly large ε" values will arise from the a.c. conductivity of the medium; further, electrode polarization may appear as well, and interfacial polarization will be found if the system is not of a single homogeneous phase. The

experimentally determined dielectric absorption is a measure of energy dissipation in the medium and, in practice; most systems will show energy losses from processes other than dielectric relaxation. Usually these will be small and related to the a.c. conductivity of the medium.

$$= \varepsilon'(\infty) + \sum \frac{(\Delta\varepsilon_i)}{1 + (j\omega\tau_i)^{(1-\alpha_i)}} + \frac{A_1}{\omega^n} - i\frac{\sigma(ac)}{\varepsilon_o \omega} - iA\omega^m \qquad (3.6)$$

Here ε′(∞) is the relative permittivity at the high frequency limit, $\Delta\varepsilon_i, \tau_i$ and α_i are the dielectric strength, relaxation time and symmetric distribution parameter $(0 \le \alpha_i \le 1)$ of the i^{th} mode respectively. The third and fourth terms in eq. (3.2) represent the contributions of electrode capacitance and ionic conductance at low frequencies, where A_1 and n are constants. σ_{ac} is the ionic conductance and ε_o is the free-space permittivity. The measured dielectric absorption ε" contains a spurious contribution above 100 KHz due to the finite resistance of ITO coated electrodes. An additional imaginary term $A\omega^m$ is added to eq. (3.2) to account partially for the ITO coated effect; A and m are constants [56]. From the conductance measurements at different temperatures and frequencies the losses (ε") were evaluated using:

$$\varepsilon'' = \frac{G_m(\omega) - G_e(\omega)}{\omega C_o} \qquad (3.7)$$

where $G_m(\omega)$ and $G_e(\omega)$ is the conductance of the cell with material and of empty cell respectively. C_o is the empty cell capacitance.

The dispersion of dielectric permittivity (ε') and dielectric losses (ε") in the cells containing DPDLC with different concentration of dye, in the frequency range 50-10^6 Hz are shown in fig. 3.20 at room temperature at voltages of 5 and 10 volts. Fig. 3.20 shows the variation of dielectric losses for these DPDLCs and exhibit that more observant dielectric losses occurred in the higher dye concentration (higher droplet size) DPDLC. For samples with a large density of small droplets, a restricted interfacial surface region becomes increasingly important between the LC and polymer in which the permittivity is low because motions of the LC molecules are suppressed. The loss peak occurs in the higher frequency range for all DPDLC samples demonstrates that an overall dipole relaxation process is present together with a

substantial conductivity-related low-frequency process (mainly Maxwell–Wagner interfacial polarization due to the difference in conductivities between the droplets and polymer matrix).

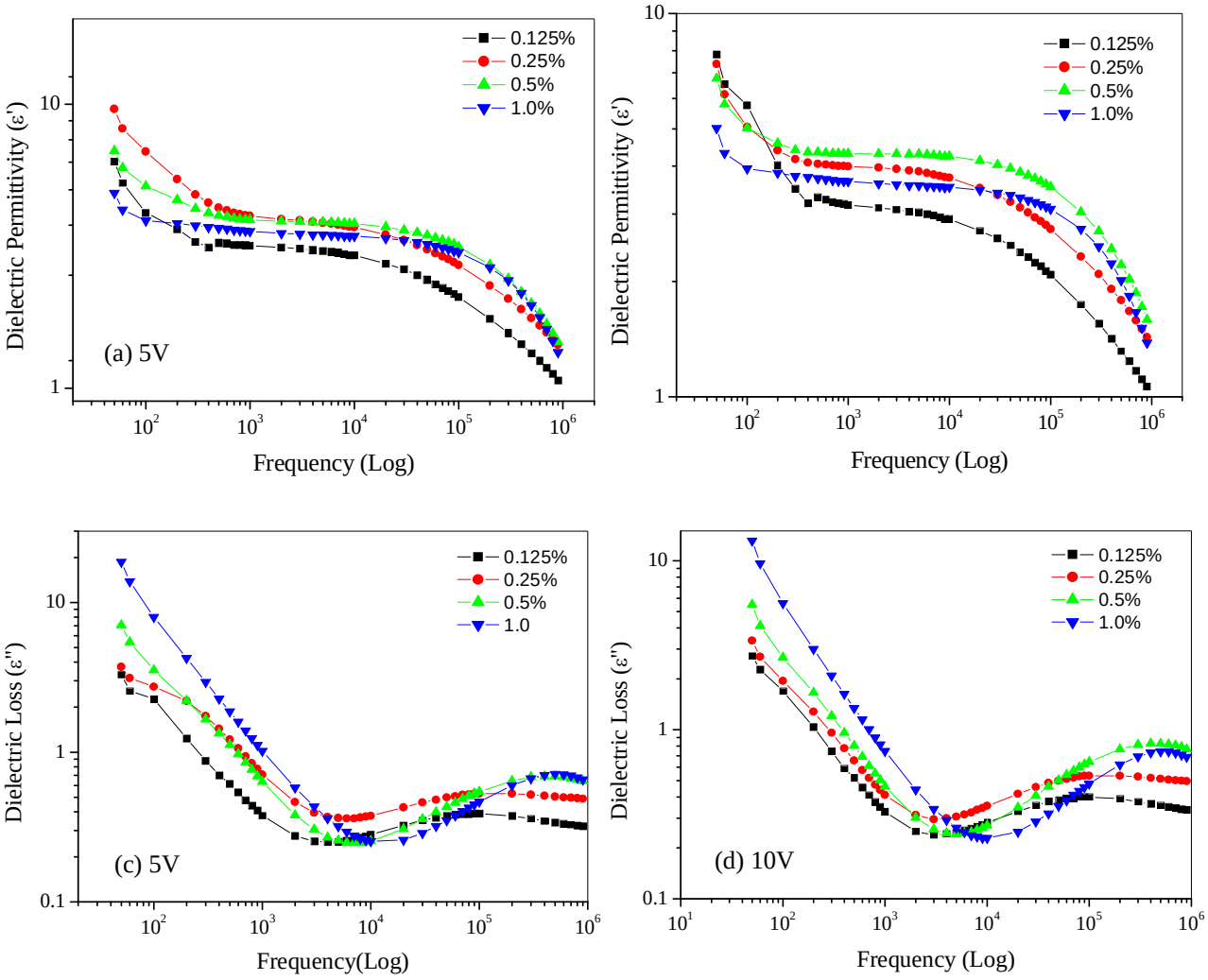

Fig.3.20 Room temperature real and imaginary part of the complex permittivity of dichroic PDLC with varying azo dye concentration at different voltage

The relaxation frequencies are 5.0 $\times 10^5$, 4.0373 $\times 10^5$, 1.0088 $\times 10^5$, and 8.9408 $\times 10^4$ Hz for 0.0625, 0.125, 0.50 and 1.0% dye with the corresponding dielectric losses 0.3864, 0.5216, 0.6853, and 0.7141 at applied field 5 volts. The relaxation frequencies are almost same at 10 volts and follow the same trends. These relaxation modes are also reflected in fig. 3.21 (a, b) in the form of Cole-Cole plots at different voltages. The addition of dye led to an increase of the dielectric absorption and to shift in the dielectric absorption peaks to lower frequencies

and can be attributed with major contribution being from the rotation of the transverse dipole moments about their long axis.

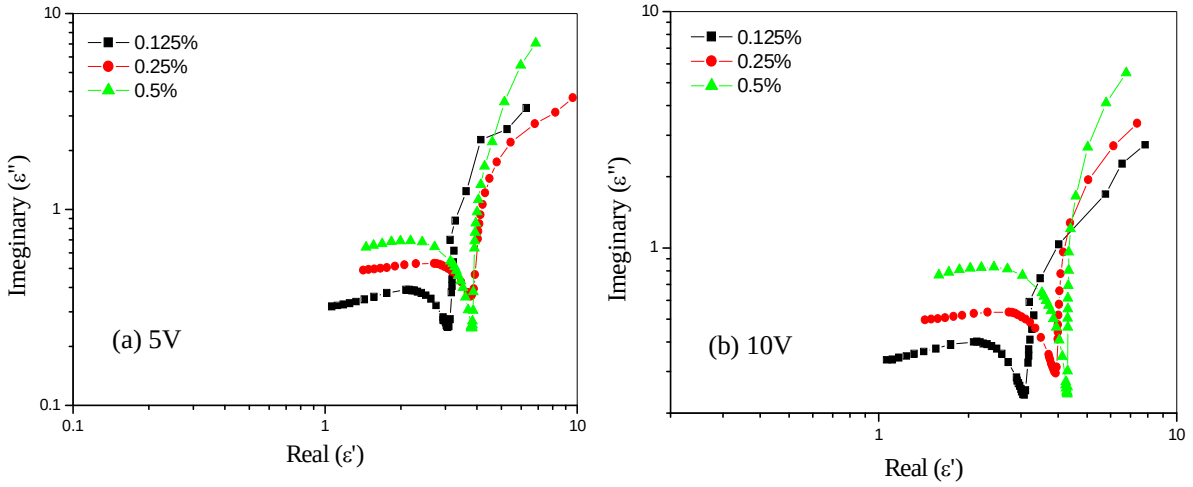

Fig. 3.21 Cole-Cole plots at different voltages of DPDLC at room temperature

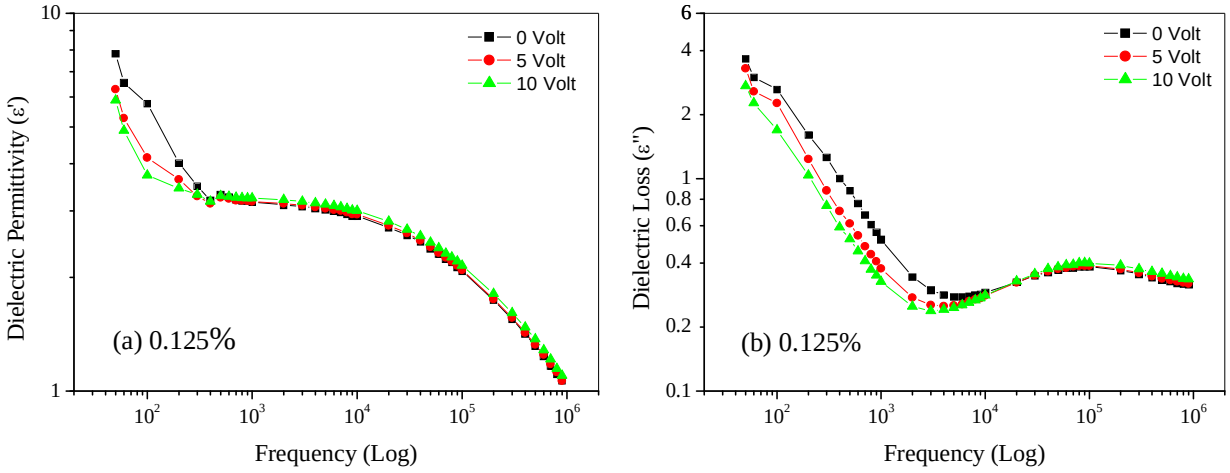

Fig. 3.22 Effect of applied voltage on real and imaginary part of the complex permittivity of DPDLC at room temperature

The dielectric permittivity (ε') with bias voltage 5 and 10 Volt at different dye concentration is shown in fig. 3.22. It is seen that dielectric permittivity is more predominant at low frequencies. Small changes in the real permittivity (ε') and loss factor (ε") with increasing applied voltage from 0 to 10 volts were observed for the DPDLC materials in low frequency range because the need of higher voltage to director realignment of the LC component.

References

[1] J. L. Fergason, SID Int. Symp. Dig. Tech. Pap. **16** (1985) 68.

[2] P. S. Drzaic, J. Appl. Phys. **60** (1986) 2142.

[3] J. W. Doane, N. A. Vaz, B. G. Wu and S. Zumer, Appl. Phys. Lett. **48** (1986) 269.

[4] N. A. Vaz, G. W. Smith and G. P. Montgomery, Mol. Cryst Liq. Cryst. **146** (1987) 1.

[5] P. S. Drazaic, Mol. Crys. Liq. Cryst. **154** (1988) 289.

[6] E. Dubois Violette and O. Parodi, J. Phys. C, **4** (1969) 57.

[7] H. G. Craighead, J. Cheng, and S. Hackwood, Appl. Phys. Lett. **40** (1982) 22.

[8] N. Kawatsuki and H. Ono, J. Appl. Poly. Sci. **55** (1995) 911.

[9] E. Shimada and T. Uchida, Jpn. J. Appl. Phys. **31** (1992) 352.

[10] J. W. Doane, A. Golemme, J. L.West, J. R. Whitehead and B. G. Wu, Mol. Cryst. Liq. Cryst. **65** (1998) 511.

[11] S. Pane, M. Caporusso and H. Hakemi, Liq. Cryst. **23** (1997) 861.

[12] L. C. Chien, C. Lin, D. S. Fredley and J. W. McCargar, Macromolecules, **25** (1992) 133.

[13] P. P. Kundu, G. Verma and K. K. Raina, J. App. Poly. Sci. **87** (2003) 284.

[14] G. Sumana and K. K. Raina, J. App. Poly. Sci. **87** (2003) 1215.

[15] P. Malik, Jasjit K. Ahuja and K. K. Raina, Current App. Phy. **3** (2003) 325.

[16] G. Sumana and K. K. Raina, J. App. Poly. Sci. **94** (2004) 159.

[17] G. Sumana and K. K. Raina, Current App. Phy. **5** (2005) 277.

[18] P. Malik and K. K. Raina, Optical Materials, **27** (2004) 613.

[19] P. Malik, Pankaj Kumar and K. K. Raina, 7^{th} Int. conf. on optoelectronics, Fiber Optics & Photonics, Cochin, India (2004) 51.

[20] K. K. Raina, Pankaj Kumar and G. Sumana, Asian Journal of Chemistry, **18** 5 (2006) 3384.

[21] K. K. Raina, Pankaj Kumar and Praveen Malik, Bull. of Mat. Sci. **29** (2006) 596.

[22] C. V. Rajaram, S. D. Hudson and L. C. Chien, Chem. Mater. **7** (1995) 2300.

[23] C. V. Rajaram, S. D. Hudson and L. C. Chien, Chem. Mater. **8** (1996) 2451.

[24] H. K. Lee, A. Kanazawa, T. Shiono and T. Ikeda, Chem. Mater. **10** (1998) 1402.

[25] O. Zaplo and J. Stumpe, Mol. Cryst. liq. Cryst. **213** (1992) 153.

[26] T. Kajiyama, H. KiKuchi and K. Nakamura, Proc. SPIE, **1911** (1993) 111.

[27] P. Palffy-Muhoray, M. A. Lee and J. A. West, Mol. Cryst. liq. Cryst. **179** (1990) 445.

[28] F. Simoni, G. Cipparrone, C. Umeton, G. Arabia and G. Chidichimo, Appl. Phy. Lett. **54** (1989) 896.

[29] F. Simoni, G. Cipparrone and C. Umeton, Appl. Phy. Lett. **57** (1990) 1949.

[30] F. Simoni, G. Cipparrone, D. Duca and I. C. Khoo, Opt. Lett. **16** (1991) 360.

[31] D. Bauman, Mol. Cryst. liq. Cryst. **159** (1988) 197.

[32] D. Bauman and W. Haase, Mol. Cryst. liq. Cryst. **168** (1989) 155.

[33] D. Bauman and H. Moryson, J. mol. Struct. **404** (1997) 113.

[34] D. Bauman, Z. X. Fan and W. Haase, Liq. Cryst. **6** (1989) 239.

[35] D. Bauman, Z. X. Fan and W. Haase, Acta Phys. Polon. A **80** (1991) 545.

[36] I. Janossy and A. D. Lloyd, Mol. Cryst. Liq. Cryst. **203** (1991) 77.

[37] I. Janossy, Phys. Rev. E **49** (1994) 2957.

[38] D. Voloshchenko, A. Khyzhhyakk, Y. Reznikov and V. Reshetnyak, Jpn. J. Appl. Phys. **34** (1995) 566.

[39] F. Simoni, L. Lucchetti, D. E. Lucchetta and O. Francescangeli, Opt. Express **9** (2001) 85.

[40] L. Lucchetti, D. E. Lucchetta, O. Francescangeli and F. Simoni, Mol. Cryst. Liq.Cryst. **375** (2002) 641.

[41] L. Lucchetti, M. D. E. Fabrizio, O. Francescangeli, F. Simoni and J. Nonlin. Opt. Phys. & Mat. **11** (2002) 13.

[42] P. S. Drzaic, R. Wiley and J. McCoy, Proc. SPIE, **1080** (1989) 41.

[43] S. Zumer, Phys. Rev. A **37** (1988) 4006.

[44] Jr. G. P. Montgomery, J.L. West and W. J. Tamura Lis, Appl. Phys. **69** (1991) 89.

[45] J. R. Kelly and D. Seekola, in Liquid Crystal Displays and Applications**,** J. W. Doane and Z. Yaniv (eds.), SPIE, **1257** (1990) 17.

[46] A. Miyamoto, H. Kikuchi, S. Kobayashi, Y. Morimura and T. Kajiyama, Macromolecules, **24** (1991) 3915.

[47] D. K. Hale, J. Mat. Sci. **11** (1976) 2105.

[48] Jin-Jei Wu, Chih-Ming Wang, Wang-Yang Li and Shu-Hsia Chen, Jpn. J. Appl. Phys. **37** (1998) 6434.

[49] G. W. Smith, Phys. Rev. Lett. **70** (1993) 198.

[50] J. E.Hall and D. A. Higgins, Poly. Mat. Sci. Eng. **88** (2003) 186.

51] E. Mei, D. A. Higgins and Langmuir **14** (1998) 1945.

[52] (a) W. Denk, J. H. Strickler and W. W. Webb, Science **248** (1990) 73.

(b) C. Xu, W. Zipfel, J. B. Shear, R. M. Williams and W. W. Webb, Proc. Nat. Acad. Sci. **93** (1996), 10763.

[53] Pankaj Kumar and K. K. Raina, Current Appl. Phy. **7** (2007) 636.

[54] Jr. G. P. Montgomery, J. L. West and W. J. Tamura Lis, J. Appl. Phys. **69** (1991) 1605.

[55] I. Janossy, A. D. Lioyd and B. S. Wherrett, Mol. Crys. Liq. Cryst. **179** (1990) 1.

[56] M J. David, John E Jensen and M. Anna Lackner, Mol. Cryst. Liq. Cryst. **68** (1981) 137.

Chapter 4

Dichroic Polymer Dispersed Ferroelectric Liquid Crystal System

Overview

Ferroelectric liquid crystals (FLCs) has developed in a new class of novel organic materials with excellent properties useful for fast electro-optical devices like flat screens, optical shutters etc. In the recent years there has been more focus on the material synthesis and their characterization for these systems. Polymer dispersed ferroelectric liquid crystal (PDFLC) composite films usually comprise of low molecular-mass liquid crystal (LC) dispersed (as micro-nano sized LC droplets) in optically transparent polymer matrix. In this chapter, we have made an effort to prepare PDFLC and some dichroic PDFLC (DPDFLC) films of these materials by polymerization induced phase separation technique using ferroelectric liquid crystal, UV curable polymer NOA 65 doped with anthraquinone blue dye. An effort also has gone in detail to investigate their FLC properties in UV curable adhesive with varying concentration of dye. The detailed investigation of droplet morphology, droplet orientation and optical responses such as transmission, spontaneous polarization, threshold voltage, contrast ratio, and response time as a function of applied voltage, temperature and dye concentration are given. These films show microseconds switching response and higher transmission at low dye concentration.

4.1 Introduction

The dispersion of ferroelectric liquid crystals in a polymer matrix also gives rise to new materials which show several interesting electro-optic effects. These composites are known as polymer dispersed ferroelectric liquid crystal (PDFLCs). PDFLC have been demonstrated to be at least three orders of magnitude faster than nematic based displays commonly used in portable computers. The switching field of PDFLC films depends on a variety of factors amongst which film morphology plays a crucial role [1-3], which is strongly dependent on composition, curing parameter, nature, kind of polymer, viscosity of the polymer, structure of

the polymer, and also the mutual solubility of ferroelectric liquid crystal (FLC) and prepolymer [4-6]. It is thus obvious that PDFLCs are very complex systems that require precise morphological and processing control. These materials exhibit unique linear and nonlinear optical properties, which are expected to find use in liquid crystal displays (LCDs).

It has also been reported that the contrast ratio and viewing angle of ferroelectric liquid crystal devices are superior to all other LC displays. It has also been reported that the performance of a PDFLC device relies on the uniformity of alignment of the liquid crystal molecules in the device. Several research groups [7, 8] investigated the behavior of ferroelectric liquid crystal (FLC) in polymer matrix although little effort has gone into understanding their morphological behavior on the basis of the concentrations of dichroic dye doped in the PDFLC.

Lee et al. [8] studied very large elliptical droplets, which are attached to the surfaces of an aligning substrate and investigated that rubbing process in PDFLC significantly improves the electro-optic switching times. This group suggested that the phase sequence and pitch (<4 μm) of FLC material also influence the size and shape of LC droplets. Molsen et al. [9] predicted that a bistable switching effect occurs in PDFLC films when the droplet size is sufficiently small. Patel et al. [10] have observed bistable switching in PDFLC samples using the ferroelectric mixture ZLI-3654. Karapinar et al. [11] reported the electro-optic properties of FLC material dispersed in polymer matrix and aligned the FLC by shearing during the phase separation process. Shearing was done by gently shearing a slide during the exposure of the sample to UV light. Zyryanov et al. [12] have created a scattering PDLC display using a FLC material DOBAMBC. Heppke et al. [13] reported the electro-clinic effect in chial smectic A material dispersed in UV polymer and noticed switching time 100 μsec to 170 μsec. Pozhidaev et al. [14] studied PDFLC samples and compared the electro-optic properties with pure FLC (FLC 3309C) material. The spontaneous polarization (P_s) value decreases one order of magnitude in comparison to pure FLC material. He suggested that a decrease in P_s may be due to the non-switching region existed near the polymer boundaries and strong anchoring of LC droplet with the polymer wall. An increase in SmC*/SmA transition in PDFLC sample by about 4.1K higher than FLC was noticed. This unexpected shift may be due to strong interaction with the surrounding polymer. Kundu et al. [15] reported the

influence of UV polymer on electro-optic properties of FLC in PDFLC samples and observed a decrease in P_s and increase in switching time.

Therefore, in the present work, an attempt has been made to study the behaviour of ferroelectric LC droplets dispersed in polymer matrices with the addition of dichroic dyes. Advanced experimental and theoretical studies on the dichroic polymer dispersed liquid crystal materials are in evolution to explore the physical parameters for the opto-electrical device and displays using ferro-electric liquid crystal. Thus in this chapter efforts were made to study the influence of dye, electric field, temperature and liquid crystal droplets size on film morphology, switching properties, electro-optic properties and also to understand the structure-property correlation of the complex system that require precise morphological and processing control. Specifically, the invention relates to DPDFLC materials based on polymers and ferroelectric liquid crystal containing dichroic dyes. In OFF state, without voltage, the DPDLC film is light scattering owing to the differences in refractive index between polymer and liquid crystal and is furthermore absorbent owing to the molecules of dye whose orientation, which dictated by that of the liquid crystal, varies randomly from one domain to the other. The electrical and optical characteristics of the DPDFLCs are such that an ac electric field applied to the FLC molecule makes its helical structure bistable resulting in optical switching [16, 17].

4.2 Experimental

4.2.1 Materials

To study the effect of dichroic dye LC film morphological, polarizing switching and their optical properties, different DPDFLC samples were prepared using the pervious standard PIPS/SIPS method. These samples were prepared using chiral ferroelectric smectic C* liquid crystal FLC-I and FLC-II with UV curable polymer NOA-65. Morphology and phase behaviour of dichroic polymer dispersed ferroelectric liquid crystal (DPDFLC) with different dye concentrations (wt./wt.) of anthraquinone dichroic dye, were studied as a function of applied voltage and temperature. Chemical structure, phase sequence and some physical parameters of the chiral ferroelectric smectic C* liquid crystals, polymer and anthraquinone dichroic dye, used in the study, are given in chapter 2. In order to ensure proper and utmost

mixing of dichroic dye in ferroelectric liquid crystal, first dye was doped with the liquid crystal and then dispersed in the polymer matrix in the wt./wt. ratio. The material FLC-I was heated at its clearing temperature (86 ^{0}C) and mixed with the NOA 65 in a fixed 50:50 weight ratio, where as PDFLC samples with material FLC-II were prepared in an 80:20 wt/wt ratio in a vial and this homogenous mixture was heated to isotropic temperature (129 ˚C) and simultaneously shaken in a vacuum chamber. In order to study the morphology and to understand the effect of dichroic dye on the FLC molecules, transmission, contrast ratio, spontaneous polarization and response time, indium tin oxide (ITO) coated glass substrates were used in sample cells.

4.2.2 Polarization switching

It is one of the most precise methods for the measurement of electro-optic parameters in FLC, PDFLC and DPDFLC materials [6]. The experimental setup used for the measurements of electro-optic parameters is shown in the fig 4.1. Here the triangular voltage (V_{in}) is applied across the PDFLC and DPDFLC sample and the output (V_{out}) is taken across a standard resistor R. The electric field was applied to the PDFLC sample through an electrode connected to conducting ITO substrates by a function generator and output is obtained on a four channel digital storage oscilloscope (Tektronix TDS 2024 having 2.0 GS/s sample rate and 200 MHz bandwidth) interfaced with computer for further data acquisition. The current and voltage pulses were detected on a digital storage oscilloscope across a resistor. In order to study the molecular re-orientation processes associated with the helix dynamics, the symmetric triangular wave pulses were applied to the samples. It reorients the dipoles between two stable polarization states (up and down). As the field is switched on, molecular alignment in the form of voltage drop is detected on the storage oscilloscope. We believe that in the PDFLC sample within the ferroelectric phase range, for a certain applied voltage V_{IN}, the current I response consists

(a) capacitive term I_C (a differentiating component which shows an abrupt jump when the slope of applied voltage changes abruptly)

(b) ionic conduction term I_R

(c) the third term is polarization current I_P, due to the charge induced by the dipole realignment in the form of polarization hump.

The schematic representation of these responses is shown in fig. 4.1. The Instantaneous value of the output current over resistor R can be presented as

$$I = I_R + I_C + I_P = \frac{V_{IN}}{R} + C\frac{dV_{IN}}{dt} + \frac{dP}{dt} \qquad (4.1)$$

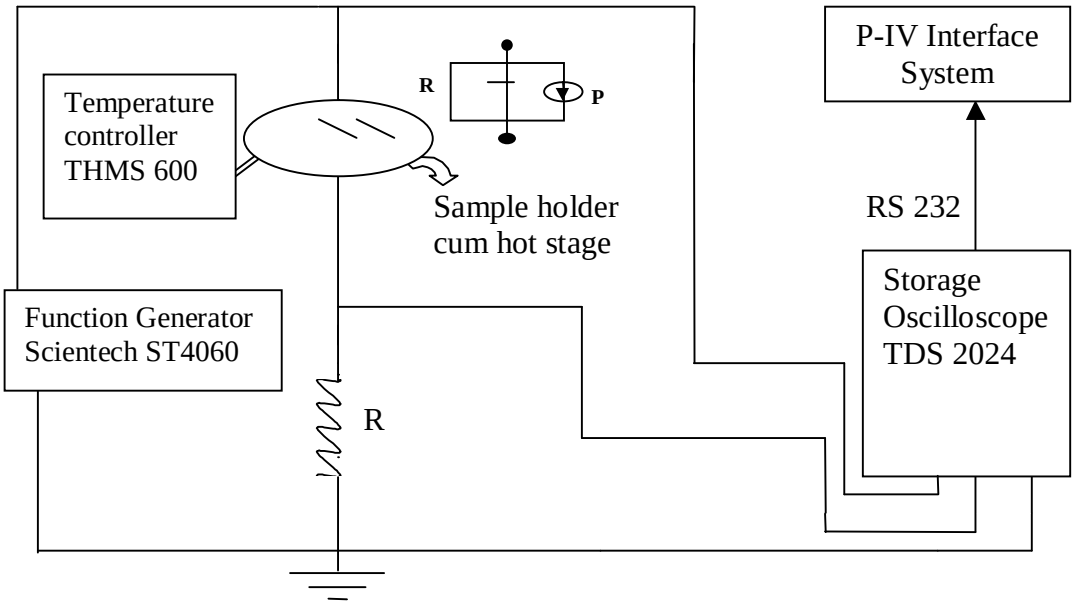

Fig. 4.1 Experimental set up to study the polarizing switching response using reversal field technique

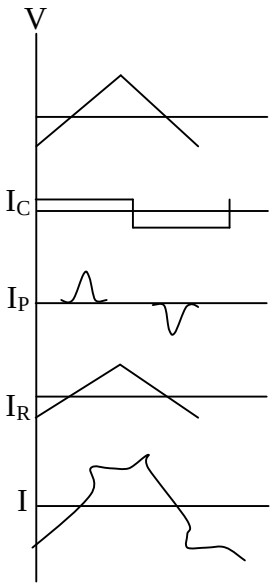

Fig. 4.2 Waveform of the output wave by the resistor method

4.2.3 Spontaneous polarization (P_s) measurement

The spontaneous polarization is the macroscopic polarization, which the sample attains due to the coupling of molecular polarization P with the electric field E within the smectic layer. The sample gets poled and attains a macroscopic polarization. At this stage the helix of the FLC in PDFLC mixture confined in the cell of a particular thickness unwinds, the macroscopic polarization becomes non-zero and the sample gets spontaneously polarized. This polarization was determined by applying the symmetric triangular wave (50Hz frequency) and separating the resistive and capacitive term from the polarization term by drawing a base line. The hump of the polarization is directly associated with dipole reorientation, corresponding to the switching between uniform stable states. Every reorienting dipole imparts a charge impulse and contributes to the polarizing reversal peak. Thus the peak incorporates total contribution of reorientation dipoles while switching between uniform states. The area under the hump is a measure of the spontaneous polarization, which is given by

$$P_s = \frac{A(i \times t)}{R(Area\,of\ Sample)} \tag{4.2}$$

Where A (i×t) is the area under the curve measured by integrating the polarization hump in terms of voltage and time [6, 7]. Thus by calculating the area of the curve by knowing current and time representing along the y-axes and x-axes, respectively the P_s can be determined. The magnitude of P_s in the ferroelectric phase of PDFLC films decrease with the rise of temperature and finally becomes zero at T_c*A, it obey the power law and given by the equation

$$P_s = P_o (T_c - T)^{\beta} \tag{4.3}$$

The critical exponent β should be 0.5 predicted by the mean field theory.

4.3 Results and discussion

4.3.1 DPDFLC morphology with FLC-I

A series PDFLC material doped by dichroic dye (DD) was obtained by the variety of the starting composition. Optical microscopic images of NOA65 dispersed FLC-I with varying dye contents are shown in fig. 4.3. It depicts that FLC droplets are not uniform as in the case of nematic LC dispersion, however the low dye concentration DPDFLC sample showed uniformity and comparatively smaller size of the droplets. The non-uniformity of FLC

droplets relatively in higher dye concentration DPDFLC may be due to the inherent property of FLC materials. The phase changes of PDFLC material can be seen from table 4.1, with an increase in isotropic temperature about 9-10 ^{o}C to the isotropic transition temperature of the FLC. The increase in dichroic dye concentration in DPDFLC results in decreased isotropic temperature as compared to PDFLC. We believe that this difference in the transition temperature may be due to some ionic impurities arising from dye molecules when dissolved in LCs. The light absorption of the dye molecules at higher concentration may also contribute to lowering the T_{N-I} [18].

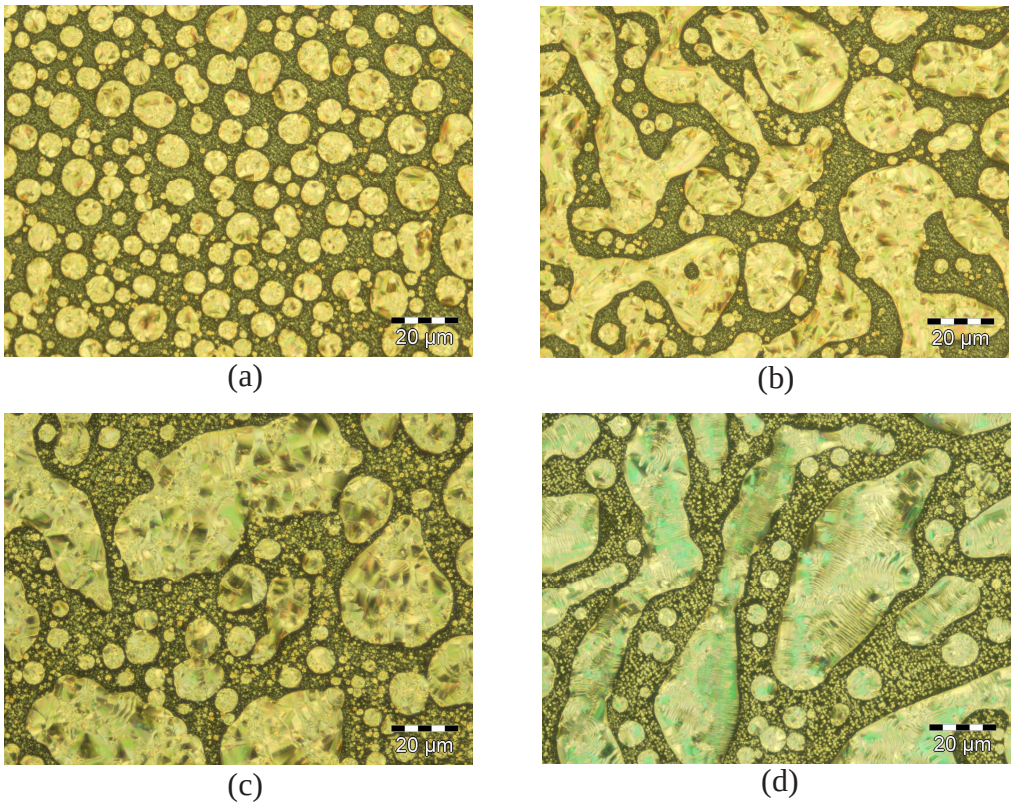

(a) (b) (c) (d)

Fig.4.3 Morphology of DPDFLCs (FLC-I + dye + NOA) with dye concentration (wt %) of 0.125% (b) 0.25% (c) 0.5% and (d) 1.0 %, respectively

Fig. 4.3 shows the morphologies of films in the voltage off state. We found that in low dye concentration (0.125%) DPDFLC material consists of FLC domains dispersed in polymer matrix are smaller in size and comparatively more uniformly distributed, as shown in fig. 4.3 (b). This may be due to the partial solubility and better mutual interaction of polymer-FLC

systems for low weight % of dichroic dye. It was also found from our results that the smaller the domain size in DPDFLC systems, the better is the electro-optic response.

4.3.1.1 Electro-optic switching and contrast ratio

The DPDFLC system depends on the birefringence of liquid crystals and takes advantage of the bistable mode in which switching occurs between 2θ [19], yielding the dark and bright states. When an applied field interacts with an FLC molecule, the molecule tends to be orientated in the direction Ps (dark state). If the field is inverted, then the FLC molecule is reoriented in the direction of Ps (bright state).

Table 4.1 Transition temperature of all the dichroic DPDFLC samples investigated

Samples	SmC* to SmA Transition (T_{C^*A} °C)	SmA to N* Transition (T_{AN^*} °C)	N* to Isotropic Transition (T_{N^*I} °C)
NOA65/ZLI- 3654	64	80	96
NOA65/ZLI-3654/B2 (0.125%wt)	62	76	92
NOA65/ZLI-3654/B2 (0.25%wt)	62	76	89.
NOA65/ZLI-3654/B2 (0.5%wt)	62	74	87
NOA65/ZLI-3654/B2 (1.0%wt)	62	74	86

Fig. 4.4 (a) shows the dye dependence of light transmission characteristic of DPDFLCs as a function of the applied voltage at frequency 50Hz, for exploring the value of threshold voltage and effect of dye. The maximum transmission of DPDFLCs decreases with increasing the concentration of dye where as the threshold voltage decreases but DPDFLC with 0.125% dye transmit better transmission than the PDFLC and 90 % transmission is achieved at dye concentration 0.125% with a threshold voltage ~ 1.57 V/μm where as the transmission is 82%

for PDFLC with a threshold value ~ 11.0 Volt. The contrast ratio is calculated from the transmission values of the dark and the bright state. Fig. 4.4 (b) shows the relationship between the contrast ratio and the dye concentration at room temperature at an applied voltage 30 V_{p-p}. The results reveal that the low dye concentration DPDFLC has a higher contrast ratio.

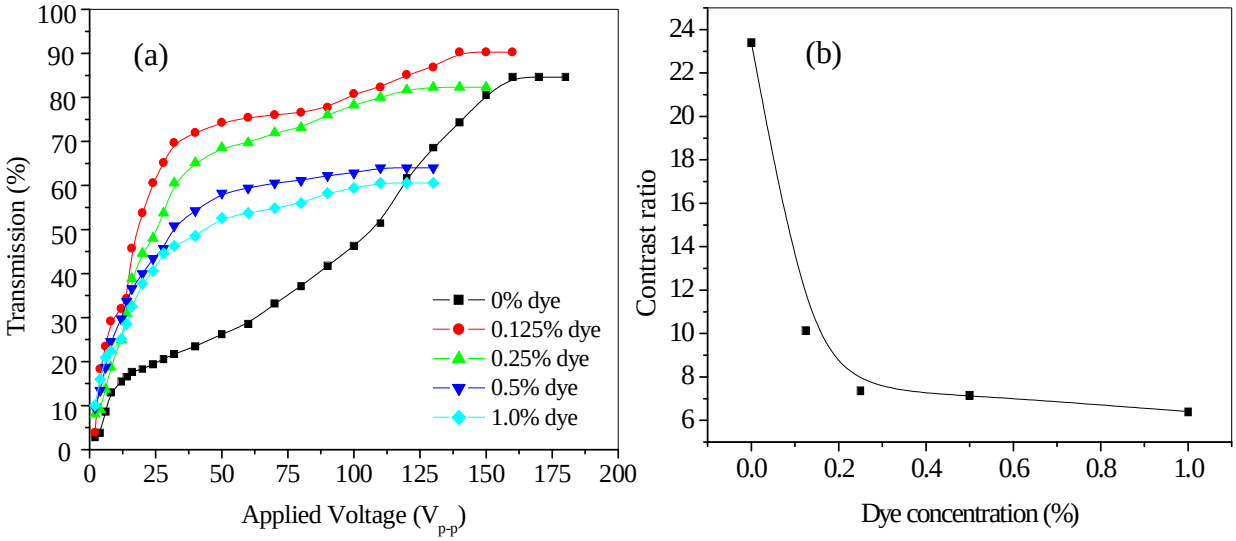

Fig.4.4 (a) Dye dependence transmission characteristics of DPDFLCs as a function of the applied voltage (50 Hz) (b) dye dependence contrast ratio of DPDFLCs at an applied voltage $30V_{p-p,}$ at room temperature

4.3.1.2 Polarization switching

Polarization switching (Ps) response and response time of the DPDFLCs of different dye concentration were calculated. The behaviour of Ps as a function of applied voltage for 0.125%, 0.5% and 1.0% DPDFLC is shown in fig. 4.5 (a-c) respectively. With the increase in the applied voltage, the spontaneous polarization increases sharply initially due to unwinding of helix and shows the same trend for all DPDFLCs in the smectic C* phase. The polarization switching with respect to temperature at different dye concentration was measured and is given in fig 4.5 (d). From the studies on dependence of Ps on temperature, it is observed that the value of Ps decreases with increase in the temperature. These trends of DPDFLCs can be explained on the basis of intra-molecular rotations and inter-molecular interactions in the presence of dye molecules in the system. The decrease in the Ps value with increase in the temperature is due to the pre-transitional effects as the transition temperature is reached and

also may be due to the weak P-E (polarization- electric field) coupling and P-θ (polarization-tilt angle) coupling in dichroic PDFLC.

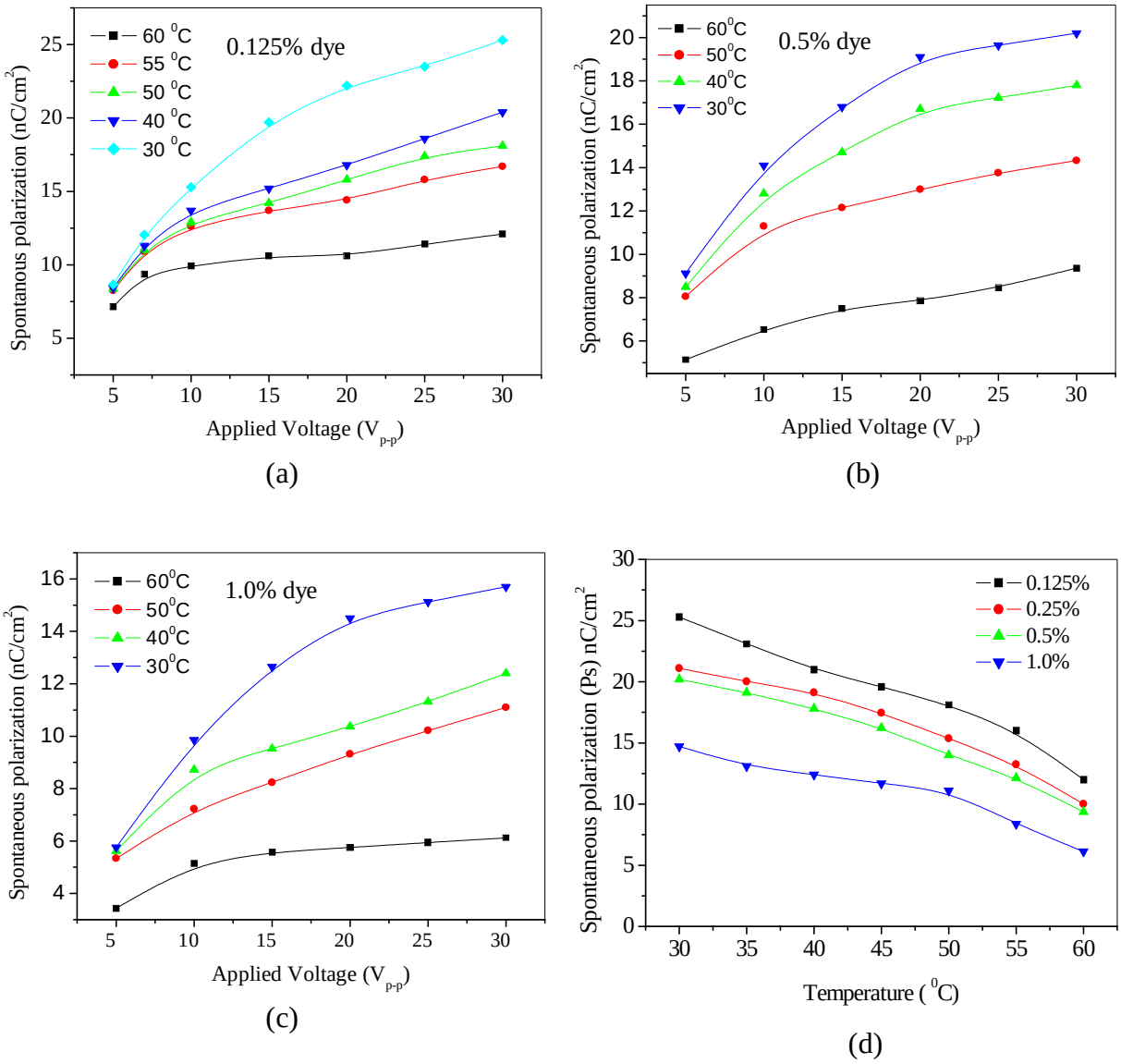

Fig.4.5 Influence of bias voltage on spontaneous polarization of (a) 0.125 % (b) 0.5 % (c) 1.0 % DPDFLCs, at different temperatures and (d) temperature dependence spontaneous polarization of all DPDFLCs at a constant bias voltage 30 V_{p-p}

Further the dye dependence Ps was also measured as shown in fig 4.6. It was found that DPDFLC containing low dye concentration shows higher polarization value. The DPDFLC containing 0.125% dye possess the Ps ~ 25.3 nC/cm^2 at a constant applied voltage 30 V_{p-p} at

30 ^{0}C however the Ps ~ 14.7 nC/cm^2 was found for the DPDFLC containing 1.0 % concentration of dye.

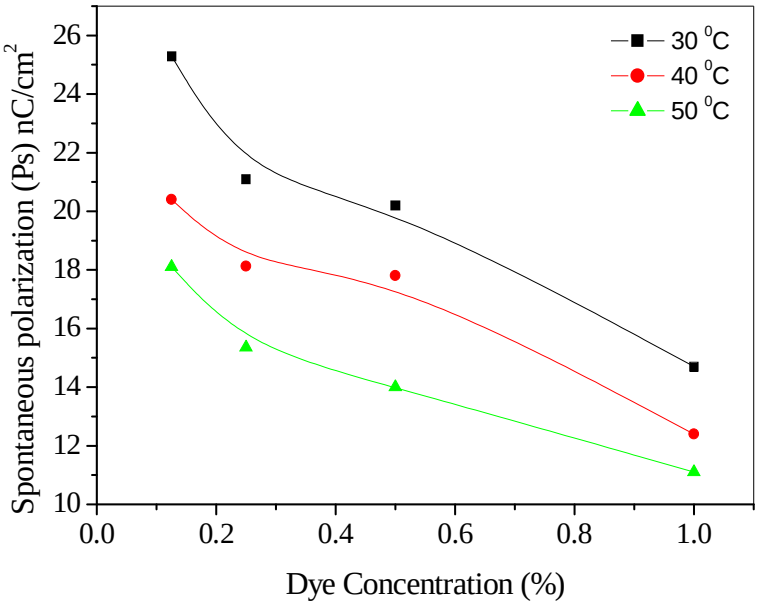

Fig.4.6 Influence of dye concentration on spontaneous polarization at a constant bias voltage 30 V_{p-p}

It stated that the dichroic dye affect the FLC molecules alignment and phase separation in DPDFLC. The higher value of Ps in low concentration of DPDFLC may be due to the induced pre helical unwinding in the system due to the orientation of ferroelectric liquid crystal molecules in the preferred direction of dye molecules in the DPDFLC. The decrease in Ps value with increasing the dye concentration may due to the weak phase separation and changed phase transition temperature because the optical tilt angle varies with temperature and optical tilt angle decreased with increasing the dichroic dye concentration [20].

Fig. 4.7 (a-c) shows the relationship between response time and the applied voltage for a fixed square-wave ac voltage on the DPDFLCs containing 0.125%, 0.5% and 1.0% concentration of dichroic dye. The response time decreased with the applied field strength. Fig. 4.7 (d) shows the response time as a function of temperature for all DPDFLCs. It was found that DPDFLC with low dye (0.125%) has sharp response time as compared to higher dye concentration DPDFLCs. With an increase of dye concentration in DPDFLC the viscosity of the FLC in the

polymer matrix is increased and the slow response time. The results were supported well by the theoretical relation (response time = viscosity/E ×Ps).

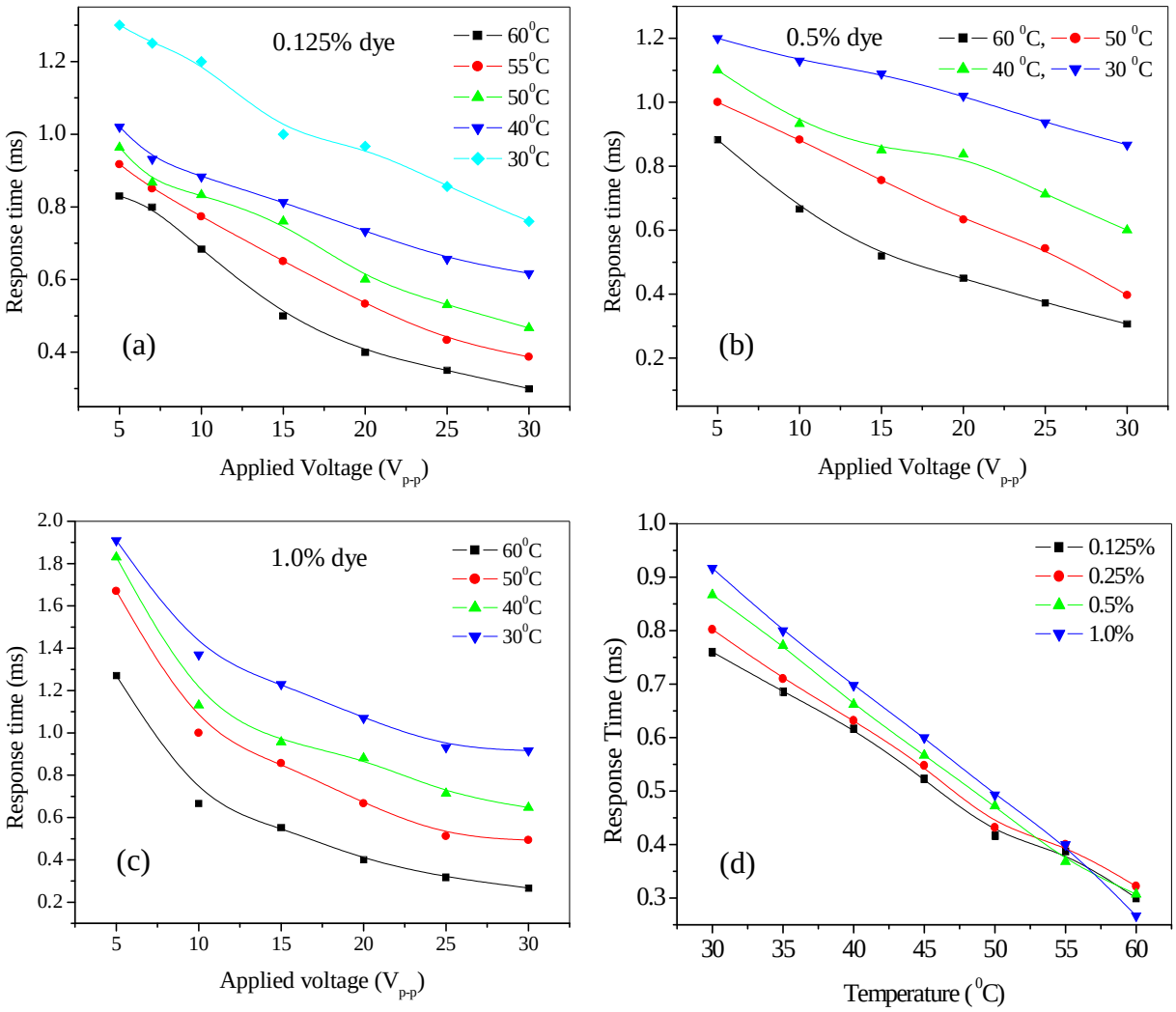

Fig.4.7 Influence of bias voltage on response time of (a) 0.125% (b) 0.5% (c) 1.0% DPDFLCs at different temperatures and (d) temperature dependence response time of all DPDFLCs

4.3.2 Phase behaviour with FLC-II

The synthesized ferroelectric liquid crystal FLC-II used in PDFLC film was studied and sequences of phases and phase transition temperatures have been determined from characteristic textures and their changes observed in polarizing microscope on cooling from isotropic phase as well as on heating from crystalline phase and confirmed by DSC. The DSC

measurements (Linseis DSC L63) were carried out on heating runs @ 5K/minute. Two mesophases namely the cholesteric and ferroelectric SmC* have been found between the isotropic and crystal phases. The DSC and microscopic textures of FLC material are shown in fig. 4.8 and fig. 4.9 respectively. The compound shows the phase sequence as

$$\text{Crystal} \xrightarrow{67\ ^{o}C} \text{SmC*} \xrightarrow{121\ ^{o}C} \text{N*} \xrightarrow{129\ ^{o}C} \text{Isotropic}$$

Morphology and phase behaviour of PDFLC (Noa 65 + FLC-II) and dichroic PDFLC containing 1% (wt/wt) blue anthraquinone dye was studied. The PDFLC film shows almost same phase behaviour as a pure FLC and fast switching characteristics between two stable states, as shown in fig. 4.10 where as a large transition temperature variation of the dichroic PDFLC film were obtained by doping the 1% (wt/wt) of dye concentration.

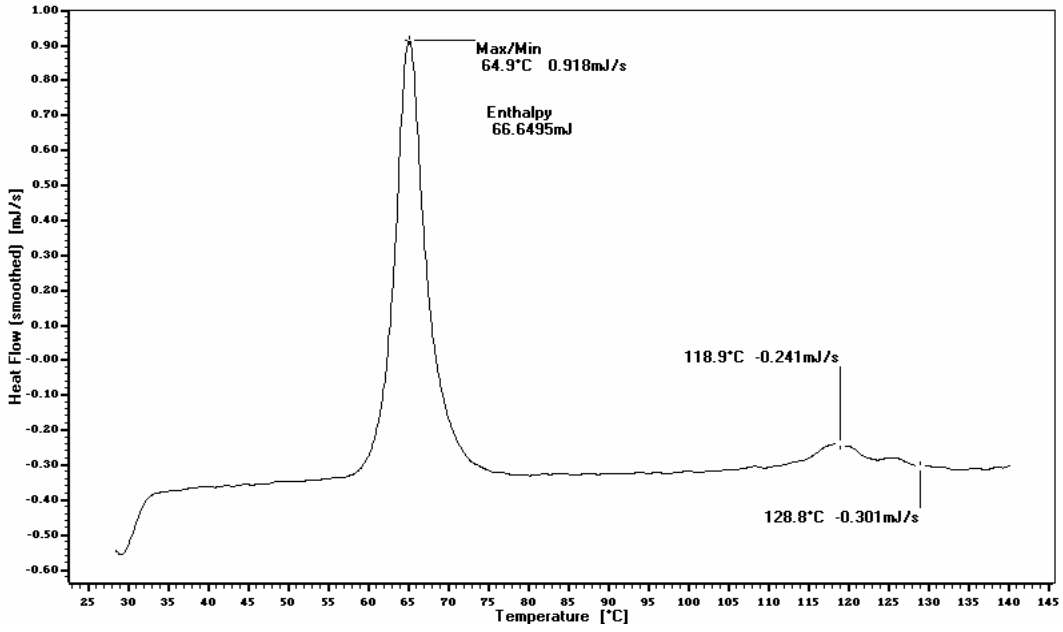

(a)

Contd.

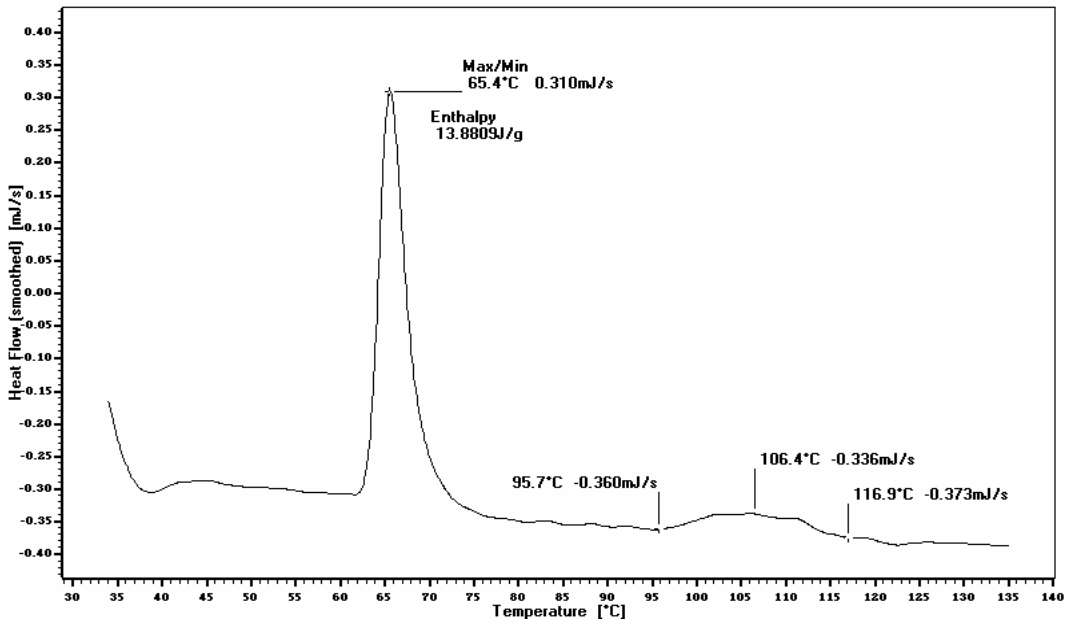

(b)

Fig.4.8 DSC plot of (a) FLC-II and (b) PDFLC

The clearing temperature is much lower for DPDFLC sample compared with PDFLC but the switching characteristics of the PDFLC film is greatly enhanced after the addition of dye as shown in fig.4.11. The phase sequence and phase transition temperatures of dichroic PDFLC have been determined from characteristic textures and their changes observed in polarizing microscope. DPDFLC showed SmC* phase only with isotropic transition temperature of 110 ˚C, may be due to the fact that much lower isotropic temperature as compared to FLC material of 129˚C as shown in fig.4.12, on cooling from isotropic phase as

$$\text{Isotropic} \xrightarrow{110\ ^0\text{C}} \text{SmC*} \xrightarrow{44\ ^0\text{C}} \text{Crystal}$$

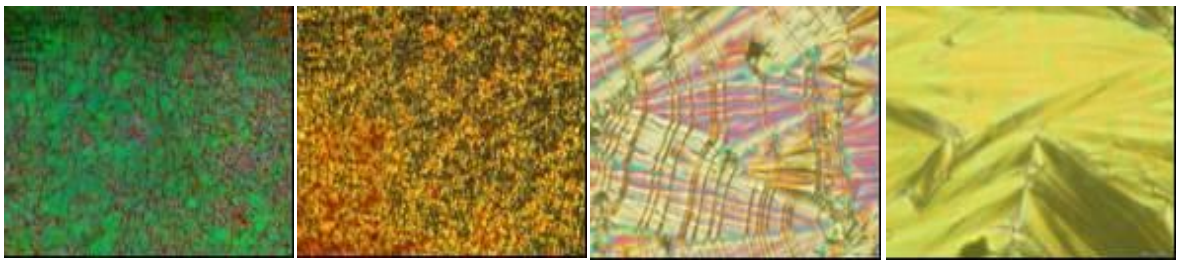

(a) (b) (c) (d)

Fig.4.9 Micro textures of FLC-II at (a) 30 ^{o}C (b) 67 ^{o}C (c) 70 ^{o}C and (d) 70 ^{o}C, at 30 V_{p-p}

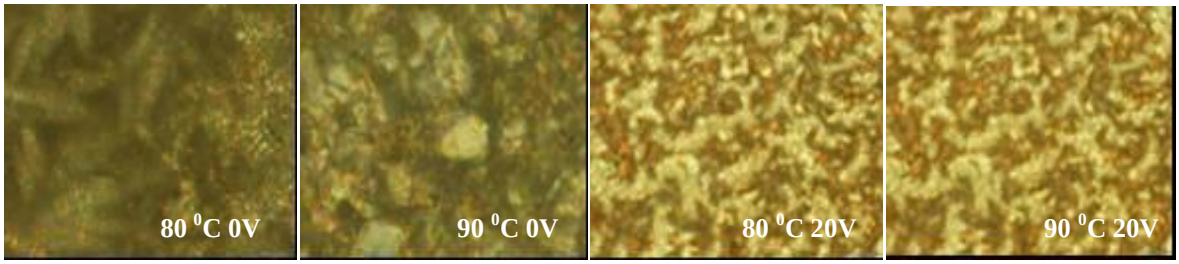

(a) (b) (c) (d)

Fig. 4.10 Optical textures of PDFLC (Noa 65 + FLC-II) film, the film shows fast switching at 20 V_{p-p}

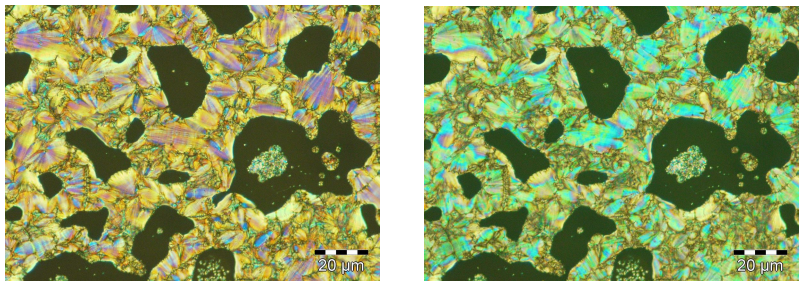

(a) (b)

Fig.4.11 Switching characteristic of dichroic PDFLC film at (a) 0 V_{p-p} and (b) 5 V_{p-p}, in chiral smectic C* phase at 50 ^{0}C

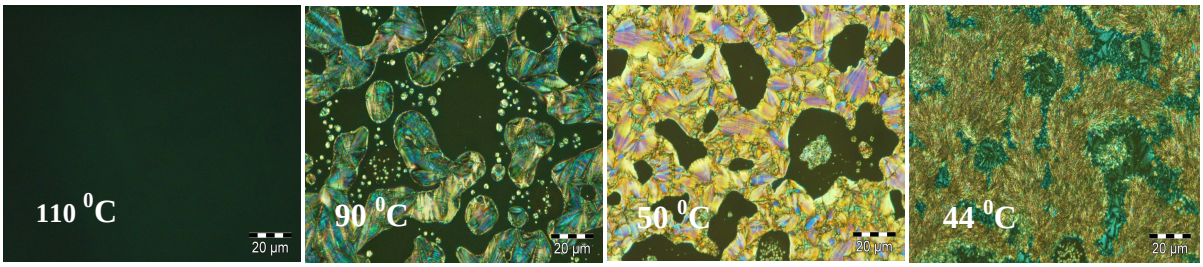

Fig.4.12 Microscopic textures of dichroic PDFLC at different temperatures at 100 X, chiral smectic C* phase changes to crystalline phase at 44 ^{0}C

4.3.2.1 Electro-optic switching

The temperature dependence of light transmission of PDFLCs was measured as a function of the applied voltage at frequency 50Hz, for exploring the value of threshold voltage as shown in fig.4.13. The transmission of PDFLC sample increases with increasing the temperature where as the threshold voltage decreases in chiral smectic C* phase. 80 % transmission is achieved at 118 ^{0}C and threshold voltage is ~ 2 V/µm and further transmission is decreased on increasing the temperature. Primarily possible reason for increasing the transmission with temperature may be due to decrease in anchoring energy between the liquid crystal and

polymer network. Secondary it may be due to the decrease in order parameter with an increase in temperature.

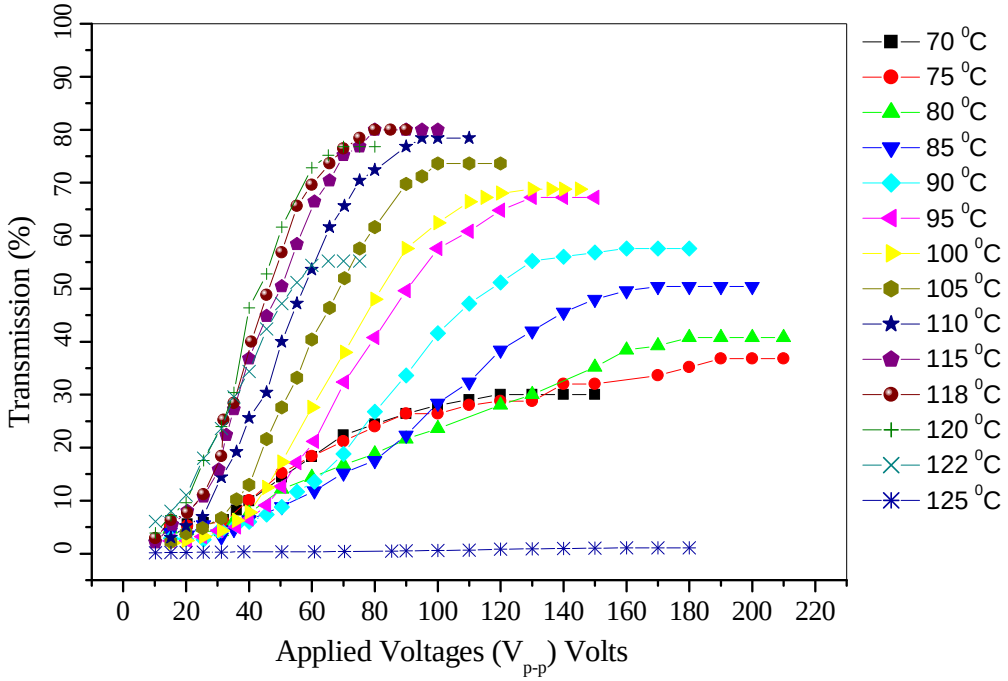

Fig.4.13 Temperature dependence transmission characteristics of PDFLC films as a function of the applied voltage (50 Hz)

4.3.2.2 Spontaneous polarization

The value of the Ps decreases with increasing temperature within smectic C* phase range as shown in fig 4.14. We found that the Ps of the PDFLC and DPDFLC samples is smaller than the FLC material. The FLC material possess the Ps ~ 200 nC/cm^2 at 60 ^{0}C however the Ps ~ 70 nC/cm^2 and Ps ~ 69.1 nC/cm^2 was found for the PDFLC and DPDFLC sample respectively. This decrease in Ps might be due to the change in wt ratio (due to that area occupied by FLC is reduced in the dispersed sample and reduction in Ps results) of the as well as the cohesive forces between the polymer and FLC domain. It also stated that the 1 % (wt/wt) dichroic dye affect the FLC molecules alignment and will course the FLC molecules alignment random due to that the spontaneous polarization decreased comparatively in DPDFLC sample. Fig. 4.15 shows the electro-optic switching times of FLC, PDFLC and DPDFLC films as a function of temperature at applied voltage 30V. The switching

characteristics were good, reaching a minimum response time of ~ 145 μs for FLC and ~ 240 μs for PDFLC device where as the DPDFLC showed the slow response time, comparatively.

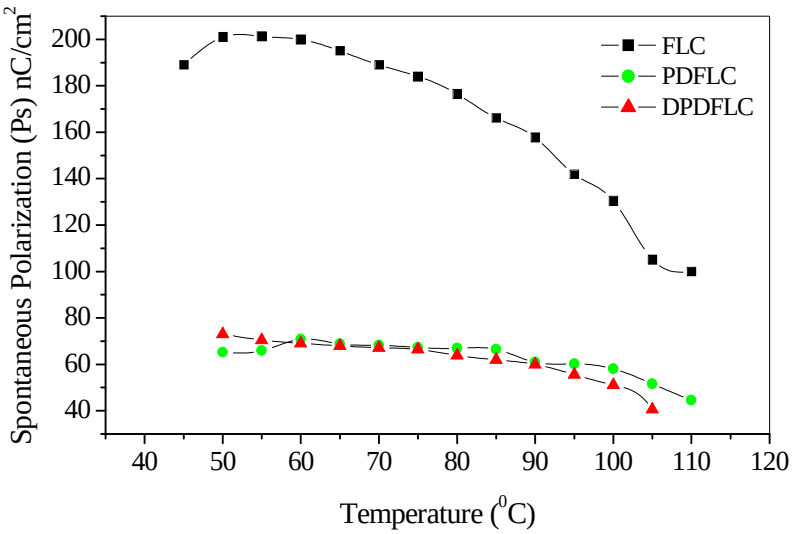

Fig.4.14 Temperature dependence spontaneous polarization of FLC, PDFLC and DPDFLC films (FLC-II + anthraquinone dye + NOA 65)

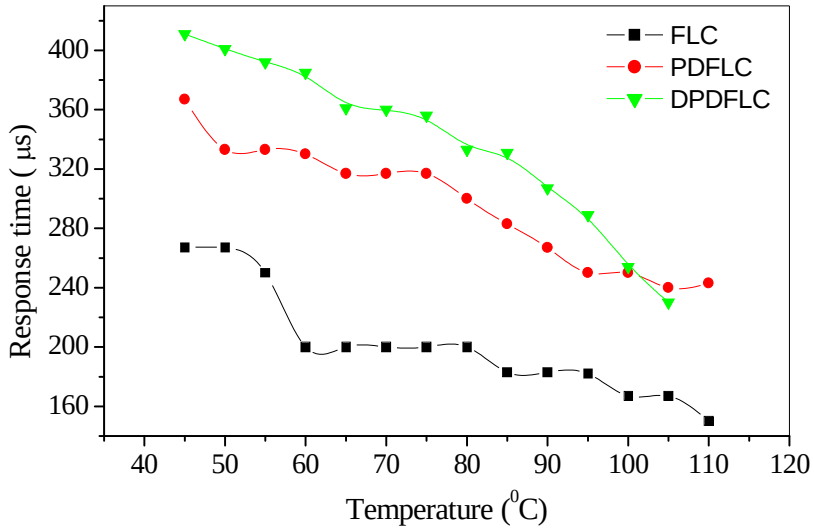

Fig.4.15 Variation of the electro-optic switching times as a function of temperature of FLC, PDFLC and DPDFLC films at applied voltage 30V.

It may be due the increased viscosity of FLC in the polymer matrix in the DPDFLC with the addition of dye concentration. The reduction in Ps will also cause the increase in response time, as explained above.

References

[1] J. L. Fergason, SID Digest, **16** (1985) 68.

[2] H. G. Craighead, J. Cheng and S. Hackwood, Appl. Phys. Lett. **40** (1982) 22.

[3] H. Liu, H.Duig and J. R. Kelly, Mol. Cryst. Liq. Cryst. **26** (1995) 99.

[4] J. W. Hax, T.J. Kaxg and G. Park, J. Korean Phys. Soc. **36** (2000) 156.

[5] P. P. Kandu, G. Verma and K. K. Raina, J. Appl. Poly. Sci. **87** (2003) 284.

[6] G. Sumana and K. K.Raina, J. Appl. Poly. Sci. **87** (2003) 1209.

[7] H. S. Kitzerow, H. Molsen and G. Heppke, Appl. Phys. Lett. **60** (1992) 25.

[8] K. P. Lee, S. W. Suh and S. D. Lee, Appl. Phys. Lett. **64** (1994) 718.

[9] H. Molsen and H. S. Kitzerow, J. Appl. Phys. **75** 710 (1994).

[10] P. Patel, D. Chu, J. L. West and S. Kumar, Soc. Inf. Disp. Dig. XXV (1994) 845.

[11] R. Karapinar and M. O. Neill, J. Phys. D Appl. Phys. **31** (1998) 900.

[12] V. Y. Zyryanov, S. L. Smorgon and V. F. Shabanov, SID Digest (1992) 776.

[13] G. Heppke, H. S. Kitzerow and H. Molsen, Mol. Cryst. Liq. Cryst. **237** (1993) 471.

[14] E. P. Pozhidaev, D. Ganzke, V.Ya. Zyryanov, S. L. Smorgon, and W. Haase, Liq. Cryst. **29** (2002) 1305.

[15] S. Kundu, T. Ray, S. K. Roy, W. Haase and R. Dabrowski, Ferrelectrics, **282** (2003) 239.

[16] Farhi, A. Andreau, E. Andreoli de Oliveira, J. P. Marcerou, H.T. Nguyen and J.M. Tarascon, Mol. Cryst. Liq. Cryst. Sci. Technol, Sect. A **365** (2001) 875.

[17] S. J. Kłosowicz, K. L. Czupryn´ski, W. Piecek Mol. Cryst. Liq. Cryst. Sci. Technol. Sect. A **351** (2000) 343.

[18] Pankaj Kumar and K. K. Raina, Current Appl. Phys. **7** (2007) 636.

[19] L. A. Beresnev, L. M. Bilnov, M. A. Osipov, and S. A. Pikin, Mol. Cryst. Liq. Cryst. **158** (1998) 3.

[20] H. Ru Lin, J. Fu Lyuu and J. Yih Lee, Mol. Cryst. Liq. Cryst. **368** (2001) 613.

Chapter 5
Conclusions

Taking into account different dye concentration, dichroic polymer dispersed liquid crystal (DPDLC) films for both nematic and ferroelectric systems have been prepared to analysis the influence of dye concentration on liquid crystal droplet morphology and their optical responses as a function of applied voltage and temperature. The use of dichroic dyes can enhance their electro-optical and thermo-optical properties. Our results show that the-

* LC domains in these DPDLC composite films are predominantly in the bipolar configuration, however different type of droplet (bipolar, axial, radial and collapsed) configuration have been observed for DPDLCs containing 0.5 % and 1.0 % anthraquinone blue dye.

* Effect of electric field on these films has been found to strongly influence the LC droplet orientation and maltese type crosses were observed at higher field.

* Transition temperature is lower for DPDLCs compared with a non doped PDLC, might be due to some contaminations arising from dye, monomer molecules when dissolved in LCs and thermal contribution of the light induced by absorption by the presence of the dye which causes a decreasing of the clearing point. The other possible reason to lowering the T_{N-I} may be that the azo molecule which shows a rod-like shape when in the trans form, but is bent and banana-like in the cis form acts like an impurity and therefore destabilizes the liquid crystalline phase.

* Use of dye allows reducing threshold voltage for switching the material from a scattered to transparent state. As dye concentration increases, the threshold voltage decreases. Threshold voltage (V_{th}) is approximately 8 V/µm for pure PDLC (without dye), where as the threshold voltages are approximately 4 V/µm, 2 V/µm and 1 V/µm for 0.125 %, 0.25 % and 0.5 % anthraquinone (blue) dye doped DPDLCs respectively, while the threshold voltages are approximately 3.5 V/µm, 1.8 V/µm, 1.5 V/µm and 1.0 V for 0.0625 % 0.125 %, 0.25 %, and 0.5 % azo (orange) dye doped DPDLCs respectively.

* We also presume that the threshold voltage in the dichroic PDLC is also affected by the droplet size. Because the surface effect is greater for smaller dichroic PDLC droplets therefore anchoring force from the surfaces is greater for the low concentration of dye (for lower droplet sizes).

* Our result indicates that lower dye concentration PDLC shows higher transmission, higher contrast ratio and better optical responses. Higher dye content results in a lower transmittance and a lower value of clearing temperature.

* The absorption coefficient is obtained by measuring the transmittances of DPDLC films. By least square fitting of the experimental data, we found that the straight line is least squares fit to the experimental data. The theory supports our experimental data.

* The dispersion of azo dye in the DPDLCs influences the dielectric parameters. The addition of dye led to an increase of the dielectric absorption and to shift in the dielectric absorption peaks to lower frequencies.

* Dichroic PDFLCs taking in account of varying concentration of anthraquinone dye have been studied in detail for transmission and optical switching. DPDFLC with 0.125 % dye transmit better transmission than the PDFLC & 90 % transmission is achieved at dye concentration of 0.125% with a threshold voltage ~ 1.57 V/μm where as the transmission is 82% for PDFLC with a threshold value ~11.0 Volt.

* The switching characteristics show response time of ~ 145 μs for FLC and ~ 240 μs for PDFLC device where as the DPDFLC showed the slow still response time, comparatively. With an increase of dye concentration in DPDFLC the viscosity of the FLC in the polymer matrix is increased and the slow response time.

* Samples with low dye concentration show higher polarization value. The DPDFLC containing 0.125 % anthraquinone dye possesses Ps ~ 25.3 nC/cm^2 at a fixed voltage 30 Vp-p at 30 ^{0}C however the Ps ~ 14.7 nC/cm^2 was found for the DPDFLC containing 1.0 % concentration of anthraquinone dye.

* Droplet size is significant factor to control the opto-electronic properties of these dichroic polymer dispersed liquid crystal systems. The materials may find suitable and promising functional electronic materials for flexible display technology.